Toxicology in Vitro 50 (2018) 347–372

Contents lists available at ScienceDirect

Toxicology in Vitro

journal homepage: www.elsevier.com/locate/toxinvit

Proteomics study of silver nanoparticles on Caco-2 cells

Sabrina Gioria[a,*], Patricia Urbán[a], Martin Hajduch[a], Paola Barboro[b], Noelia Cabaleiro[a], Rita La Spina[a], Hubert Chassaigne[a]

[a] European Commission, Joint Research Centre (JRC), Directorate F - Health, Consumers and Reference Materials, Via Enrico Fermi 2749, I-21027 Ispra, VA, Italy
[b] Academic Unit of Medical Oncology, Ospedale Policlinico San Martino, L.go R. Benzi 10, 16132 Genova, Italy

ARTICLE INFO

Keywords:
Nanomaterial safety assessment
Systems biology analysis
2D-gel based proteomic approach
Label-free MS-based proteomic approach
Qualitative and quantitative proteomics

ABSTRACT

Silver nanoparticles (AgNPs) have been incorporated into several consumer products. While these advances in technology are promising and exciting, the effects of these nanoparticles have not equally been studied. Due to the size, AgNPs can penetrate the body through oral exposure and reach the gastrointestinal tract. The present study was designed as a comparative proteomic analysis of Caco-2 cells, used as an in vitro model of the small intestine, exposed to 30 nm citrate stabilized-silver nanoparticles (AgNPs) for 24 or 72 h. Using two complementary proteomic approaches, 2D gel-based and label-free mass spectrometry, we present insight into the effects of AgNPs at proteins level. Exposure of 1 or 10 μg/mL AgNPs to Caco-2 cells resulted in 56 and 88 altered proteins at 24 h and 72 h respectively, by 2D gel-based technique. Ten of these proteins were found to be common between the two time-points. Using label-free mass spectrometry technique, 291 and 179 altered proteins were found at 24 h and 72 h, of which 24 were in common. Analysis of the proteomes showed several major biological processes altered, from which, cell cycle, cell morphology, cellular function and maintenance were the most affected.

1. Introduction

Silver nanoparticles (AgNPs) are the most commercialised nanotechnological products on the market according to the Consumer Products Inventory (2016), with over 400 registered applications to date (Calderón-Jiménez et al., 2017). Due to their unique antibacterial properties against both Gram-positive and negative bacteria (Panáček et al., 2006), AgNPs have been incorporated into a large number of consumer products. AgNPs are found in clothing, kitchenware, toys, cosmetics, medicinal products, medical devices, food packaging materials, plant protection and biocidal products.

Considering the broad application of AgNPs, a wide public is likely exposed to them on a regular basis. The increased rate of introduction of NPs-based consumer products to the market prompts the need for a better understanding of the fate and potential impacts on the biological systems.

Silver is considered to be more toxic than other metals when in nanoscale form (Bar-Ilan et al., 2009) and AgNPs have a different toxicity mechanism compared to dissolved silver ions (Li et al., 2013). The mechanism employed for the uptake of NPs and their effects on cellular function appear to be critically dependent on the particle characteristics, such as the size (of the primary particle and potential aggregates/agglomerates), hydrophobicity, surface modification, and shape (Win and Feng, 2005). However, less research has been done to evaluate these interactions and their impact on human health. Previous works have shown that AgNPs can induce potential harmful effects, including the generation of dangerous radicals (Li et al., 2013).

Due to their size, NPs can readily penetrate the body and cells through various routes. It has been reported that inhaled NPs cleared by mucociliary escalator, can be ingested and reach the gastrointestinal tract (Teow et al., 2011). It is estimated that the average person in a developed country is exposed orally to 10^{12} to 10^{14} man-made fin (0.1–1 μm) to ultrafine (< 100 nm) particles every day (Lomer et al., 2002, Kim et al., 2010, Hartemann et al., 2015). As the Caco-2 human epithelial cell line is one of the most relevant in vitro models to study intestinal functions (Lefebvre et al., 2015), it was selected to investigate AgNPs toxicity.

The present study was designed to elucidate the effects of AgNPs when interacting with Caco-2 cells and to address the limited literature available. We had previously shown the advantages of 2D gel-based proteomics as a potent tool to accurately quantify and identify proteins involved in cellular events, underlying nano-bio interactions and understanding the potential mechanism of actions (Gioria et al., 2016). Here, we have applied the technique to unravel the cellular networks regulated by AgNPs.

We report on the two complementary proteomic approaches for the

* Corresponding author: European Commission, Joint Research Centre, Directorate F - Health, Consumers and Reference Materials, via E. Fermi 2749, 21027 Ispra, VA, Italy.
E-mail address: sabrina.gioria@ec.europa.eu (S. Gioria).

https://doi.org/10.1016/j.tiv.2018.03.015
Received 15 January 2018; Received in revised form 28 March 2018; Accepted 29 March 2018
Available online 04 April 2018

investigation of the interactions of AgNPs with Caco-2 cells: (i) the 2D gel-based proteomics, which included two-dimensional gel electrophoresis (2DE), coupled with ultra-high-performance liquid chromatography high-resolution mass spectrometry (UHPLC-HRMS/MS); and (ii) the label-free MS-based proteomics, based on UHPLC-HRMS/MS, followed by extensive bioinformatics and data mining procedures. Also, the two proteomic approaches were complemented with additional analytical techniques for a complete analysis of cellular response to NPs.

Overall this research advances the mechanistic understanding of AgNP toxicity and contribute to a more effective assessment of the growing number of new nanomaterials, which is difficult to achieve by traditional, single end-point approaches (Costa and Fadeel, 2016) (Matysiak et al., 2016). In addition, data sharing in mass-spectrometry (MS)-based proteomics opens a plethora of opportunities (Martens and Vizcaíno, 2017) for scientific progress.

2. Materials and methods

A schematic diagram of the experimental design of the 2D-gel based and label-free MS-based approaches and bioinformatics tools employed is provided in Fig. 1.

2.1. AgNPs synthesis

In controlling the colloidal stability, citrate was used as a capping agent. The synthesis of AgNPs was carried out by the reduction of $AgNO_3$ with citrate and tannic acid based on the procedure described in (Dadosh, 2009) with some modifications. More specifically, 120 µL of tannic acid (2 mM) were added to 6 mL of citrate 28 mM, the solution was and stirred at 60 °C for 15 min. Then, 6 mL of this solution were added to 94 mL of $AgNO_3$ 0.55 mM in boiling condition under vigorous stirring. The mixture was kept at 97 °C for further 40 min. The solution was heated up using a microwave synthesis reactor (Discover S by CEM corporation) to ensure a highly reproducible rapid heating. Afterwards, the solution was rapidly cooled down at 40 °C, and then to room temperature. The nanoparticles were directly characterized after synthesis.

2.2. AgNPs characterisation

The size and size distribution of the synthesized AgNPs in dispersion solution were assessed by Centrifugal Liquid Sedimentation (CLS), and Dynamic Light Scattering (DLS) while the shape and size were verified by Scanning Electron Microscopy (SEM) imaging. The CLS measurements (instrument model DC24000UHR, CPS Instruments Inc., USA) were performed in an 8 wt%–24 wt% sucrose density gradient with a disc speed of 22,000 rpm. Each sample injection of 100 µL was preceded by a calibration step using certified polyvinyl chloride (PVC) particle size standards with a weight mean size of 280 nm. Measurements of particle size distribution by DLS were done using a Zetasizer Nano-ZS by Malvern Ltd., UK. Each sample was measured in triplicate at 25 °C after an equilibration step of 120 s using an acquisition time of 80 s. The hydrodynamic diameter was calculated using the DLS internal software.

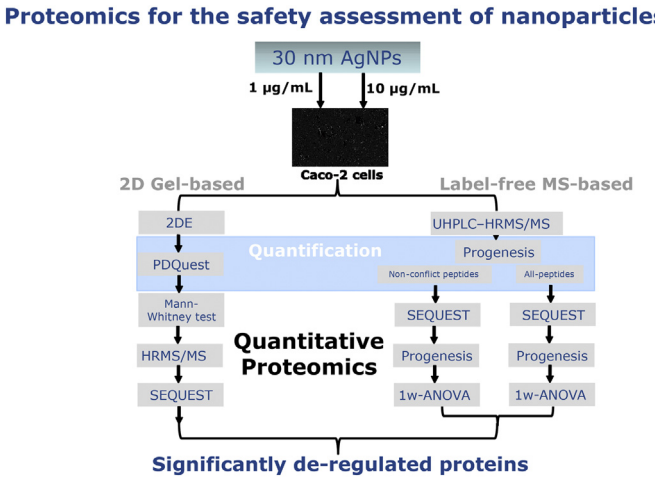

Fig. 1. Schematic diagram of the experimental design of the 2D-gel based and label-free MS-based.

The size distribution and shape of the particles were also verified using TEM image. The software ImageJ was used for image analysis with a minimum of 100 particles being counted for size and size distribution calculations.

The behaviour of citrate-stabilized AgNPs in complete culture medium was monitored by DLS analysis for up to 72 h at 37 °C.

The particle stock suspension was analysed for potential endotoxin contamination using a commercially available endotoxin quantitation kit (Thermo Fisher Scientific, 88,282) according to the manufacturer's instructions and no endotoxin contamination was detected.

2.3. Quantification of dissolved ionic silver and internalised AgNPs by ICP-MS

The amount of dissolved ionic Ag was evaluated by ultrafiltration in 1 and 10 µg/mL AgNPs suspensions in Caco-2 complete culture media. Two mL of the stock was filtered through Amicon Ultra Centrifugal Filter of regenerated cellulose (cut off 3KDa). To 500 µL of the resulting filtrate, 200 µL of concentrated nitric acid was added (Carlo Erba SpA, Italy) and the solution was made up to 3 mL with Milli-Q water (Millipore, USA) before analysis by ICP-MS (Agilent ICP-MS 7700x, Agilent Technologies, Santa Clara, USA). The instrument was operated using collision cell technology (CCT) with He gas (4.3 mL/min) and monitoring isotope Ag^{107}. Rhodium (50 µg/L) was added on-line as an internal standard.

Total concentration of Ag internalised in cells incubated for 24 h, or 72 h was evaluated after 10 min microwave digestion (200 °C, 300 W, 400 psi) with 2 mL of HNO_3 and 0.4 mL H_2O_2 using a microwave acid digestion system (Discover SP-D, CEM Co., USA). Samples were diluted with milli-Q water before ICP-MS analysis, as described above. ICP-MS was also performed on initial solution of 1 and 10 µg/mL (t = 0) in order to calculate the percentage of dissolved ionic Ag.

2.4. Cell culture conditions and AgNP exposure

Human colon adenocarcinoma Caco-2 cells were obtained from the American Type Culture Collection (LGC standards, Milano, Italy). Caco-2 cells (passage 43–49) were cultured in complete culture medium, composed of Dulbecco's Modified Eagle Medium (DMEM) high glucose (4500 g/L) supplemented with 10% (v/v) Fetal Bovine Serum (FBS, North America Origin), 0.5% (v/v) penicillin/streptomycin, 4 mM L-glutamine and 1% (v/v) not essential amino acids. All cell culture reagents were purchased from Life Technologies, Italy. For routine culture, cells were maintained in a sub-confluent state under standard cell culture conditions in a humidified incubator (37 °C, 5% CO_2, 95% humidity) (Heraeus Thermo Fisher®, Belgium).

2.5. Sample preparation

For proteomic experiments, 1×10^6 Caco-2 cells between passage 43 and 49 were seeded in 5 mL complete culture medium in 100 × 20 mm Petri dish (Corning, Italy). For treatment, the medium was replaced with 30 nm AgNPs at final concentrations of 1 or 10 µg/mL. In each experiment, untreated cells were used as control. Six biological replicates were performed for each experimental condition. Proteins extraction from the cytoplasmatic compartment was performed at 24 and 72 h of exposure time as described in our previous work (Gioria et al., 2014).

For 2D gel-based experiments, protein pellets were re-suspended in the buffer for two-dimensional polyacrylamide gel electrophoresis. Experiments were run using an equal protein amount of 100 µg per sample (control or treated). For each experimental condition (Control and treated), six replicate gels were run.

For MS-based proteomic experiments, protein pellets (100 µg protein each) were re-suspended in 100 µL 0.2% (w/v) RapiGest solution and vortexed. 5 µL of 50 mM DTT solution was added, and the sample was heated at 60 °C for 30 min at 300 rpm using a Thermomixer. The sample was cooled to room temperature, and 10 µL of 100 mM iodoacetamide (IoAc) solution was added. The sample was placed in the dark at room temperature for 30 min and 40 µL 0.1 µg/µL of trypsin solution was added to the protein tube (1:50, protease: protein ratio). Samples were incubated at 37 °C for 12 h (Thermomixer at 300 rpm) for optimum enzymatic digestion. 5 µL of 500 mM HCl solution was then added to neutralise the RapiGest. The sample was transferred into molecular-mass cut-off filtration units (3000 MWCO) and the units were centrifuged at 14,000 × *g* for 10 min before LC-MS/MS analysis.

2.6. 2D gel-based quantitative proteomic experiments

2.6.1. 2D gel electrophoresis and 2D map differential analysis

In order to better estimate the difference between untreated (control) and AgNPs-treated cells, a randomised block design on 6 biological replicates for each experimental condition (control, 1 or 10 µg/mL AgNPs) was performed to reduce the bias and variance in the 2D-gel protein patterns.

The 2D gel electrophoresis technique was described in our previous work (Gioria et al., 2014). Briefly, protein samples were separated by isoelectric focusing using immobilised non-linear pH range 3.0–10.0 strips (GE Healthcare) followed by SDS-PAGE in a 16 × 14 cm 8–14% linear gradient. After 2D electrophoresis, gels stained with fluorescent dye Sypro Ruby (Molecular Probe Inc., Lifetechnologies, Italy) were scanned with a GS-800 imaging densitometer (BioRad) under the same scanning conditions. For each 2D map protein pattern analysis, background subtraction, spot detection, gel alignment and spot matching were performed using PDQuest v. 7.3.0 software package (BioRad) as already reported (Gioria et al., 2016). Using Mann-Whitney test along with ± two folds change in expression level, differentially regulated proteins were selected. Apparent molecular weight (MW) and isoelectric points (pI) were established by comparison with known proteins used as internal standards.

2.6.2. Preparative 2D gels and protein spot picking

A preparative experiment was run using 200 µg of protein from control and treated samples. Experimental conditions for electrophoresis were the same as the ones described for the analytical gel. The gels were Sypro Ruby stained and digitized for image analysis. Preparative gels were matched with analytical gels for protein selection in the 2D map using PDQuest software. Corresponding spots were listed and numbered accordingly for further MS/MS identification. Selected protein spots were excised and transferred to a 96-well plate using a ProteomeWorks Plus Spot Cutter System (BioRad).

2.6.3. In-gel protein hydrolysis and peptide extraction

Sample preparation was carried out under a laminar flow cabinet using powder-free gloves and sterile equipment. Protein spots were washed three times with Milli-Q water and dried three times with acetonitrile (CH_3CN), reduced (using 10 mM DTT in 50 mM ammonium bicarbonate for 30 min at 56 °C) and alkylated (using 50 mM iodoacetamide in 50 mM ammonium bicarbonate for 30 min in the dark). The enzymatic digestion (using 1 ng/µl sequencing grade trypsin in 50 mM ammonium bicarbonate) was performed at 37 °C overnight. The resulting hydrolysates were extracted three times with a total volume of 40 µl solution (CH_3CN 100%) and transferred into Eppendorf tubes. Extracts were combined (120 µl) and samples were evaporated to dryness using a rotary evaporator equipped with a vacuum system and re-suspended in 20 µL solution of 0.1% formic acid (HCOOH) in milli-Q water: methanol, 95:5.

2.7. Label-free MS-based quantitative proteomic experiments

2.7.1. Capillary-UHPLC and LTQ Orbitrap mass spectrometry

For label-free MS-based quantitative proteomics, the UHPLC-HRMS/MS configuration and experimental conditions were similar as described for the 2D-gel based approach (Protein spot identification by UHPLC-HRMS/MS, Supplementary Methods). 6 biological replicates were analysed to increase the impact of this study. Peptides extracted from the digested gel were transferred to the Ultimate 3000 autosampler. A 5 µL aliquot of the extract was injected and loaded onto the pre-column. Experiment design involved the analysis of quality control (QC) samples (Waters Mass PREP Digestion standard bovine serum albumin in establishing the repeatability of the method), analytical blanks (for possible contamination) and the study samples (control and treated). Control and treated samples were run in randomised order with the analytical blanks and QCs during the sequence. Peptides extracted from the digested gel were transferred to the Ultimate 3000 autosampler. A 5 µL aliquot of the extract was injected and loaded onto the pre-column. An experimental design table was created for each of the 6 batches of analysis (not shown). To each batch was associated a *.csv file containing the following information on the analysis sequence: sample name (QC, blank, sample), sample code, file name and treatment, nanoparticle size.

2.7.2. HRMS/MS data processing

The raw data obtained from the label-free MS-based proteomic analysis (*.raw) were imported and processed using Progenesis QI for Proteomics software (NonLinear Dynamics, UK). The software processed the raw data in two steps. Firstly, each sample run was subjected to peak extraction and alignment. The sample run that yielded most features (i.e. peptide ions) was used as the reference run to which retention time of all of the other runs was aligned, and peak intensities were normalised. The Progenesis peptide quantification algorithm calculates peptide abundance as the sum of the peak areas. Each abundance value is then transformed to a normalised abundance value by applying a global scaling factor. Protein abundance was calculated as the sum of the abundances of all peptide ions identified as coming from the same protein. For the purpose of this experiment, the quantification based on i) all peptides and ii) non-conflict peptides was performed and compared. A number of criteria were used to filter the data before exporting the MS/MS output files for protein identification; (1) peptide features with analysis of variance (ANOVA) p-value ≤ 0.05 between experimental groups, (2) mass peaks with charge states from +2 to +4, and (3) maximum number of MS/MS spectra per mass set to 5. All MS/MS spectra were exported from Progenesis software as a MASCOT generic file (*.mgf) and used for peptide identification with Proteome Discoverer 1.4 (Thermo Fisher Scientific) using the SEQUEST algorithm, (licence Thermo Scientific, registered trademark University of Washington, USA) against the UniProtKB database (taxonomy: *Homo sapiens*). The search parameters used were as follows: (1) peptide mass tolerance set to 20 ppm, (2) MS/MS mass tolerance set to 0.6 Da, (3) up to two missed cleavages were allowed, (4) carbamidomethylation set as a fixed modification and (5) methionine oxidation set as a variable modification. A number of criteria were applied to assign a protein as identified; proteins with ≥2 peptides matched, a ≥ 1.5 fold difference in abundance. For re-importation back into Progenesis LC–MS software for further analysis, only peptides with XCorr scores > 1.9 for singly charged ions, > 2.2 for doubly charged ions and > 3.75 for triply charged ions or more (from SEQUEST) were selected. A number of criteria were applied to ensure proper identification of proteins, including an ANOVA score between experimental groups of ≤0.05 and proteins with ≥2 peptides matched. The quantitative protein data

(normalised abundances) for each sample of biological replicated analysis were exported into Excel file.

2.7.3. Identification of differentially abundant proteins

In detecting statistically significant alterations in protein abundances between control and treated samples, one-way ANOVA was used to compare the different treatments (control, 1 μg/mL AgNPs, 10 μg/mL AgNPs).

2.7.4. Systems biology analysis

The relation between the identified proteins was evaluated using the software Ingenuity Pathways Analysis (IPA) (Ingenuity Systems®, Redwood City, CA, USA). A pair-wise analysis of deregulated protein was performed throughout the experiment. This pair-wise comparison of proteins-features is a representation of data where the individual values contained in the table were represented as colours. The range was set from −0.58 to 0.58 (Base 2 logarithm = 0.58), where < −0.58 was set to green, 0 to black and > 0.58 to red. The values in between are shown as colour gradients. The significantly different features are the ones that are lower than −0.58 and higher than 0.58. Identified proteins were analysed using Ingenuity Pathways Analysis (IPA) (Ingenuity Systems®, Redwood City, CA, USA). Identified proteins were mapped onto Ingenuity's Knowledge Database to generate networks on the base of their algorithmic connectivity. Canonical pathway analysis identified the most significant ones from the IPA library, based on the number of molecules from the data set that map the pathway. Functional analysis of networks revealed the biological functions most significant to the molecules in the network ($p < 0.05$, right-tailed Fisher's exact test).

2.8. Other techniques used

For complementary techniques (immunocytochemistry analysis, cytokines and apoptosis array membrane) refer to Supplementary methods.

3. Results

3.1. Physico-chemical characterisation of AgNPs

In controlling the colloidal stability of the AgNPs, citrate was used as a capping agent. The main physicochemical properties of the NPs used in this work are summarised in Table 1Sa. The behaviour of citrate-stabilized AgNPs in complete culture medium was monitored by DLS analysis for up to 72 h of incubation at 37 °C. The NPs remained well dispersed with no aggregation.

Initial preliminary experiments were performed to confirm the suitability of regenerated cellulose filters for quantifying ionic silver release. To this end, different aqueous Ag^+ solutions in the range 5–1000 μg/L were submitted to ultrafiltration and recoveries were calculated. The values ranged from 92.4–98.4%, thus confirming negligible Ag^+ adsorption to the ultrafiltration units and therefore the suitability of the chosen regenerated cellulose material for ionic release quantification (data not shown).

The amount of dissolved ionic silver was measured through ICP-MS in complete cell culture medium, and it was found < 0.01% and 0.075% for AgNPs 1 and 10 μg/mL respectively at the highest time point of 72 h (Table 1Sb).

3.2. Cell viability

The cytotoxic effect of AgNPs and $AgNO_3$ on Caco-2 cells was quantified with the analysis of DAPI-stained nuclei using the IN Cell Analyzer. Cell viability was calculated by determining the number of nuclei in the exposure conditions compared to the number of nuclei in negative control wells. The analysis showed that at 24 h exposure,

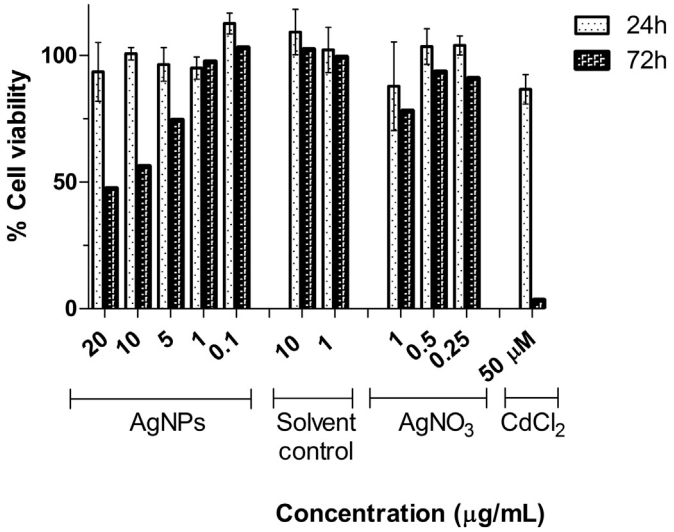

Fig. 2. Cell viability of CaCo-2, assessed by PI/Hoechst staining using IN Cell Analyzer 2200 (GE Healthcare®). Cells were exposed to AgNPs (0.1, 1, 5, 10 and 20 μg/mL) for 24 and 72 *H. medium* control, solvent controls, $AgNO_3$ (1, 0.5 and 0.25 μg/mL) and a positive control for toxicity (50 μM $CdCl_2$) were used. Data are expressed as the mean ± standard deviation, and three independent experiments were performed in triplicates.

AgNPs for all concentrations that tested up to 20 μg/mL did not induce a significant reduction in cell number compared to the negative control (Fig. 2). However, after 72 h exposure, the cell numbers were significantly reduced for concentrations above 1 μg/mL with a calculated IC_{50} of 15.4 μg/mL. At lower concentrations of AgNPs, no significant differences in cell number were detected ($p > 0.05$).

Based on the dose-response toxicity results for Caco-2 cells exposed to 30 nm AgNPs, two concentrations were selected for the proteomic analysis: 1 and 10 μg/mL, corresponding to a low and high toxic concentration at 72 h exposure.

Citrate used to stabilise the NPs was also tested at the same concentrations selected for the study (1 or 10 μg/mL) as solvent control, and no effects on cell viability were observed. $AgNO_3$ was used as a control for silver ions release. The data shows no effects due to Ag ions for concentrations of $AgNO_3$ below 0.5 μg/mL. These controls indicate that the toxicity observed for AgNPs is caused by the NPs and not by impurities derived from the synthesis process or by silver ion leaching.

3.3. AgNPs internalization

The amount of AgNPs bound to the cells and internalised have been quantified through ICP-MS. Data shows that at the highest concentration and exposure time, only approximately 1% of the initial amount of AgNPs exposed to the cells is internalised or bound to the external cell membrane (Fig. 1S).

3.4. Investigation of the differentially expressed proteins using the 2D gel-based method

We assessed the differences between the cytoplasmic proteome of Caco-2 cells exposed to 30 nm AgNPs (1 or 10 μg/mL) at two-time points (24 or 72 h), on the untreated cells.

As preliminary work, we assessed if there were any differences in the proteome profile of the untreated cells compared to cells exposed to the solvent of the NPs at the same doses intended to use in the study (1 or 10 μg/mL). The results showed that there were very few significant differences: two proteins in the case of Control vs. solvent of 1 μg/mL AgNPs and three proteins in the case of control vs. solvent of 10 μg/mL AgNPs-treated cells. Therefore, untreated cells were considered as the

Table 1
List of deregulated proteins identified in individual 2D gel spots of Caco-2 cytoplasmic extracts. Proteins have been classified according to their main function, based on UniProtKB/Swiss-Prot and Gene Ontology (GO). 24 h and 72 h data are presented.

	Accession Number	Protein code	Ag1 vs C 24h		Ag10 vs C 24h		Ag1 vs Ag10 24h		Ag1 vs C 72h		Ag10 vs C 72h		Ag1 vs Ag10 72h	
			p value	Fc	*p* value	Fc	*p* value	Fc	p value	Fc	p value	Fc	p value	Fc
Metabolism														
Amino Acids														
Aspartate aminotransferase OS=Homo sapiens GN=GOT2 PE=3 SV=1 - [A0A024R6W0_HUMAN]	A0A024R6W0	GOT2	0.037	3.742										
Glutamate dehydrogenase OS=Homo sapiens PE=2 SV=1 - [B4DMF5_HUMAN]	B4DMF5								0.006	6.826				
Adenosylhomocysteinase	Q1RMG2	AHCY					0.017	4.588						
Methylcrotonoyl-CoA carboxylase beta chain, mitochondrial OS=Homo sapiens GN=MCCC2 PE=1 SV=1 - [MCCB_HUMAN]	Q9HCC0	MCCC2									0.009	-21.346		
Serine hydroxymethyltransferase (Fragment) OS=Homo sapiens GN=SHMT2 PE=2 SV=1 - [Q5BJF5_HUMAN]	Q5BJF5	SHMT2							0.030	-3.226				
Pyrroline-5-carboxylate reductase OS=Homo sapiens PE=2 SV=1 - [E7D7X9_HUMAN]	E7D7X9				0.007	22.732								
Lipid and sterol														
Isoform 2 of Enoyl-CoA delta isomerase 1, mitochondrial OS=Homo sapiens GN=ECI1 - [ECI1_HUMAN]	P42126-2	ECI1							0.006	-13.945				
Isoform 3 of Prostaglandin E synthase 3 OS=Homo sapiens GN=PTGES3 - [TEBP_HUMAN]	Q15185-3	PTGES3									0.002	-9.645		
cDNA FLJ54509, highly similar to Trifunctional enzyme subunit alpha, mitochondrial OS=Homo sapiens PE=2 SV=1 - [B4DRH6_HUMAN]	B4DRH6		0.027	2.446	0.028	2.252								
Phosphoinositide phospholipase C (Fragment) OS=Homo sapiens GN=DKFZp434N101 PE=2 SV=1 - [Q9UFY1_HUMAN]	Q9UFY1	DKFZp434N101	0.044	3.375	0.015	3.104								
Purine biosynthesis														
Carboxilic acid														
Carbohydrate														
UDP-glucose 6-dehydrogenase OS=Homo sapiens GN=UGDH PE=1 SV=1 - [UGDH_HUMAN]	O60701	UGDH							0.008	8.854	0.006	17.405		
L-lactate dehydrogenase B chain OS=Homo sapiens GN=LDHB PE=1 SV=2 - [LDHB_HUMAN]	P07195	LDHB			0.014	-2.738								
Energy														
Glycolysis														
Pyruvate kinase OS=Homo sapiens GN=PKM2 PE=2 SV=1 - [Q504U3_HUMAN]	Q504U3	PKM2							0.044	-12.458				
Pyruvate kinase PKM OS=Homo sapiens GN=PKM PE=1 SV=4 - [KPYM_HUMAN]	P14618	PKM							0.022	6.000	0.007	5.134		
Glyceraldehyde-3-phosphate dehydrogenase OS=Homo sapiens GN=GAPDH PE=1 SV=3 - [G3P_HUMAN]	P04406	GAPDH	0.016	-6.738	0.012	-16.250	0.010	-16.918			0.033	4.434	0.023	5.329
Alpha-enolase OS=Homo sapiens GN=ENO1 PE=1 SV=2 - [ENOA_HUMAN]	P06733	ENO1	0.014	11.466	0.014	-13.504	0.020	-16.807						
Pyruvate														
Acetyltransferase component of pyruvate dehydrogenase complex OS=Homo sapiens PE=2 SV=1 - [B4DJX1_HUMAN]	B4DJX1				0.009	2.299	0.007	2.289			0.011	3.003		
Gluconeogenesis														
Aldehyde dehydrogenase, mitochondrial OS=Homo sapiens GN=ALDH2 PE=1 SV=2 - [ALDH2_HUMAN]	P05091	ALDH2	0.013	3.044										
Penthose phosphate pathway														
TCA pathway														
Isocitrate dehydrogenase 1 (Fragment) OS=Homo sapiens GN=IDH1 PE=2 SV=1 - [Q0QER2_HUMAN]	Q0QER2	IDH1							0.010	-2.395				
Isoform Cytoplasmic of Fumarate hydratase, mitochondrial OS=Homo sapiens GN=FH - [FUMH_HUMAN]	P07954-2	FH	0.027	2.773										
Malate dehydrogenase, cytoplasmic OS=Homo sapiens GN=MDH1 PE=1 SV=4 - [MDHC_HUMAN]	P40925	MDH1							0.020	-2.476				
Aconitate hydratase, mitochondrial OS=Homo sapiens PE=2 SV=1 - [B4DZ08_HUMAN]	B4DZ08				0.034	3.118								
Citrate synthase OS=Homo sapiens GN=CS PE=1 SV=1 - [A0A0C4DGI3_HUMAN]	A0A0C4DGI3	CS							0.029	5.386				
Respiration														
E-transport														
ATP synthase subunit alpha, mitochondrial OS=Homo sapiens GN=ATP5A1 PE=1 SV=1 - [ATPA_HUMAN]	P25705	ATP5A1	0.025	72.591	0.008	17.436								
Electron transfer flavoprotein subunit alpha, mitochondrial (Fragment) OS=Homo sapiens GN=ETFA PE=1 SV=1 - [H0YLU7_HUMAN]	H0YLU7	ETFA					0.042	96.434						
Transcription														
RNA transport														
Insulin-like growth factor 2 mRNA-binding protein 1 OS=Homo sapiens GN=IGF2BP1 PE=1 SV=2 - [IF2B1_HUMAN]	Q9NZI8	IGF2BP1											0.027	-6.485
Transcription regulation														
cDNA, FLJ93125, highly similar to Homo sapiens cleavage and polyadenylation specific factor 5, 25 kDa(CPSF5), mRNA OS=Homo sapiens PE=2 SV=1 - [B2R6U8_HUMAN]	B2R6U8		0.013	5.135										
Isoform 2 of Transcription intermediary factor 1-beta OS=Homo sapiens GN=TRIM28 - [TIF1B_HUMAN]	Q13263-2	TRIM28									0.005	4.967	0.043	5.261
Transcription termination factor 2 OS=Homo sapiens GN=TTF2 PE=1 SV=2 - [TTF2_HUMAN]	Q9UNY4	TTF2					0.035	-10.618						
Putative uncharacterized protein DKFZp686P17171 OS=Homo sapiens GN=DKFZp686P17171 PE=2 SV=1 - [Q63HR1_HUMAN	Q63HR1	DKFZp686P17171									0.041	-10.057		
Ribosomal proteins														
RNA binding														
Isoform 4 of Heterogeneous nuclear ribonucleoprotein Q OS=Homo sapiens GN=SYNCRIP - [HNRPQ_HUMAN]	O60506-4	SYNCRIP							0.011	-20.666			0.008	9.290
cDNA FLJ54552, highly similar to Heterogeneous nuclear ribonucleoprotein K OS=Homo sapiens PE=2 SV=1 - [B4DUQ1_HUMAN]	B4DUQ1		0.046	2.268										
Ribonuclease H2 subunit A OS=Homo sapiens GN=RNASEH2A PE=1 SV=2 - [RNH2A_HUMAN]	O75792	RNASEH2A			0.039	2.679							0.043	47.477
Far upstream element-binding protein 2 OS=Homo sapiens GN=KHSRP PE=1 SV=1 - [A0A087WTP3_HUMAN]	A0A087WTP3	KHSRP					0.034	3.947						
DNA binding														
AT-rich interactive domain-containing protein 4A (Fragment) OS=Homo sapiens GN=ARID4A PE=1 SV=1 - [H7C485_HUMAN]	H7C485	ARID4A							0.024	-5.566				
cDNA FLJ52237, highly similar to Creatine kinase B-type (EC 2.7.3.2) OS=Homo sapiens PE=2 SV=1 - [B4DP56_HUMAN]	B4DP56										0.045	29.266	0.042	20.872

(*continued on next page*)

Table 1 (*continued*)

	Accession Number	Protein code	Ag1 vs C 24h		Ag10 vs C 24h		Ag1 vs Ag10 24h		Ag1 vs C 72h		Ag10 vs C 72h		Ag1 vs Ag10 72h	
			p value	Fc	*p* value	Fc	*p* value	Fc	p value	Fc	p value	Fc	p value	Fc
Protein														
Folding and stability														
Peptidyl-prolyl cis-trans isomerase OS=Homo sapiens PE=2 SV=1 - [Q71V99_HUMAN]	Q71V99		0.007	17.929										
T-complex protein 1 subunit delta OS=Homo sapiens PE=2 SV=1 - [B7Z9L0_HUMAN]	B7Z9L0										0.015	2.693		
T-complex protein 1 subunit delta OS=Homo sapiens PE=2 SV=1 - [B7Z2F4_HUMAN]	B7Z2F4		0.048	16.058	0.018	16.273								
Isoform 3 of Protein disulfide-isomerase A6 OS=Homo sapiens GN=PDIA6 - [PDIA6_HUMAN]	Q15084-3	PDIA6											0.042	3.805
Proteolysis														
cDNA FLJ77744, highly similar to Homo sapiens kallikrein B, plasma (Fletcher factor) 1 (KLKB1), mRNA OS=Homo sapiens PE=2 SV=1 - [A8K9A9_HUMAN]	A8K9A9												0.005	-3.636
26S protease regulatory subunit 6A OS=Homo sapiens GN=PSMC3 PE=1 SV=1 - [E9PM69_HUMAN]	E9PM69	PSMC3											0.007	-7.904
Protein modification														
Isoform 2 of Protein Dok-7 OS=Homo sapiens GN=DOK7 - [DOK7_HUMAN]	Q18PE1-2	DOK7	0.008	-13.123										
Protein synthesis														
Elongation factor 2 OS=Homo sapiens GN=EEF2 PE=1 SV=4 - [EF2_HUMAN]	P13639	EEF2							0.010	-3.527	0.038	5.473	0.007	20.931
Eukaryotic elongation factor 2 kinase OS=Homo sapiens GN=EEF2K PE=1 SV=2 - [EF2K_HUMAN]	Q504U3	PKM2							0.044	-12.458				
Elongation factor Tu, mitochondrial OS=Homo sapiens GN=TUFM PE=1 SV=2 - [EFTU_HUMAN]	P49411	TUFM											0.006	7.613
Inorganic pyrophosphatase OS=Homo sapiens GN=PPA1 PE=1 SV=2 - [IPYR_HUMAN]	Q15181	PPA1									0.041	-3.395		
cDNA FLJ52573, highly similar to Elongation factor 1-alpha 1 OS=Homo sapiens PE=2 SV=1 - [B4DNE0_HUMAN]	B4DNE0				0.004	2.957								
Mitochondrial elongation factor G OS=Homo sapiens PE=3 SV=1 - [E5KND7_HUMAN]	E5KND7												0.010	-16.918
Protein transport														
Isoform 3 of Syndetin OS=Homo sapiens GN=VPS50 - [VPS50_HUMAN]	Q96JG6-3	VPS50											0.047	11.511
Charged multivesicular body protein 4b OS=Homo sapiens GN=CHMP4B PE=1 SV=1 - [CHM4B_HUMAN]	Q9H444	CHMP4B									0.055	-2.470	0.047	-2.601
Cell morphology and transport														
Cytoskeleton														
cDNA FLJ58286, highly similar to Actin, cytoplasmic 2 OS=Homo sapiens PE=2 SV=1 - [B4DVQ0_HUMAN]	B4DVQ0		0.025	8.376										
KRT8 protein OS=Homo sapiens PE=2 SV=1 - [Q7L4M3_HUMAN]	Q7L4M3				0.047	-8.006								
KRT18 protein (Fragment) OS=Homo sapiens GN=KRT18 PE=2 SV=1 - [I6L965_HUMAN]	I6L965	KRT18											0.024	4.258
Peptidyl-prolyl cis-trans isomerase FKBP4 OS=Homo sapiens GN=FKBP4 PE=1 SV=3 - [FKBP4_HUMAN]	Q02790	FKBP4							0.028	-2.595				
Cofilin 1 (Non-muscle), isoform CRA_a OS=Homo sapiens GN=CFL1 PE=1 SV=1 - [G3V1A4_HUMAN]	G3V1A4	CFL1					0.026	-33.979						
DNA FLJ55253, highly similar to Actin, cytoplasmic 1 OS=Homo sapiens PE=2 SV=1 - [B4DW52_HUMAN]	B4DW52										0.000	9.105	0.000	7.164
cDNA FLJ11352 fis, clone HEMBA1000220, highly similar to Tubulin beta-2C chain OS=Homo sapiens PE=2 SV=1 - [B3KML9_HUMAN]	B3KML9												0.036	3.309
Glial fibrillary acidic protein (Fragment) OS=Homo sapiens GN=GFAP PE=1 SV=1 - [K7EJU1_HUMAN]	K7EJU1	GFAP											0.047	-4.259
T-complex protein 1 subunit alpha OS=Homo sapiens GN=TCP1 PE=1 SV=1 - [TCPA_HUMAN]	P17987	TCP1							0.048	-2.315				
T-complex protein 1 subunit theta OS=Homo sapiens GN=CCT8 PE=1 SV=4 - [TCPQ_HUMAN]	P50990	CCT8											0.020	2.340
cDNA FLJ32131 fis, clone PEBLM2000267, highly similar to Tubulin alpha-ubiquitous chain OS=Homo sapiens PE=2 SV=1 - [B3KPS3_HUMAN]	B3KPS3												0.027	3.347
cDNA FLJ52068, highly similar to Microtubule-associated protein RP/EB family member 1 OS=Homo sapiens PE=2 SV=1 - [B4DM33_HUMAN]	B4DM33												0.043	47.477
cDNA FLJ53327, highly similar to Gelsolin OS=Homo sapiens PE=2 SV=1 - [B7Z2X4_HUMAN]	B7Z2X4								0.060	-5.611				
Actin-related protein 2/3 complex subunit 5 OS=Homo sapiens GN=ARPC5 PE=1 SV=3 - [ARPC5_HUMAN]	O15511	ARPC5									0.012	-6.389		
cDNA FLJ54184, highly similar to Tropomyosin alpha-4 chain OS=Homo sapiens PE=2 SV=1 - [B4DVY2_HUMAN]	B4DVY2										0.011	-4.678		
Isoform 3 of Intraflagellar transport protein 88 homolog OS=Homo sapiens GN=IFT88 - [IFT88_HUMAN]	Q13099-3	IFT88							0.044	3.484				
Tubulin beta-4B chain OS=Homo sapiens GN=TUBB4B PE=1 SV=1 - [TBB4B_HUMAN]	P68371	TUBB4B							0.019	13.544	0.004	33.080		
Cell adhesion														
Isoform 1 of Vinculin OS=Homo sapiens GN=VCL - [VINC_HUMAN]	P18206-2	VCL			0.014	-3.971								
Veside mediated transport														
Isoform 4 of Perilipin-3 OS=Homo sapiens GN=PLIN3 - [PLIN3_HUMAN]	O60664-4	PLIN3			0.007	-76.711	0.023	-64.189					0.040	-102.332
Isoform 2 of Protein SEC13 homolog OS=Homo sapiens GN=SEC13 - [SEC13_HUMAN]	P55735-2	SEC13											0.027	4.496
AP-1 complex subunit gamma-1 (Fragment) OS=Homo sapiens GN=AP1G1 PE=1 SV=1 - [H3BR36_HUMAN]	H3BR36	AP1G1							0.018	-6.258				
Cell-Cell junction														
Cell cycle and proliferation														
Isoform 2 of Annexin A11 OS=Homo sapiens GN=ANXA11 - [ANX11_HUMAN]	P50995-2	ANXA11							0.019	-2.871				
Isoform 5 of Protein phosphatase 1 regulatory subunit 12A OS=Homo sapiens GN=PPP1R12A - [MYPT1_HUMAN]	O14974-5	PPP1R12A			0.048	-11.963								
Nuclear migration protein nudC OS=Homo sapiens GN=NUDC PE=1 SV=1 - [NUDC_HUMAN]	Q9Y266	NUDC									0.035	-2.978	0.007	-7.756

(*continued on next page*)

Table 1 (*continued*)

	Accession Number	Protein code	Ag1 vs C 24h		Ag10 vs C 24h		Ag1 vs Ag10 24h		Ag1 vs C 72h		Ag10 vs C 72h		Ag1 vs Ag10 72h	
			p value	Fc	*p* value	Fc	*p* value	Fc	p value	Fc	p value	Fc	p value	Fc
Stress response														
Isoform Beta of Heat shock protein 105 kDa OS=Homo sapiens GN=HSPH1 - [HS105_HUMAN]	Q92598-2	HSPH1			0.036	3.133								
Mitochondrial heat shock 60kD protein 1 variant 1 OS=Homo sapiens GN=HSPD1 PE=2 SV=1 - [B3GQS7_HUMAN]	B3GQS7	HSPD1											0.016	-4.869
Protein disulfide-isomerase OS=Homo sapiens GN=P4HB PE=1 SV=3 - [PDIA1_HUMAN]	P07237	P4HB	0.005	-4.363										
cDNA FLJ54328, highly similar to Heat shock 70 kDa protein 1 OS=Homo sapiens PE=2 SV=1 - [B4DI39_HUMAN]	B4DI39				0.083	-2.278								
cDNA FLJ54407, highly similar to Heat shock 70 kDa protein 1 OS=Homo sapiens PE=2 SV=1 - [B4E388_HUMAN]	B4E388		0.016	-9.057					0.022	13.704	0.039	9.938		
Serpin H1 OS=Homo sapiens GN=SERPINH1 PE=1 SV=2 - [SERPH_HUMAN]	P50454	SERPINH1									0.047	-30.304	0.007	-25.182
cDNA FLJ54023, highly similar to Heat shock protein HSP 90-beta OS=Homo sapiens PE=2 SV=1 - [B4DMA2_HUMAN]	Q2VPJ6	HSP90AA1									0.010	5.499		
Hypoxia up-regulated protein 1 OS=Homo sapiens GN=HYOU1 PE=1 SV=1 - [A0A087X054_HUMAN]	A0A087X054	HYOU1							0.039	10.906				
cDNA FLJ54023, highly similar to Heat shock protein HSP 90-beta OS=Homo sapiens PE=2 SV=1 - [B4DMA2_HUMAN]	B4DMA2				0.027	10.978					0.010	5.499		
3-mercaptopyruvate sulfurtransferase OS=Homo sapiens GN=MPST PE=1 SV=3 - [THTM_HUMAN]	P25325	MPST							0.025	-12.585				
Glutathione synthetase OS=Homo sapiens GN=GSS PE=1 SV=1 - [GSHB_HUMAN]	P48637	GSS											0.042	20.872
Peroxiredoxin-1 (Fragment) OS=Homo sapiens GN=PRDX1 PE=1 SV=1 - [A0A0A0MSI0_HUMAN]	A0A0A0MSI0	PRDX1							0.011	-3.264			0.014	4.250
Glutaredoxin-3 OS=Homo sapiens GN=GLRX3 PE=1 SV=2 - [GLRX3_HUMAN]	O76003	GLRX3									0.032	12.195	0.036	64.563
cDNA FLJ50510, highly similar to Heat shock 70 kDa protein 4 OS=Homo sapiens PE=2 SV=1 - [B4DH02_HUMAN]	B4DH02												0.016	-4.990
Heat shock 70 kDa protein 1A OS=Homo sapiens GN=HSPA1A PE=1 SV=1 - [HS71A_HUMAN]	P0DMV8	HSPA1A			0.007	2.039							0.002	2.590
cDNA FLJ54912, highly similar to 60 kDa heat shock protein, mitochondrial OS=Homo sapiens PE=2 SV=1 - [B7Z4F6_HUMAN]	B7Z4F6				0.045	2.652							0.017	-2.229
superoxide metabolism														
Isoform 2 of SH3 and PX domain-containing protein 2A OS=Homo sapiens GN=SH3PXD2A - [SPD2A_HUMAN]	Q5TCZ1-2	SH3PXD2A											0.035	7.036
Cytokines production														
Isoform 3 of Nuclear factor of activated T-cells, cytoplasmic 2 OS=Homo sapiens GN=NFATC2 - [NFAC2_HUMAN]	Q13469-3	NFATC2	0.165	12.048										
Apoptosis														
Isoform 3 of Apoptosis-inducing factor 1, mitochondrial OS=Homo sapiens GN=AIFM1 - [AIFM1_HUMAN]	O95831-3	AIFM1			0.104	2.238			0.045	-4.772			0.020	8.221
Proteasome subunit alpha type-5 OS=Homo sapiens GN=PSMA5 PE=1 SV=3 - [PSA5_HUMAN]	P28066	PSMA5			0.010	-2.033								
Guanine nucleotide-binding protein subunit beta-2-like 1 OS=Homo sapiens GN=GNB2L1 PE=1 SV=3 - [GBLP_HUMAN]	P63244	GNB2L1					0.022	6.205						
Voltage-dependent anion-selective channel protein 1 OS=Homo sapiens GN=VDAC1 PE=1 SV=2 - [VDAC1_HUMAN]	P21796	VDAC1							0.046	6.945				
Annexin A5 OS=Homo sapiens GN=ANXA5 PE=1 SV=2 - [ANXA5_HUMAN]	P08758	ANXA5									0.004289915	-5.957	0.013	-5.715
Proteasome subunit alpha type-5 OS=Homo sapiens GN=PSMA5 PE=1 SV=3 - [PSA5_HUMAN]	P28066	PSMA5											0.023	-21.221
78 kDa glucose-regulated protein OS=Homo sapiens GN=HSPA5 PE=1 SV=2 - [GRP78_HUMAN]	P11021	HSPA5									0.014792316	-48.694	0.015	-37.999
Cell death														
Heme-binding protein 2 OS=Homo sapiens GN=HEBP2 PE=1 SV=1 - [HEBP2_HUMAN]	Q9Y5Z4	HEBP2			0.013	-16.076	0.007	-13.588						
Others														
calcium binding														
Annexin A2 OS=Homo sapiens GN=ANXA2 PE=1 SV=2 - [ANXA2_HUMAN]	P07355	ANXA2	0.008	-8.475										
cDNA FLJ90381 fis, clone NT2RP2005035, highly similar to Calumenin OS=Homo sapiens PE=2 SV=1 - [B3KQF5_HUMAN]	B3KQF5										0.01899192	-52.456	0.015	-48.004
Reticulocalbin-1 OS=Homo sapiens GN=RCN1 PE=1 SV=1 - [RCN1_HUMAN]	Q15293	RCN1									0.011442502	-2.019		
CALM3 protein OS=Homo sapiens PE=1 SV=1 - [Q9BRL5_HUMAN]	Q9BRL5												0.001	-7.660
inflammatory response														
Leukotriene A-4 hydrolase OS=Homo sapiens GN=LTA4H PE=1 SV=2 - [LKHA4_HUMAN]	P09960	LTA4H	0.049	-3.971			0.016	3.338						
Cellular component														
Disintegrin and metalloproteinase domain-containing protein 28 (Fragment) OS=Homo sapiens GN=ADAM28 PE=1 SV=1 - [H0YBQ8_HUMAN]	H0YBQ8	ADAM28							0.025	-4.996				
NUMA1 protein OS=Homo sapiens PE=2 SV=1 - [Q7Z757_HUMAN]	Q7Z757								0.012	-3.840				
cDNA FLJ77988 OS=Homo sapiens PE=2 SV=1 - [A8K5X8_HUMAN]	A8K5X8		0.021	13.073										
Transgelin-2 (Fragment) OS=Homo sapiens GN=TAGLN2 PE=1 SV=1 - [X6RJP6_HUMAN]	X6RJP6	TAGLN2	0.015	-6.379	0.009	-9.730								
Protein PRRC1 OS=Homo sapiens GN=PRRC1 PE=1 SV=1 - [PRRC1_HUMAN]	Q96M27	PRRC1					0.026	4.967						
Kanadaptin OS=Homo sapiens GN=SLC4A1AP PE=1 SV=1 - [A0A087X0M4_HUMAN]	A0A087X0M4	SLC4A1AP											0.0157108	-32.037
Prohibitin variant (Fragment) OS=Homo sapiens PE=2 SV=1 - [Q53FV0_HUMAN]	Q53FV0										0.043671127	-2.629		
SPRY domain-containing protein 4 OS=Homo sapiens GN=SPRYD4 PE=1 SV=2 - [SPRY4_HUMAN]	Q8WW59	SPRYD4							0.088	-3.149				
ST13 protein (Fragment) OS=Homo sapiens GN=ST13 PE=2 SV=1 - [Q0IJ56_HUMAN]	Q0IJ56	ST13											0.0753278	-5.072
cDNA, FLJ94417, highly similar to Homo sapiens WD repeat domain 57 (U5 snRNP specific) (WDR57), mRNA OS=Homo sapiens PE=2 SV=1 - [B2R9I9_HUMAN]	B2R9I9								0.015	-4.721				
Serine/threonine-protein kinase D3 (Fragment) OS=Homo sapiens GN=PRKD3 PE=1 SV=6 - [H7C172_HUMAN]	H7C172	PRKD3							0.024	-11.310				
Isoform 2 of DENN domain-containing protein 2C OS=Homo sapiens GN=DENND2C - [DEN2C_HUMAN]	Q68D51-2	DENND2C							0.023	-64.731				
Plasma kallikrein (Fragment) OS=Homo sapiens GN=KLKB1 PE=1 SV=1 - [H0YAC1_HUMAN]	H0YAC1	KLKB1											0.0319136	-16.271
cDNA FLJ56274, highly similar to Transketolase (EC 2.2.1.1) OS=Homo sapiens PE=2 SV=1 - [B4E022_HUMAN]	B4E022												0.0080662	-37.458
Docking protein 4 (Fragment) OS=Homo sapiens GN=DOK4 PE=4 SV=1 - [H3BVB4_HUMAN]	H3BVB4	DOK4									0.020341132	-4.085204375	0.0158593	-4.197

Table 2
List of deregulated proteins identified by the label-free nano UHPLC-Orbitrap MS/MS analysis of Caco-2 cytoplasmic extracts. Proteins have been classified according to their main function, based on UniProtKB/Swiss-Prot and Gene Ontology (GO). a) 24 h and b) 72 h experiment.

(a)

Description	Accession Number	Anova (p)	Ag1 vs C	Ag10 vs C	Ag1 vs Ag10	Peptide count	Confidence score
Metabolism							
Amino Acids							
D-amino-acid oxidase OS=Homo sapiens GN=DAO PE=1 SV=3 - [OXDA_HUMAN]	Q99062	0.00013			-2.49556	2	3.35997
Dihydropyrimidine dehydrogenase [NADP(+)] OS=Homo sapiens GN=DPYD PE=1 SV=2 - [DPYD_HUMAN]	Q9HC77	0.00088		2.45006		2	3.31567
Sugars and polysaccharides							
Polypeptide N-acetylgalactosaminyltransferase 10 OS=Homo sapiens GN=GALNT10 PE=1 SV=2 - [GLT10_HUMAN]	A6NCL7	0.00582			-2.63257	2	2.41047
Polypeptide N-acetylgalactosaminyltransferase 9 OS=Homo sapiens GN=GALNT9 PE=2 SV=3 - [GALT9_HUMAN]	A8K2U0;F8WDL3	0.01815		2.93223		3	4.61742
Alpha-1,3-mannosyl-glycoprotein 4-beta-N-acetylglucosaminyltransferase B OS=Homo sapiens GN=MGAT4B PE=1 SV=1 - [MGT4B_HUMAN]	O00370	0.00406			-2.27995	2	3.33770
Fucose-1-phosphate guanylyltransferase OS=Homo sapiens GN=FPGT PE=1 SV=2 - [FPGT_HUMAN]	P30041	0.02394	-2.32552			3	4.61782
Lipid and sterol							
Acyl-coenzyme A synthetase ACSM1, mitochondrial OS=Homo sapiens GN=ACSM1 PE=1 SV=1 - [ACSM1_HUMAN]	A4UGR9	0.00582		2.35584		2	2.30820
Long-chain-fatty-acid--CoA ligase ACSBG2 OS=Homo sapiens GN=ACSBG2 PE=1 SV=2 - [ACBG2_HUMAN]	O15226	0.02160			-2.54738	2	2.81827
Malonyl-CoA decarboxylase, mitochondrial OS=Homo sapiens GN=MLYCD PE=1 SV=3 - [DCMC_HUMAN]	P26358	0.03282		2.41296		2	3.30347
Sialidase-1 OS=Homo sapiens GN=NEU1 PE=1 SV=1 - [NEUR1_HUMAN]	Q14865	0.00923		-2.44966		2	3.07293
Serine incorporator 1 OS=Homo sapiens GN=SERINC1 PE=1 SV=1 - [SERC1_HUMAN]	Q8N3R9	0.00014		2.15121		2	2.73937
Other							
NAD(P)H-hydrate epimerase OS=Homo sapiens GN=APOA1BP PE=1 SV=2 - [NNRE_HUMAN]	P21860	0.01198	-2.31300			2	4.44309
Energy							
Glycolysis							
Glyceraldehyde-3-phosphate dehydrogenase OS=Homo sapiens GN=GAPDH PE=1 SV=3 - [G3P_HUMAN]	Q6BAA4-4	0.04965	-2.29394			7	40.98491
Gluconeogenesis							
Penthose phosphate pathway							
TCA pathway							
Respiration							
Ubiquinol-cytochrome-c reductase complex assembly factor 2 OS=Homo sapiens GN=UQCC2 PE=1 SV=1 - [UQCC2_HUMAN]	Q13616	0.02051			-2.37539	2	2.82323
E-transport							
ATP synthase subunit alpha, mitochondrial OS=Homo sapiens GN=ATP5A1 PE=1 SV=1 - [ATPA_HUMAN]	P40937	0.04369			-2.34775	8	21.20712
Cell growth / division							
Meiosis							
Ankyrin repeat, SAM and basic leucine zipper domain-containing protein 1 OS=Homo sapiens GN=ASZ1 PE=2 SV=1 - [ASZ1_HUMAN]	P13942	0.03432			-2.32981	2	2.90225
DNA synthesis /replication							
DNA polymerase nu OS=Homo sapiens GN=POLN PE=1 SV=2 - [DPOLN_HUMAN]	A6NCI4	0.01467		2.43701		2	3.15201
LINE-1 retrotransposable element ORF2 protein OS=Homo sapiens PE=1 SV=1 - [LORF2_HUMAN]	P38159	0.00090			-2.42229	3	4.25731
DNA polymerase subunit gamma-1 OS=Homo sapiens GN=POLG PE=1 SV=1 - [DPOG1_HUMAN]	Q5FVE4	0.00105			-2.89946	3	4.40526
Replication factor C subunit 5 OS=Homo sapiens GN=RFC5 PE=1 SV=1 - [RFC5_HUMAN]	Q9HCQ5	0.00006		2.53856		2	3.21655
DNA replication licensing factor MCM4 OS=Homo sapiens GN=MCM4 PE=1 SV=5 - [MCM4_HUMAN]	Q9UQ53	0.00035			-2.70142	2	3.99255
Recombination / repair							
DNA repair protein RAD50 OS=Homo sapiens GN=RAD50 PE=1 SV=1 - [RAD50_HUMAN]	B4DQ52	0.00994	2.93103			2	3.50885
Endonuclease 8-like 3 OS=Homo sapiens GN=NEIL3 PE=1 SV=3 - [NEIL3_HUMAN]	P83110	0.03680			-2.53299	2	3.15105
Cell cycle							
Centromere protein J OS=Homo sapiens GN=CENPJ PE=1 SV=2 - [CENPJ_HUMAN]	O15018	0.02280	-2.24054			3	6.78401
Rootletin OS=Homo sapiens GN=CROCC PE=1 SV=1 - [CROCC_HUMAN]	P07355	0.03954		2.36497		3	8.09869
Hemicentin-1 OS=Homo sapiens GN=HMCN1 PE=1 SV=2 - [HMCN1_HUMAN]	Q8NEA0	0.04529			-2.31489	2	3.33964
Cytokinesis							
Protein asunder homolog OS=Homo sapiens GN=ASUN PE=1 SV=2 - [ASUN_HUMAN]	Q13029	0.00064			-2.32101	2	2.56925
Growth regulators							
Transforming growth factor beta receptor type 3 OS=Homo sapiens GN=TGFBR3 PE=1 SV=3 - [TGBR3_HUMAN]	A5D8V7	0.04894			-2.38154	2	3.61514
Growth hormone variant OS=Homo sapiens GN=GH2 PE=1 SV=3 - [SOM2_HUMAN]	P01024	0.04443		-2.30755		2	3.24594
Epidermal growth factor receptor substrate 15-like 1 OS=Homo sapiens GN=EPS15L1 PE=1 SV=1 - [EP15R_HUMAN]	P30101	0.00670			-2.33929	2	2.42459
Other							
Paraneoplastic antigen Ma3 OS=Homo sapiens GN=PNMA3 PE=2 SV=2 - [PNMA3_HUMAN]	Q93034	0.01915			-2.48895	2	4.60896
DNA (cytosine-5)-methyltransferase 1 OS=Homo sapiens GN=DNMT1 PE=1 SV=2 - [DNMT1_HUMAN]	Q96JN2	0.02372			-2.47027	2	3.27609
Centrosomal protein of 152 kDa OS=Homo sapiens GN=CEP152 PE=1 SV=4 - [CE152_HUMAN]	Q9H579-2	0.00112			-2.45894	2	3.62924

(*continued on next page*)

Table 2 (*continued*)

(a) continue

Description	Accession Number	Anova (p)	Ag1 vs C	Ag10 vs C	Ag1 vs Ag10	Peptide count	Confidence score
Transcription							
rRNA synthesis							
Treacle protein OS=Homo sapiens GN=TCOF1 PE=1 SV=3 - [TCOF_HUMAN]	O00148	0.00685			-2.85401	3	5.62121
Pescadillo homolog OS=Homo sapiens GN=PES1 PE=1 SV=1 - [PESC_HUMAN]	Q7Z745	0.00024			-2.44386	2	2.48494
tRNA synthesis							
Mediator of RNA polymerase II transcription subunit 17 OS=Homo sapiens GN=MED17 PE=1 SV=2 - [MED17_HUMAN]	A2RUS2	0.02219			-2.56532	3	6.07272
mRNA synthesis							
RNA-binding motif protein, X chromosome OS=Homo sapiens GN=RBMX PE=1 SV=3 - [RBMX_HUMAN]	O15083	0.00522			-2.38921	3	4.29116
Prohibitin-2 OS=Homo sapiens GN=PHB2 PE=1 SV=2 - [PHB2_HUMAN]	O75116	0.02182			2.38622	6	17.38419
RNA polymerase II elongation factor ELL2 OS=Homo sapiens GN=ELL2 PE=1 SV=2 - [ELL2_HUMAN]	P35498	0.02545			-2.28394	3	5.75095
General TFs							
Specific TFs							
Max-like protein X OS=Homo sapiens GN=MLX PE=1 SV=2 - [MLX_HUMAN]	P34931	0.00000			-2.64354	2	3.54598
Dachshund homolog 2 OS=Homo sapiens GN=DACH2 PE=2 SV=1 - [DACH2_HUMAN]	P48995	0.02606			-2.38492	2	3.92321
Tumor protein 63 OS=Homo sapiens GN=TP63 PE=1 SV=1 - [P63_HUMAN]	Q13129	0.04369		2.29451		2	3.86574
Transcription factor E2F7 OS=Homo sapiens GN=E2F7 PE=1 SV=3 - [E2F7_HUMAN]	Q5VWQ0	0.03804			2.46362	2	4.12722
AF4/FMR2 family member 1 OS=Homo sapiens GN=AFF1 PE=1 SV=1 - [AFF1_HUMAN]	Q6ZWH5	0.01130			-2.80431	3	4.61582
Prospero homeobox protein 1 OS=Homo sapiens GN=PROX1 PE=1 SV=2 - [PROX1_HUMAN]	Q9UFD9	0.01392			-2.38061	2	4.48365
Chromatin							
Putative Polycomb group protein ASXL3 OS=Homo sapiens GN=ASXL3 PE=2 SV=3 - [ASXL3_HUMAN]	E9PJ16	0.00838			-2.93317	4	7.09230
Histone-lysine N-methyltransferase NSD3 OS=Homo sapiens GN=WHSC1L1 PE=1 SV=1 - [NSD3_HUMAN]	O00541	0.01916		3.30190		4	5.99754
Methylcytosine dioxygenase TET3 OS=Homo sapiens GN=TET3 PE=1 SV=3 - [TET3_HUMAN]	O15164	0.02208		-2.54505		2	2.49076
Protein Jumonji OS=Homo sapiens GN=JARID2 PE=1 SV=2 - [JARD2_HUMAN]	O43166	0.02599	2.78575			2	3.79340
Nipped-B-like protein OS=Homo sapiens GN=NIPBL PE=1 SV=2 - [NIPBL_HUMAN]	O75581	0.00222			-2.43497	3	4.69683
Helicase SRCAP OS=Homo sapiens GN=SRCAP PE=1 SV=3 - [SRCAP_HUMAN]	Q5XXA6	0.02740	-2.26202			2	4.38184
Tudor domain-containing protein 3 OS=Homo sapiens GN=TDRD3 PE=1 SV=1 - [TDRD3_HUMAN]	Q6ZUU3	0.00015			-2.50123	2	3.29468
Trinucleotide repeat-containing gene 18 protein OS=Homo sapiens GN=TNRC18 PE=1 SV=3 - [TNC18_HUMAN]	Q8IXI1;Q9Y3L5	0.01313			-2.50921	4	6.34712
Histone-lysine N-methyltransferase 2A OS=Homo sapiens GN=KMT2A PE=1 SV=5 - [KMT2A_HUMAN]	Q96AQ1	0.00331			-2.71504	6	9.49496
Hepatoma-derived growth factor-related protein 2 OS=Homo sapiens GN=HDGFRP2 PE=1 SV=1 - [HDGR2_HUMAN]	Q96AV8	0.01419			-2.35099	2	2.88397
Chromodomain-helicase-DNA-binding protein 2 OS=Homo sapiens GN=CHD2 PE=1 SV=2 - [CHD2_HUMAN]	Q9H252	0.01968			-2.72227	2	2.44186
Cohesin subunit SA-1 OS=Homo sapiens GN=STAG1 PE=1 SV=3 - [STAG1_HUMAN]	Q9UH92	0.00381			-2.60045	2	3.61684
mRNA processing							
Iron-responsive element-binding protein 2 OS=Homo sapiens GN=IREB2 PE=1 SV=3 - [IREB2_HUMAN]	O14978	0.02148			2.61441	4	5.58109
ATP-dependent RNA helicase DDX39A OS=Homo sapiens GN=DDX39A PE=1 SV=2 - [DX39A_HUMAN]	Q03701	0.04140	-2.19845			2	2.96731
Peptidylprolyl isomerase domain and WD repeat-containing protein 1 OS=Homo sapiens GN=PPWD1 PE=1 SV=1 - [PPWD1_HUMAN]	Q13367	0.00203		2.88570		2	3.53191
RNA-binding protein 25 OS=Homo sapiens GN=RBM25 PE=1 SV=3 - [RBM25_HUMAN]	Q14055	0.00005		2.44842		2	2.37275
Serine/arginine repetitive matrix protein 1 OS=Homo sapiens GN=SRRM1 PE=1 SV=2 - [SRRM1_HUMAN]	Q15878	0.00499			-2.52474	2	3.03465
Probable ATP-dependent RNA helicase DDX23 OS=Homo sapiens GN=DDX23 PE=1 SV=3 - [DDX23_HUMAN]	Q2TB10	0.04089			-2.20592	2	2.40416
Eukaryotic translation initiation factor 4 gamma 3 OS=Homo sapiens GN=EIF4G3 PE=1 SV=2 - [IF4G3_HUMAN]	Q68CJ6	0.01465	-2.29174			2	3.02692
Serine/arginine-rich splicing factor 1 OS=Homo sapiens GN=SRSF1 PE=1 SV=2 - [SRSF1_HUMAN]	Q8NBV4	0.00462			-2.81446	2	2.82459
G patch domain and KOW motifs-containing protein OS=Homo sapiens GN=GPKOW PE=1 SV=2 - [GPKOW_HUMAN]	Q8NFS9	0.00889			-2.45521	2	3.68633
Probable ATP-dependent RNA helicase YTHDC2 OS=Homo sapiens GN=YTHDC2 PE=1 SV=2 - [YTDC2_HUMAN]	Q9H6U6	0.04008			-2.22185	3	5.26442
ATP-dependent RNA helicase DHX29 OS=Homo sapiens GN=DHX29 PE=1 SV=2 - [DHX29_HUMAN]	Q9NQG6	0.03275			2.41454	3	4.98648
Serine/arginine-rich splicing factor 4 OS=Homo sapiens GN=SRSF4 PE=1 SV=2 - [SRSF4_HUMAN]	Q9Y6N3	0.00511		-2.37703		2	3.40955
RNA transport							
Insulin-like growth factor 2 mRNA-binding protein 1 OS=Homo sapiens GN=IGF2BP1 PE=1 SV=2 - [IF2B1_HUMAN]	Q96T58	0.01757			-2.39719	4	5.86446
Regulation							
AT-rich interactive domain-containing protein 5B OS=Homo sapiens GN=ARID5B PE=1 SV=3 - [ARI5B_HUMAN]	Q13325	0.04515	-2.22317			2	3.03138
Zinc finger protein 318 OS=Homo sapiens GN=ZNF318 PE=1 SV=2 - [ZN318_HUMAN]	Q13474	0.00140		-2.72242		5	8.21042
Forkhead box protein Q1 OS=Homo sapiens GN=FOXQ1 PE=2 SV=2 - [FOXQ1_HUMAN]	Q13936	0.00170			-2.46775	2	3.30467
Zinc finger protein 407 OS=Homo sapiens GN=ZNF407 PE=1 SV=2 - [ZN407_HUMAN]	Q16099	0.00813			-2.48973	4	5.90753
Zinc finger protein 692 OS=Homo sapiens GN=ZNF692 PE=1 SV=1 - [ZN692_HUMAN]	A6NM28	0.03066		-2.86850		2	2.88780
Zinc finger and BTB domain-containing protein 12 OS=Homo sapiens GN=ZBTB12 PE=1 SV=1 - [ZBT12_HUMAN]	A8K8P3	0.01339			-2.31631	3	6.05587
RE1-silencing transcription factor OS=Homo sapiens GN=REST PE=1 SV=3 - [REST_HUMAN]	Q5VUA4	0.01027		2.34238		2	2.61182
Class E basic helix-loop-helix protein 40 OS=Homo sapiens GN=BHLHE40 PE=1 SV=1 - [BHE40_HUMAN]	Q6ZRK6	0.00046			-2.46578	2	2.73358
Msx2-interacting protein OS=Homo sapiens GN=SPEN PE=1 SV=1 - [MINT_HUMAN]	Q6ZRS2	0.01434		2.60802		5	7.09579
Putative Polycomb group protein ASXL2 OS=Homo sapiens GN=ASXL2 PE=1 SV=1 - [ASXL2_HUMAN]	Q8IY34	0.04533			-2.97962	3	5.13868
Zinc finger protein 263 OS=Homo sapiens GN=ZNF263 PE=1 SV=2 - [ZN263_HUMAN]	Q8IY63	0.01542		2.52394		2	2.34939
NF-kappa-B-repressing factor OS=Homo sapiens GN=NKRF PE=1 SV=2 - [NKRF_HUMAN]	Q8IYB3	0.01149		2.93477		2	2.38026
Transcription intermediary factor 1-alpha OS=Homo sapiens GN=TRIM24 PE=1 SV=3 - [TIF1A_HUMAN]	Q8N7U6	0.03272		2.73983		3	4.67399
Zinc finger protein 92 homolog OS=Homo sapiens GN=ZFP92 PE=2 SV=3 - [ZFP92_HUMAN]	Q92786	0.04793	-2.19560			2	3.92927
Zinc finger and SCAN domain-containing protein 1 OS=Homo sapiens GN=ZSCAN1 PE=1 SV=2 - [ZSCA1_HUMAN]	Q92917	0.02572		2.47131		2	3.90502
Retinoic acid-induced protein 1 OS=Homo sapiens GN=RAI1 PE=1 SV=2 - [RAI1_HUMAN]	Q96T17	0.04308			-2.20801	2	3.39680
Protein capicua homolog OS=Homo sapiens GN=CIC PE=1 SV=1 - [I3L2J0_HUMAN]	Q99623	0.00126			-2.01408	3	4.02281
Bromodomain and WD repeat-containing protein 1 OS=Homo sapiens GN=BRWD1 PE=1 SV=4 - [BRWD1_HUMAN]	Q9BUQ8	0.01220	-2.30232			2	3.71030
PAX-interacting protein 1 OS=Homo sapiens GN=PAXIP1 PE=1 SV=2 - [PAXI1_HUMAN]	Q9C009	0.01044			-2.40621	2	2.83687
Zinc finger protein 800 OS=Homo sapiens GN=ZNF800 PE=1 SV=1 - [ZN800_HUMAN]	Q9H270	0.00906			-2.64707	5	7.66673
PR domain-containing protein 11 (Fragment) OS=Homo sapiens GN=PRDM11 PE=1 SV=1 - [H3BSZ2_HUMAN]	Q9H3D4	0.00908			-2.46290	2	4.06476
CCAAT/enhancer-binding protein zeta OS=Homo sapiens GN=CEBPZ PE=1 SV=3 - [CEBPZ_HUMAN]	Q9H6S0	0.04175			-2.37302	5	8.21778
Zinc finger protein RlF OS=Homo sapiens GN=RLF PE=1 SV=2 - [RLF_HUMAN]	Q9HD20	0.00491			-2.27252	2	3.45209
Probable JmjC domain-containing histone demethylation protein 2C OS=Homo sapiens GN=JMJD1C PE=1 SV=2 - [JHD2C_HUMAN]	Q9NRL3;H0YIY1	0.00923		2.09583		5	6.68819
RING finger protein 207 OS=Homo sapiens GN=RNF207 PE=2 SV=2 - [RN207_HUMAN]	Q9NZM3	0.00355			-2.86070	2	3.84226
PR domain zinc finger protein 2 OS=Homo sapiens GN=PRDM2 PE=1 SV=3 - [PRDM2_HUMAN]	O14772	0.00339			-2.75207	3	5.72624
Cyclin-L1 OS=Homo sapiens GN=CCNL1 PE=1 SV=1 - [CCNL1_HUMAN]	Q9Y2D4	0.00126			-2.57191	2	4.45213

(*continued on next page*)

Table 2 (*continued*)

(a) continue

Description	Accession Number	Anova (p)	Ag1 vs C	Ag10 vs C	Ag1 vs Ag10	Peptide count	Confidence score
Protein Synthesis							
Ribosomal proteins							
ATP-binding cassette sub-family F member 1 OS=Homo sapiens GN=ABCF1 PE=1 SV=2 - [ABCF1_HUMAN]	C9JQI7	0.03370		2.34203		2	3.64116
Other							
Probable threonine--tRNA ligase 2, cytoplasmic OS=Homo sapiens GN=TARSL2 PE=1 SV=1 - [SYTC2_HUMAN]	Q9Y4D1	0.00520			-2.33285	3	3.80631
Protein destination and storage							
Folding and stability							
Heat shock 70 kDa protein 1A OS=Homo sapiens GN=HSPA1A PE=1 SV=1 - [HS71A_HUMAN]	A0FGR8	0.04891	-2.20270			3	10.76717
Heat shock 70 kDa protein 1-like OS=Homo sapiens GN=HSPA1L PE=1 SV=2 - [HS71L_HUMAN]	A2RTX5	0.04978	-2.19593			5	13.02335
DnaJ homolog subfamily A member 4 OS=Homo sapiens GN=DNAJA4 PE=1 SV=1 - [DNJA4_HUMAN]	Q3SXZ7	0.03865			-2.35478	2	3.51728
UDP-glucose:glycoprotein glucosyltransferase 1 OS=Homo sapiens GN=UGGT1 PE=1 SV=3 - [UGGG1_HUMAN]	Q96QF0	0.01225			-2.34499	2	1.89421
Thioredoxin-like protein 1 (Fragment) OS=Homo sapiens GN=TXNL1 PE=1 SV=1 - [K7EML9_HUMAN]	Q9P219;Q9H0W7	0.02528	2.59347			2	3.20519
Targeting							
Exocyst complex component 6B OS=Homo sapiens GN=EXOC6B PE=1 SV=3 - [EXC6B_HUMAN]	O75369	0.01067		2.50587		2	3.75363
Rab-3A-interacting protein OS=Homo sapiens GN=RAB3IP PE=1 SV=1 - [RAB3I_HUMAN]	Q3SXM0	0.00778			-2.27797	3	5.95337
Mitochondrial dynamics protein MID51 OS=Homo sapiens GN=MIEF1 PE=1 SV=1 - [MID51_HUMAN]	Q96DT5	0.01913			-2.32693	2	2.95212
Metallophosphoesterase 1 OS=Homo sapiens GN=MPPE1 PE=1 SV=2 - [MPPE1_HUMAN]	Q96HI0	0.03179			-2.48313	2	4.12560
Modification							
Mannosyl-oligosaccharide 1,2-alpha-mannosidase IA OS=Homo sapiens GN=MAN1A1 PE=1 SV=3 - [MA1A1_HUMAN]	P0C671	0.00324			-2.42678	2	3.12672
N-acetyllactosaminide beta-1,6-N-acetylglucosaminyl-transferase, isoform C OS=Homo sapiens GN=GCNT2 PE=2 SV=2 - [GNT2C_HUMAN]	Q13034	0.00139		-2.50919		2	3.14393
Protein Daple OS=Homo sapiens GN=CCDC88C PE=1 SV=3 - [DAPLE_HUMAN]	Q8NE71	0.00011			-2.48801	4	5.71397
Glycosyltransferase-like protein LARGE1 OS=Homo sapiens GN=LARGE PE=1 SV=1 - [LARGE_HUMAN]	Q9H4G4	0.03913			-2.55932	2	3.55526
Ubiquitin-associated protein 1-like OS=Homo sapiens GN=UBAP1L PE=2 SV=1 - [UBA1L_HUMAN]	Q9UHR4	0.03083	2.46176			2	2.43940
E3 ubiquitin-protein ligase DTX3L OS=Homo sapiens GN=DTX3L PE=1 SV=1 - [DTX3L_HUMAN]	Q9UK58	0.04944	-2.20598			3	4.79957
Proteolysis							
ATP-dependent Clp protease ATP-binding subunit clpX-like, mitochondrial OS=Homo sapiens GN=CLPX PE=1 SV=2 - [CLPX_HUMAN]	O75718	0.00005			-2.75373	2	3.73987
Sentrin-specific protease 1 OS=Homo sapiens GN=SENP1 PE=1 SV=2 - [SENP1_HUMAN]	Q6KC79;O15247	0.00130		2.43397		2	2.70462
Ankyrin repeat and SOCS box protein 15 OS=Homo sapiens GN=ASB15 PE=2 SV=3 - [ASB15_HUMAN]	Q6NY19	0.00010		2.64768		2	4.75995
Alpha-2-macroglobulin-like protein 1 OS=Homo sapiens GN=A2ML1 PE=1 SV=3 - [A2ML1_HUMAN]	Q6ZWJ8	0.04990			-2.20151	2	2.76684
Cullin-5 OS=Homo sapiens GN=CUL5 PE=1 SV=4 - [CUL5_HUMAN]	Q7Z5Q5	0.00002		2.40044		2	3.00721
Cullin-1 OS=Homo sapiens GN=CUL1 PE=1 SV=2 - [CUL1_HUMAN]	Q86YZ3	0.00159			-2.81229	2	4.83614
Sentrin-specific protease 5 OS=Homo sapiens GN=SENP5 PE=1 SV=3 - [SENP5_HUMAN]	Q92878	0.00010			-2.51049	2	3.43679
Serine protease HTRA3 OS=Homo sapiens GN=HTRA3 PE=1 SV=2 - [HTRA3_HUMAN]	Q99959	0.03342		2.45044		2	2.35946
Transporters							
Ions							
Voltage-dependent L-type calcium channel subunit alpha-1C OS=Homo sapiens GN=CACNA1C PE=1 SV=4 - [CAC1C_HUMAN]	P01242	0.00166			-2.81879	3	4.44110
Voltage-dependent R-type calcium channel subunit alpha-1E OS=Homo sapiens GN=CACNA1E PE=1 SV=3 - [CAC1E_HUMAN]	P48729-3	0.00123			-2.52479	2	3.13602
Calcium-activated chloride channel regulator family member 3 OS=Homo sapiens GN=CLCA3P PE=1 SV=1 - [CLCA3_HUMAN]	P49796	0.01294			-2.36683	2	3.79602
Glutamate receptor ionotropic, kainate 4 OS=Homo sapiens GN=GRIK4 PE=2 SV=2 - [GRIK4_HUMAN]	Q0VDD8;Q9UFE4	0.01781			-2.18503	2	2.99293
Potassium voltage-gated channel subfamily H member 6 OS=Homo sapiens GN=KCNH6 PE=1 SV=1 - [KCNH6_HUMAN]	Q86SR1	0.00003			-2.54454	2	3.29565
Sodium channel protein type 1 subunit alpha OS=Homo sapiens GN=SCN1A PE=1 SV=2 - [SCN1A_HUMAN]	Q8NEP3	0.04786		2.66401		3	4.77960
Short transient receptor potential channel 1 OS=Homo sapiens GN=TRPC1 PE=1 SV=1 - [TRPC1_HUMAN]	Q8TDB6	0.04883	-2.18750			2	3.67644
Anoctamin-1 OS=Homo sapiens GN=ANO1 PE=1 SV=1 - [ANO1_HUMAN]	Q8WWH4	0.00232			-2.42109	2	2.95583
Solute carrier family 15 member 3 OS=Homo sapiens GN=SLC15A3 PE=2 SV=2 - [S15A3_HUMAN]	Q9NVM9	0.00883			-2.80951	2	2.47476
Sodium channel protein type 11 subunit alpha OS=Homo sapiens GN=SCN11A PE=1 SV=2 - [SCNBA_HUMAN]	Q9NZR2	0.00060			-2.47176	2	1.68033
Sugars							
Solute carrier family 2, facilitated glucose transporter member 14 OS=Homo sapiens GN=SLC2A14 PE=2 SV=1 - [GTR14_HUMAN]	Q7Z478	0.04387	2.42564			2	3.82114
Lipids							
Extended synaptotagmin-2 OS=Homo sapiens GN=ESYT2 PE=1 SV=1 - [ESYT2_HUMAN]	Q9UL41	0.03213			-2.53788	3	4.62919
Transport ATPases							
Manganese-transporting ATPase 13A1 OS=Homo sapiens GN=ATP13A1 PE=1 SV=2 - [AT131_HUMAN]	P48200	0.00076			-2.35075	3	8.62736
Other							
DENN domain-containing protein 3 OS=Homo sapiens GN=DENND3 PE=1 SV=2 - [DEND3_HUMAN]	Q8N841	0.00581			-2.26668	2	3.25645
Lysosomal-trafficking regulator OS=Homo sapiens GN=LYST PE=1 SV=3 - [LYST_HUMAN]	Q9H7E2	0.01773			-2.37406	3	4.43551
Intracellular traffic							
Endosome							
AP-3 complex subunit beta-2 OS=Homo sapiens GN=AP3B2 PE=1 SV=2 - [AP3B2_HUMAN]	P05787;L0R512	0.02716		2.56042		2	3.68614

(*continued on next page*)

Table 2 (*continued*)

(a) continue

Description	Accession Number	Anova (p)	Ag1 vs C	Ag10 vs C	Ag1 vs Ag10	Peptide count	Confidence score
Cell structure							
Cytoskeleton							
Collagen alpha-2(IX) chain OS=Homo sapiens GN=COL9A2 PE=1 SV=2 - [CO9A2_HUMAN]	A6NIX2	0.04546	-2.21351			2	3.94438
KN motif and ankyrin repeat domain-containing protein 3 OS=Homo sapiens GN=KANK3 PE=1 SV=1 - [KANK3_HUMAN]	A8TX70	0.03329		2.61796		3	5.48168
MAGUK p55 subfamily member 5 OS=Homo sapiens GN=MPP5 PE=1 SV=3 - [MPP5_HUMAN]	F5GYI3	0.04845			-2.23081	2	2.13294
Keratin, type II cytoskeletal 1b OS=Homo sapiens GN=KRT77 PE=2 SV=3 - [K2C1B_HUMAN]	O00472	0.00382		2.69538		3	5.14948
Dystrophin OS=Homo sapiens GN=DMD PE=1 SV=3 - [DMD_HUMAN]	P06241	0.02778			-2.35906	2	3.10943
Talin-2 OS=Homo sapiens GN=TLN2 PE=1 SV=4 - [TLN2_HUMAN]	P19013	0.01485			-2.38078	2	3.44798
Disheveled-associated activator of morphogenesis 1 OS=Homo sapiens GN=DAAM1 PE=1 SV=2 - [DAAM1_HUMAN]	P49802	0.02483			-2.23010	2	3.05422
ERC protein 2 OS=Homo sapiens GN=ERC2 PE=1 SV=3 - [ERC2_HUMAN]	P50454	0.01834			-2.48027	4	5.83825
Tubulin polyglutamylase TTLL6 OS=Homo sapiens GN=TTLL6 PE=1 SV=2 - [TTLL6_HUMAN]	P54098	0.01309			-2.61082	3	4.47843
Xin actin-binding repeat-containing protein 2 OS=Homo sapiens GN=XIRP2 PE=1 SV=2 - [XIRP2_HUMAN]	P60709	0.00800			-2.78743	6	9.49751
Disheveled-associated activator of morphogenesis 2 OS=Homo sapiens GN=DAAM2 PE=1 SV=3 - [DAAM2_HUMAN]	Q08AH1	0.00000		5.06117		2	4.15765
Actin, cytoplasmic 1 OS=Homo sapiens GN=ACTB PE=1 SV=1 - [ACTB_HUMAN]	Q09MP3	0.04962		2.78993		2	6.27124
Keratin, type I cuticular Ha5 OS=Homo sapiens GN=KRT35 PE=2 SV=5 - [KRT35_HUMAN]	Q12955	0.01900			-2.42948	3	5.38338
Filamin-B OS=Homo sapiens GN=FLNB PE=1 SV=2 - [FLNB_HUMAN]	Q14093	0.00732			-2.36994	3	5.07697
Dynamin-1 OS=Homo sapiens GN=DNM1 PE=1 SV=2 - [DYN1_HUMAN]	Q14249	0.00117		2.91701		4	6.88843
IQ motif and SEC7 domain-containing protein 1 OS=Homo sapiens GN=IQSEC1 PE=1 SV=1 - [IQEC1_HUMAN]	Q5T764	0.03335		2.50303		2	3.04020
Keratin, type II cytoskeletal 4 OS=Homo sapiens GN=KRT4 PE=1 SV=4 - [K2C4_HUMAN]	Q6DN90	0.01336			-2.31886	3	3.51542
Dynein heavy chain 14, axonemal OS=Homo sapiens GN=DNAH14 PE=2 SV=3 - [DYH14_HUMAN]	Q6ZW49	0.03906			-2.29016	6	9.29252
Actin, aortic smooth muscle OS=Homo sapiens GN=ACTA2 PE=1 SV=1 - [ACTA_HUMAN]	Q76G19	0.00226			-2.45667	5	14.46846
Ankyrin-3 OS=Homo sapiens GN=ANK3 PE=1 SV=3 - [ANK3_HUMAN]	Q7Z4V5	0.03251			-2.29172	2	2.99881
Dynein heavy chain 11, axonemal OS=Homo sapiens GN=DNAH11 PE=1 SV=4 - [DYH11_HUMAN]	Q7Z5J4	0.03532			-2.31809	3	4.64857
Regulator of microtubule dynamics protein 2 OS=Homo sapiens GN=RMDN2 PE=1 SV=2 - [RMD2_HUMAN]	Q8IYT3	0.01122	-2.38466			2	3.75986
Signal-induced proliferation-associated 1-like protein 1 OS=Homo sapiens GN=SIPA1L1 PE=1 SV=4 - [SI1L1_HUMAN]	Q8TAT5	0.00654			-2.38750	2	3.49832
Focal adhesion kinase 1 OS=Homo sapiens GN=PTK2 PE=1 SV=2 - [FAK1_HUMAN]	Q8TDY2	0.00277		2.57936		3	4.93705
Keratin, type II cytoskeletal 8 OS=Homo sapiens GN=KRT8 PE=1 SV=7 - [K2C8_HUMAN]	Q8WW22	0.01268			-2.55074	7	20.41354
Filamin-A-interacting protein 1 OS=Homo sapiens GN=FILIP1 PE=1 SV=1 - [FLIP1_HUMAN]	Q8WXK1	0.01588		2.48364		2	3.36857
Talin-1 OS=Homo sapiens GN=TLN1 PE=1 SV=3 - [TLN1_HUMAN]	Q92630	0.01724			-2.42096	2	2.43976
Brain-specific angiogenesis inhibitor 1-associated protein 2-like protein 1 OS=Homo sapiens GN=BAIAP2L1 PE=1 SV=2 - [BI2L1_HUMAN]	Q92833	0.00121			-2.53723	3	4.20520
Collagen alpha-5(VI) chain OS=Homo sapiens GN=COL6A5 PE=1 SV=1 - [CO6A5_HUMAN]	Q96N16	0.04765			-2.19173	4	5.81246
Collagen alpha-2(XI) chain OS=Homo sapiens GN=COL11A2 PE=1 SV=5 - [COBA2_HUMAN]	Q96SM3	0.01917			-2.33419	4	6.47921
FH2 domain-containing protein 1 OS=Homo sapiens GN=FHDC1 PE=1 SV=2 - [FHDC1_HUMAN]	Q9BRT2	0.01042			-2.38345	2	4.06934
Probable tubulin polyglutamylase TTLL9 OS=Homo sapiens GN=TTLL9 PE=2 SV=3 - [TTLL9_HUMAN]	Q9BZ95	0.00055			-2.62418	2	2.60414
Breast carcinoma-amplified sequence 3 OS=Homo sapiens GN=BCAS3 PE=1 SV=3 - [BCAS3_HUMAN]	Q9C0G0	0.01191			-2.41009	3	5.26351
MAP7 domain-containing protein 2 OS=Homo sapiens GN=MAP7D2 PE=1 SV=2 - [MA7D2_HUMAN]	Q9HB29	0.00579			-2.40755	3	5.36784
Janus kinase and microtubule-interacting protein 1 OS=Homo sapiens GN=JAKMIP1 PE=1 SV=1 - [JKIP1_HUMAN]	Q9P265	0.00676		2.05652		5	8.53623
Leiomodin-1 OS=Homo sapiens GN=LMOD1 PE=1 SV=3 - [LMOD1_HUMAN]	Q9UI33	0.04676		2.41247		2	2.95155
Nucleus							
Endocytosis							
Endosome							
Vacuolar protein sorting-associated protein 11 homolog OS=Homo sapiens GN=VPS11 PE=1 SV=1 - [VPS11_HUMAN]	Q13127	0.01400			2.86083	2	3.04452
Kinesin-like protein KIF16B OS=Homo sapiens GN=KIF16B PE=1 SV=2 - [KI16B_HUMAN]	Q8NFI3	0.00367			-2.43335	3	5.34676
Cell cycle							
Protein SFI1 homolog OS=Homo sapiens GN=SFI1 PE=1 SV=2 - [SFI1_HUMAN]	Q5TB30	0.00087			-2.67147	2	3.45664
Organelle transport							
Cell-Cell junction							
Cell proliferation							
Other							
Coiled-coil domain-containing protein 151 OS=Homo sapiens GN=CCDC151 PE=1 SV=1 - [CC151_HUMAN]	Q9ULL0	0.00165			-2.71169	4	8.39674
Signal transduction							
Receptors							
Granulocyte colony-stimulating factor receptor OS=Homo sapiens GN=CSF3R PE=1 SV=1 - [CSF3R_HUMAN]	E7EW31	0.02892			-2.29206	2	4.08372
Interleukin-1 receptor-like 2 OS=Homo sapiens GN=IL1RL2 PE=1 SV=2 - [IILRL2_HUMAN]	P52179	0.03612	2.90080			2	2.58005
Contactin-associated protein-like 2 OS=Homo sapiens GN=CNTNAP2 PE=1 SV=1 - [CNTP2_HUMAN]	Q8N9Z2	0.04990	2.90089			2	3.97375
Kinases							
Isoform 3 of Casein kinase I isoform alpha OS=Homo sapiens GN=CSNK1A1 - [KC1A_HUMAN]	O43432	0.01441	-2.27324			2	2.96572
Serine/threonine-protein kinase Nek10 OS=Homo sapiens GN=NEK10 PE=2 SV=3 - [NEK10_HUMAN]	Q15772	0.01445			-2.40803	2	2.57895
Dual specificity tyrosine-phosphorylation-regulated kinase 2 OS=Homo sapiens GN=DYRK2 PE=1 SV=3 - [DYRK2_HUMAN]	Q6ZRF8	0.04661			-2.36321	2	4.03283
Receptor tyrosine-protein kinase erbB-3 OS=Homo sapiens GN=ERBB3 PE=1 SV=1 - [ERBB3_HUMAN]	Q17RM4	0.00154		2.37087		2	3.06179
Striated muscle preferentially expressed protein kinase OS=Homo sapiens GN=SPEG PE=1 SV=4 - [SPEG_HUMAN]	Q68DQ2	0.03874			-2.28828	5	8.49920
Rho-associated protein kinase 2 OS=Homo sapiens GN=ROCK2 PE=1 SV=4 - [ROCK2_HUMAN]	Q8N123	0.04905			-2.46870	2	3.06404
Serine/threonine-protein kinase N2 OS=Homo sapiens GN=PKN2 PE=1 SV=1 - [PKN2_HUMAN]	Q8TDW7	0.04782			-2.24929	2	2.47704
Tyrosine-protein kinase Fyn OS=Homo sapiens GN=FYN PE=1 SV=3 - [FYN_HUMAN]	Q8WY22	0.03295			-2.45182	2	2.92408
Serine-protein kinase ATM OS=Homo sapiens GN=ATM PE=1 SV=4 - [ATM_HUMAN]	Q96LZ7	0.02177			-2.21418	3	5.69819
Phosphatases							
Probable lipid phosphate phosphatase PPAPDC3 OS=Homo sapiens GN=PPAPDC3 PE=2 SV=1 - [PPAC3_HUMAN]	P46093	0.02020		2.67587		2	2.85927
G proteins							
Regulator of G-protein signaling 3 OS=Homo sapiens GN=RGS3 PE=1 SV=2 - [RGS3_HUMAN]	Q53F39	0.03277	-2.40649			2	2.24651
G-protein coupled receptor 4 OS=Homo sapiens GN=GPR4 PE=2 SV=2 - [GPR4_HUMAN]	Q86XD8	0.00661			-2.97639	2	2.99308
PDZ domain-containing protein 2 OS=Homo sapiens GN=PDZD2 PE=1 SV=4 - [PDZD2_HUMAN]	Q8NB25	0.00157			-2.50602	3	4.81889
Regulator of G-protein signaling 7 OS=Homo sapiens GN=RGS7 PE=1 SV=3 - [RGS7_HUMAN]	Q8NDA2	0.02694			-2.21535	2	2.87577
BTB/POZ domain-containing protein KCTD16 OS=Homo sapiens GN=KCTD16 PE=2 SV=1 - [KCD16_HUMAN]	Q9NZI8	0.03573	-2.26013			2	3.49912
Other							
Cartilage-associated protein OS=Homo sapiens GN=CRTAP PE=1 SV=1 - [CRTAP_HUMAN]	A6NCM1	0.00177			-2.86289	2	2.68777
1-phosphatidylinositol 4,5-bisphosphate phosphodiesterase delta-1 OS=Homo sapiens GN=PLCD1 PE=1 SV=2 - [PLCD1_HUMAN]	A8MU93	0.01954			-2.98160	2	3.58925
DEP domain-containing protein 1A OS=Homo sapiens GN=DEPDC1 PE=1 SV=2 - [DEP1A_HUMAN]	O15013	0.04496	-2.20350			2	3.90607
Striatin-4 OS=Homo sapiens GN=STRN4 PE=1 SV=2 - [STRN4_HUMAN]	Q13315	0.03299	-2.29511			2	3.21902
Mitochondrial Rho GTPase 2 OS=Homo sapiens GN=RHOT2 PE=1 SV=2 - [MIRO2_HUMAN]	Q5T0N1	0.03641			-2.25045	2	3.81024
A-kinase anchor protein SPHKAP OS=Homo sapiens GN=SPHKAP PE=1 SV=1 - [SPKAP_HUMAN]	Q8N2E2	0.00021			-2.47859	3	4.88310
NADPH oxidase 1 OS=Homo sapiens GN=NOX1 PE=1 SV=2 - [NOX1_HUMAN]	Q8TDB8	0.01897			-2.91352	2	3.64382
Very large A-kinase anchor protein OS=Homo sapiens GN=CRYBG3 PE=1 SV=3 - [CRBG3_HUMAN]	Q9BZF9	0.00508			-2.39490	3	5.33229
Natural cytotoxicity triggering receptor 1 OS=Homo sapiens GN=NCR1 PE=1 SV=1 - [NCTR1_HUMAN]	Q9P0U3	0.01565			-2.47376	2	3.51368
Kielin/chordin-like protein OS=Homo sapiens GN=KCP PE=2 SV=2 - [KCP_HUMAN]	Q9Y5S8	0.02613	-2.49201			2	3.91916

(*continued on next page*)

Table 2 (*continued*)

(a) continue

Description	Accession Number	Anova (p)	Ag1 vs C	Ag10 vs C	Ag1 vs Ag10	Peptide count	Confidence score
Disease / defence							
Cell death							
Endonuclease G, mitochondrial OS=Homo sapiens GN=ENDOG PE=1 SV=4 - [NUCG_HUMAN]	O43151	0.00090			-2.39019	2	4.22420
Uveal autoantigen with coiled-coil domains and ankyrin repeats OS=Homo sapiens GN=UACA PE=1 SV=2 - [UACA_HUMAN]	P49756	0.01052			-2.26968	2	3.27282
Defence-related							
Interferon-induced protein with tetratricopeptide repeats 1B OS=Homo sapiens GN=IFIT1B PE=2 SV=1 - [IFT1B_HUMAN]	Q96N23	0.02223			-2.33925	3	4.85809
Interferon-induced protein with tetratricopeptide repeats 5 OS=Homo sapiens GN=IFIT5 PE=1 SV=1 - [IFIT5_HUMAN]	Q9NUD7	0.00731			-2.82881	2	3.18421
Stress response							
Peroxiredoxin-6 OS=Homo sapiens GN=PRDX6 PE=1 SV=3 - [PRDX6_HUMAN]	Q8NCW5	0.00306			-2.42278	4	8.43253
Other							
Isoform 4 of Fc receptor-like B OS=Homo sapiens GN=FCRLB - [FCRLB_HUMAN]	Q9Y490	0.02789			-2.81343	2	2.29661
Unclear classification							
Coiled-coil domain-containing protein 73 OS=Homo sapiens GN=CCDC73 PE=2 SV=2 - [CCD73_HUMAN]	O00533	0.00778			-2.74957	2	4.86648
Low-density lipoprotein receptor-related protein 1B OS=Homo sapiens GN=LRP1B PE=1 SV=2 - [LRP1B_HUMAN]	O14647	0.04071			-2.33849	3	5.43258
17 beta-hydroxysteroid dehydrogenase OS=Homo sapiens GN=17BHSDI PE=3 SV=1 - [Q13034_HUMAN]	O75955	0.00552		2.52003		2	3.25594
Dystrophin-related protein 2 OS=Homo sapiens GN=DRP2 PE=2 SV=2 - [DRP2_HUMAN]	O76031	0.00136		2.71389		2	2.69163
Low-density lipoprotein receptor-related protein 6 OS=Homo sapiens GN=LRP6 PE=1 SV=2 - [LRP6_HUMAN]	P11047	0.00850			-2.53454	2	3.66119
RB1-inducible coiled-coil protein 1 OS=Homo sapiens GN=RB1CC1 PE=1 SV=3 - [RBCC1_HUMAN]	P20594	0.04787	-2.20117			3	4.56900
Intersectin-2 OS=Homo sapiens GN=ITSN2 PE=1 SV=3 - [ITSN2_HUMAN]	P33908;Q6P1N9	0.00208			-2.57533	2	2.33191
Cytosolic endo-beta-N-acetylglucosaminidase OS=Homo sapiens GN=ENGASE PE=1 SV=1 - [ENASE_HUMAN]	P33991	0.04927	-2.19788			2	4.88180
Semaphorin-4F OS=Homo sapiens GN=SEMA4F PE=2 SV=2 - [SEM4F_HUMAN]	P51178	0.00009			3.26777	3	4.77767
Flotillin-1 OS=Homo sapiens GN=FLOT1 PE=1 SV=3 - [FLOT1_HUMAN]	P51825	0.01782			-2.46170	2	3.09900
Protein disulfide-isomerase A3 OS=Homo sapiens GN=PDIA3 PE=1 SV=4 - [PDIA3_HUMAN]	Q03164	0.03236		2.25422		6	14.55174
Cylicin-2 OS=Homo sapiens GN=CYLC2 PE=2 SV=1 - [CYLC2_HUMAN]	Q05397	0.02635			-2.23225	3	4.00290
TBC1 domain family member 10B OS=Homo sapiens GN=TBC1D10B PE=1 SV=3 - [TB10B_HUMAN]	Q05586	0.01197		2.69650		2	2.29240
Neural cell adhesion molecule L1-like protein OS=Homo sapiens GN=CHL1 PE=1 SV=4 - [NCHL1_HUMAN]	Q07955	0.02382			-2.99616	3	4.32921
Laminin subunit gamma-1 OS=Homo sapiens GN=LAMC1 PE=1 SV=3 - [LAMC1_HUMAN]	Q12882;Q8NGN8	0.04364			-2.15350	2	3.22330
Alsin OS=Homo sapiens GN=ALS2 PE=1 SV=2 - [ALS2_HUMAN]	Q14520	0.01539		-2.49310		2	2.23861
Glutamate receptor ionotropic, NMDA 1 OS=Homo sapiens GN=GRIN1 PE=1 SV=1 - [NMDZ1_HUMAN]	Q16513	0.02622		2.40546		2	3.70622
Nuclear GTPase SLIP-GC OS=Homo sapiens GN=NUGGC PE=2 SV=3 - [SLIP_HUMAN]	Q68DU8	0.04658	-2.22754			2	3.81828
Hyaluronan-binding protein 2 OS=Homo sapiens GN=HABP2 PE=1 SV=1 - [HABP2_HUMAN]	Q6IPM2	0.00056		2.59811		2	4.14606
Pleckstrin homology domain-containing family A member 7 OS=Homo sapiens GN=PLEKHA7 PE=1 SV=2 - [PKHA7_HUMAN]	Q6ZQQ6	0.01284			-2.30867	3	4.41091
Serpin H1 OS=Homo sapiens GN=SERPINH1 PE=1 SV=2 - [SERPH_HUMAN]	Q76L83	0.02142			-2.34270	9	22.79801
Chondroitin sulfate glucuronyltransferase OS=Homo sapiens GN=CHPF2 PE=2 SV=2 - [CHPF2_HUMAN]	Q86T65	0.00790			-2.69190	2	4.18128
Cilia- and flagella-associated protein 54 OS=Homo sapiens GN=CFAP54 PE=2 SV=3 - [CFA54_HUMAN]	Q8N8C3	0.03341		2.70867		4	5.89849
Hemicentin-2 OS=Homo sapiens GN=HMCN2 PE=2 SV=2 - [HMCN2_HUMAN]	Q8WVM7	0.04813			-2.49282	9	13.61151
Plakophilin-2 OS=Homo sapiens GN=PKP2 PE=1 SV=2 - [PKP2_HUMAN]	Q96Q42	0.01093			-2.30306	3	5.70954
Transmembrane protein 232 OS=Homo sapiens GN=TMEM232 PE=2 SV=2 - [TM232_HUMAN]	Q96RW7	0.02531			-2.36160	2	4.29479
Myomesin-1 OS=Homo sapiens GN=MYOM1 PE=1 SV=2 - [MYOM1_HUMAN]	Q99519	0.01106		2.40241		4	7.10053
Cilia- and flagella-associated protein 70 OS=Homo sapiens GN=CFAP70 PE=2 SV=3 - [CFA70_HUMAN]	Q99698	0.04240			-2.40895	4	6.27854
Round spermatid basic protein 1 OS=Homo sapiens GN=RSBN1 PE=1 SV=2 - [RSBN1_HUMAN]	Q9BU19	0.00005			-2.55795	2	2.87834
Golgi-associated plant pathogenesis-related protein 1 OS=Homo sapiens GN=GLIPR2 PE=1 SV=3 - [GAPR1_HUMAN]	Q9C0D6	0.03697		2.63154		2	2.59858
Annexin A2 OS=Homo sapiens GN=ANXA2 PE=1 SV=2 - [ANXA2_HUMAN]	Q9C0F0	0.00013			-2.73189	11	28.28074
Complement C3 OS=Homo sapiens GN=C3 PE=1 SV=2 - [CO3_HUMAN]	Q9NRX5	0.02192		2.61328		2	2.13876
Rho guanine nucleotide exchange factor 10 OS=Homo sapiens GN=ARHGEF10 PE=1 SV=4 - [ARHGA_HUMAN]	Q9NSI6	0.03837		2.44466		3	4.88130
Wilms tumor protein 1-interacting protein OS=Homo sapiens GN=WTIP PE=1 SV=3 - [WTIP_HUMAN]	Q9NYU2	0.03345			-2.78055	2	3.19162
Protocadherin Fat 3 OS=Homo sapiens GN=FAT3 PE=2 SV=2 - [FAT3_HUMAN]	Q9P2D6	0.01202	-2.28014			2	3.72581
Dynein assembly factor 1, axonemal OS=Homo sapiens GN=DNAAF1 PE=1 SV=5 - [DAAF1_HUMAN]	Q9P2E5	0.01986			2.99477	3	4.82100
Atrial natriuretic peptide receptor 2 OS=Homo sapiens GN=NPR2 PE=1 SV=1 - [ANPRB_HUMAN]	Q9UBC2	0.00347			-2.85674	2	2.89056
Unclasified							
von Willebrand factor D and EGF domain-containing protein OS=Homo sapiens GN=VWDE PE=2 SV=4 - [VWDE_HUMAN]	H3BSZ2	0.04100			-2.23206	2	2.18033
FOXL2 neighbor protein OS=Homo sapiens GN=FOXL2NB PE=2 SV=1 - [FOXNB_HUMAN]	F8WEY1	0.04827			-2.15730	2	2.77811
Maestro heat-like repeat-containing protein family member 2B OS=Homo sapiens GN=MROH2B PE=2 SV=3 - [MRO2B_HUMAN]	I3L2J0	0.03637			-2.03691	5	9.14316
Uncharacterized protein KIAA1107 OS=Homo sapiens GN=KIAA1107 PE=1 SV=2 - [K1107_HUMAN]	K7EML9	0.04749			-2.36538	2	3.62545
IQ domain-containing protein E OS=Homo sapiens GN=IQCE PE=1 SV=2 - [IQCE_HUMAN]	O14503	0.01747		2.51312		3	4.82031
Isoform 2 of Protein MROH8 OS=Homo sapiens GN=MROH8 - [MROH8_HUMAN]	O15417	0.02108		2.43741		3	4.72667
Coiled-coil domain-containing protein 142 OS=Homo sapiens GN=CCDC142 PE=2 SV=1 - [CC142_HUMAN]	O76036	0.04688			-2.52647	3	5.41430
Semenogelin-2 OS=Homo sapiens GN=SEMG2 PE=1 SV=1 - [SEMG2_HUMAN]	O94986	0.04124	-2.89476			2	3.53720
Protein FAM184A OS=Homo sapiens GN=FAM184A PE=2 SV=3 - [F184A_HUMAN]	O95461	0.04115	-2.61224			2	3.60002
Hornerin OS=Homo sapiens GN=HRNR PE=1 SV=2 - [HORN_HUMAN]	O95754	0.00549			-2.73674	2	3.08306
Uncharacterized protein KIAA1210 OS=Homo sapiens GN=KIAA1210 PE=2 SV=3 - [K1210_HUMAN]	O95822	0.00331			-2.08860	2	2.77701
IQ and AAA domain-containing protein 1-like OS=Homo sapiens GN=IQCA1L PE=3 SV=2 - [IQCAL_HUMAN]	P04406	0.01483			-2.26450	2	2.62556
Protein WWC2 OS=Homo sapiens GN=WWC2 PE=1 SV=2 - [WWC2_HUMAN]	P0DMV8	0.00000		13.84321		2	3.05959
PDZ domain-containing protein 4 OS=Homo sapiens GN=PDZD4 PE=1 SV=1 - [PDZD4_HUMAN]	P11532	0.00207			-2.55216	4	7.91782
FLJ44955 protein OS=Homo sapiens GN=FLJ44955 PE=2 SV=1 - [Q0VFX3_HUMAN]	P14920	0.03574		2.68278		2	3.28018
Uncharacterized protein C6orf222 OS=Homo sapiens GN=C6orf222 PE=1 SV=1 - [CF222_HUMAN]	P25705	0.00448			-2.34849	3	5.00742
Coiled-coil domain-containing protein 74A OS=Homo sapiens GN=CCDC74A PE=2 SV=1 - [CC74A_HUMAN]	P29536	0.04867	2.84386			2	2.42102
Ankyrin repeat domain-containing protein 33B OS=Homo sapiens GN=ANKRD33B PE=3 SV=1 - [AN33B_HUMAN]	P62736	0.01832		2.80325		2	3.93040
AN1-type zinc finger protein 4 OS=Homo sapiens GN=ZFAND4 PE=2 SV=2 - [ZFAN4_HUMAN]	Q02383	0.00154		2.97671		3	3.99111
Disco-interacting protein 2 homolog B OS=Homo sapiens GN=DIP2B PE=1 SV=3 - [DIP2B_HUMAN]	Q03167	0.00002		2.40044		2	3.89269
Uncharacterized protein C20orf96 OS=Homo sapiens GN=C20orf96 PE=2 SV=2 - [CT096_HUMAN]	Q05193	0.01092			-2.45066	2	3.41435
DDB1- and CUL4-associated factor 4-like protein 1 OS=Homo sapiens GN=DCAF4L1 PE=2 SV=1 - [DC4L1_HUMAN]	Q08170	0.04994			-2.20170	2	3.61347
Coiled-coil domain-containing protein 84 OS=Homo sapiens GN=CCDC84 PE=1 SV=1 - [E9PJ16_HUMAN]	Q0VFX3	0.00264			-2.86220	2	3.02196
cDNA FLJ58923 OS=Homo sapiens PE=2 SV=1 - [B4DQ52_HUMAN]	Q13428	0.00027			-2.47199	2	3.41989
Coiled-coil domain-containing protein 170 OS=Homo sapiens GN=CCDC170 PE=1 SV=3 - [CC170_HUMAN]	Q15652	0.04394		2.25213		2	2.56597
Protein FAM135A OS=Homo sapiens GN=FAM135A PE=1 SV=2 - [F135A_HUMAN]	Q2M3C7	0.02191			-2.60482	2	3.42314
WD repeat-containing protein 87 OS=Homo sapiens GN=WDR87 PE=1 SV=3 - [WDR87_HUMAN]	Q4KMP7	0.00741			-2.31220	5	7.41356
RIMS-binding protein 3A OS=Homo sapiens GN=RIMBP3 PE=1 SV=4 - [RIM3A_HUMAN]	Q5TZA2	0.00208			-2.38198	3	3.93504
von Willebrand factor A domain-containing protein 3A OS=Homo sapiens GN=VWA3A PE=2 SV=3 - [VWA3A_HUMAN]	Q6AWC2	0.00213			-2.85408	2	4.21103
Angiomotin-like protein 1 OS=Homo sapiens GN=AMOTL1 PE=1 SV=1 - [AMOL1_HUMAN]	Q6IQ23	0.01646			-2.25666	2	2.94944
Probable carboxypeptidase X1 OS=Homo sapiens GN=CPXM1 PE=2 SV=2 - [CPXM1_HUMAN]	Q7Z794	0.00038		-2.96885		2	3.39455
Uncharacterized protein C17orf100 OS=Homo sapiens GN=C17orf100 PE=2 SV=1 - [CQ100_HUMAN]	Q7Z7B0	0.02769	-2.57082			2	2.94914
Coiled-coil domain-containing protein 136 OS=Homo sapiens GN=CCDC136 PE=1 SV=3 - [CC136_HUMAN]	Q8NBB4	0.03187	-2.21683			2	2.80959
Proline-rich basic protein 1 OS=Homo sapiens GN=PROB1 PE=2 SV=2 - [PROB1_HUMAN]	Q92764	0.00874			-2.34252	3	4.80982
EF-hand domain-containing family member B OS=Homo sapiens GN=EFHB PE=2 SV=4 - [EFHB_HUMAN]	Q96BP3	0.00944			-2.32806	2	3.70613
BRI3-binding protein OS=Homo sapiens GN=BRI3BP PE=1 SV=1 - [BRI3B_HUMAN]	Q96L93	0.02563			-2.31336	2	3.07474
cDNA FLJ39672 fis, clone SMINT2009233 OS=Homo sapiens PE=2 SV=1 - [Q8N8C3_HUMAN]	Q96NX9	0.00505		2.42430		2	3.12145
HCG2019382 OS=Homo sapiens GN=MGC44328 PE=2 SV=1 - [Q8NEA0_HUMAN]	Q9NVC6	0.00000		2.45039		2	4.95528
5'-nucleotidase domain-containing protein 2 OS=Homo sapiens GN=NT5DC2 PE=4 SV=1 - [F8WEY1_HUMAN]	Q9UHC6	0.02261	-2.25086			2	2.23402
CPX chromosomal region candidate gene 1 protein OS=Homo sapiens GN=CPXCR1 PE=2 SV=2 - [CPXCR_HUMAN]	Q9UPP5	0.00025			-2.46802	2	3.13097
RAD51-associated protein 2 OS=Homo sapiens GN=RAD51AP2 PE=1 SV=1 - [R51A2_HUMAN]	Q9Y330	0.00008		-2.79116		3	5.53504
Coiled-coil domain-containing protein 71L OS=Homo sapiens GN=CCDC71L PE=2 SV=2 - [CC71L_HUMAN]	Q9Y4G6	0.00273		2.63076		2	2.04108

(*continued on next page*)

Table 2 (*continued*)

(b)

Description	Accession	Anova (p)	Ag1 vs C	Ag10 vs C	Ag1 vs Ag10	Peptide number	Confidence score
Metabolism							
Amino Acids							
Methionine synthase OS=Homo sapiens GN=MTR PE=1 SV=2 - [METH_HUMAN]	Q8N3C7	0.02626			2.45262	3	4.55757
Sugars and polysaccharides							
Lipid and sterol							
Cytochrome P450 2D6 OS=Homo sapiens GN=CYP2D6 PE=1 SV=2 - [CP2D6_HUMAN]	Q9H867	0.00305		-7.72521		2	3.35675
Other							
Energy							
Glycolysis							
Glycerol-3-phosphate dehydrogenase, mitochondrial OS=Homo sapiens GN=GPD2 PE=1 SV=3 - [GPDM_HUMAN]	Q1MSJ5	0.00936		-3.43154		3	3.80769
Gluconeogenesis							
Penthose phosphate pathway							
TCA pathway							
Respiration							
E-transport							
Cell growth / division							
Meiosis							
DNA synthesis /replication							
Nucleolar GTP-binding protein 1 OS=Homo sapiens GN=GTPBP4 PE=1 SV=3 - [NOG1_HUMAN]	Q04844	0.03381			6.22622	2	3.06145
Protein timeless homolog OS=Homo sapiens GN=TIMELESS PE=1 SV=2 - [TIM_HUMAN]	Q5FWE3	0.00000		-4.48210		2	2.02461
Recombination / repair							
DNA damage-binding protein 1 OS=Homo sapiens GN=DDB1 PE=1 SV=1 - [DDB1_HUMAN]	Q70CQ2	0.00531			3.65086	2	3.54617
Cell cycle							
Hemicentin-1 OS=Homo sapiens GN=HMCN1 PE=1 SV=2 - [HMCN1_HUMAN]	Q96JI7	0.02529			-2.42105	2	3.46974
Rootletin OS=Homo sapiens GN=CROCC PE=1 SV=1 - [CROCC_HUMAN]	Q96NS5	0.03643	2.36851			4	9.58848
Golgin subfamily A member 2 OS=Homo sapiens GN=GOLGA2 PE=1 SV=3 - [GOGA2_HUMAN]	Q96SB8	0.00795			9.44598	2	2.70282
Cyclin-F OS=Homo sapiens GN=CCNF PE=1 SV=2 - [CCNF_HUMAN]	Q9BZ95	0.00370			3.83669	2	3.40588
Cytokinesis							
Dedicator of cytokinesis protein 7 OS=Homo sapiens GN=DOCK7 PE=1 SV=4 - [DOCK7_HUMAN]	Q5S007	0.02800			2.31898	2	3.80531
Centrosome and spindle pole-associated protein 1 OS=Homo sapiens GN=CSPP1 PE=1 SV=4 - [CSPP1_HUMAN]	Q8IY84;Q09(	0.00486			2.15382	2	3.26154
Protein regulator of cytokinesis 1 OS=Homo sapiens GN=PRC1 PE=1 SV=2 - [PRC1_HUMAN]	Q92854	0.04458			3.48330	2	4.23651
Growth regulators							
Transforming growth factor beta receptor type 3 OS=Homo sapiens GN=TGFBR3 PE=1 SV=3 - [TGBR3_HUMAN]	P51795	0.04541			2.05372	2	3.26711
Other							
Centrosomal protein of 70 kDa OS=Homo sapiens GN=CEP70 PE=1 SV=2 - [CEP70_HUMAN]	A6NFN9	0.00207			3.13514	2	2.55840
Oral-facial-digital syndrome 1 protein OS=Homo sapiens GN=OFD1 PE=1 SV=1 - [OFD1_HUMAN]	O60449	0.00453			2.14306	2	4.74019
Transcription							
rRNA synthesis							
tRNA synthesis							
Mediator of RNA polymerase II transcription subunit 17 OS=Homo sapiens GN=MED17 PE=1 SV=2 - [MED17_HUMAN]	Q96NX9	0.00000			-2.70088	3	5.89224
mRNA synthesis							
DNA-directed RNA polymerase, mitochondrial OS=Homo sapiens GN=POLRMT PE=1 SV=2 - [RPOM_HUMAN]	Q32P51	0.02333			2.89537	2	2.96891
General TFs							
General transcription factor 3C polypeptide 1 OS=Homo sapiens GN=GTF3C1 PE=1 SV=4 - [TF3C1_HUMAN]	O76013	0.01261			2.55145	3	4.31069
Specific TFs							
Dachshund homolog 2 OS=Homo sapiens GN=DACH2 PE=2 SV=1 - [DACH2_HUMAN]	A6NDB9	0.00829		-2.40889		2	3.46345
Transcription elongation factor A protein-like 1 OS=Homo sapiens GN=TCEAL1 PE=1 SV=2 - [TCAL1_HUMAN]	V9HVX8	0.00543			4.32400	2	3.21461
Chromatin							
Teashirt homolog 3 OS=Homo sapiens GN=TSHZ3 PE=1 SV=2 - [TSH3_HUMAN]	O15083	0.00390		-2.59974		2	2.77866
Histone deacetylase 9 OS=Homo sapiens GN=HDAC9 PE=1 SV=2 - [HDAC9_HUMAN]	P16157	0.00235			2.36180	4	5.32437
Histone-lysine N-methyltransferase NSD3 OS=Homo sapiens GN=WHSC1L1 PE=1 SV=1 - [NSD3_HUMAN]	Q16531	0.00786			3.55613	2	2.98018
Histone-lysine N-methyltransferase NSD2 OS=Homo sapiens GN=WHSC1 PE=1 SV=1 - [NSD2_HUMAN]	Q6ZUU3	0.00269			-2.57431	2	3.11195
Nucleosome assembly protein 1-like 3 OS=Homo sapiens GN=NAP1L3 PE=2 SV=2 - [NP1L3_HUMAN]	Q8IZP9	0.00143		-17.77406		2	2.65080
mRNA processing							
Protein SCAF11 OS=Homo sapiens GN=SCAF11 PE=1 SV=2 - [SCAFB_HUMAN]	O75369	0.00321			-2.19737	2	2.19372
Splicing factor 45 OS=Homo sapiens GN=RBM17 PE=1 SV=1 - [SPF45_HUMAN]	P62736	0.00583			3.99501	2	2.34158
Splicing factor, suppressor of white-apricot homolog OS=Homo sapiens GN=SFSWAP PE=1 SV=3 - [SFSWA_HUMAN]	Q6WRX3	0.01142		-2.44745		5	7.40227
Pre-mRNA cleavage complex 2 protein Pcf11 OS=Homo sapiens GN=PCF11 PE=1 SV=3 - [PCF11_HUMAN]	Q6ZPA5	0.00352			2.17500	4	6.33357
Heterogeneous nuclear ribonucleoprotein A1-like 2 OS=Homo sapiens GN=HNRNPA1L2 PE=2 SV=2 - [RA1L2_HUMAN]	Q99707	0.01076			2.41766	6	16.86664
Terminal uridylyltransferase 4 OS=Homo sapiens GN=ZCCHC11 PE=1 SV=3 - [TUT4_HUMAN]	Q9HCU4	0.00001			-2.29413	4	6.04731
rRNA processing							
WD repeat-containing protein 3 OS=Homo sapiens GN=WDR3 PE=1 SV=1 - [WDR3_HUMAN]	O96028	0.00770			2.52710	3	4.59716
Ribosomal RNA processing protein 1 homolog B OS=Homo sapiens GN=RRP1B PE=1 SV=3 - [RRP1B_HUMAN]	Q8N130;Q02	0.00579		-3.08110		2	3.10301
RNA transport							
Germinal-center associated nuclear protein OS=Homo sapiens GN=MCM3AP PE=1 SV=2 - [GANP_HUMAN]	Q0P6D6	0.00249			-2.67851	3	5.40109
Regulation							
Transcription regulator protein BACH1 OS=Homo sapiens GN=BACH1 PE=1 SV=2 - [BACH1_HUMAN]	A6NCL7	0.04841			3.44606	2	3.80936
Putative zinc finger and SCAN domain-containing protein 5D OS=Homo sapiens GN=ZSCAN5D PE=5 SV=1 - [ZSA5D_HUMAN]	A8K8P3	0.00188			2.07423	2	3.65083
DBF4-type zinc finger-containing protein 2 OS=Homo sapiens GN=ZDBF2 PE=1 SV=3 - [ZDBF2_HUMAN]	O60336	0.00224			8.75390	3	3.12220
Zinc finger ZZ-type and EF-hand domain-containing protein 1 OS=Homo sapiens GN=ZZEF1 PE=1 SV=6 - [ZZEF1_HUMAN]	P0DMV8	0.00186		19.48378		3	3.69340
Protein CBFA2T3 OS=Homo sapiens GN=CBFA2T3 PE=1 SV=2 - [MTG16_HUMAN]	Q06210	0.04297			-3.49716	2	3.06214
Msx2-interacting protein OS=Homo sapiens GN=SPEN PE=1 SV=1 - [MINT_HUMAN]	Q08378	0.02130			2.25580	3	4.20975
Zinc finger protein 254 OS=Homo sapiens GN=ZNF254 PE=2 SV=3 - [ZN254_HUMAN]	Q13905	0.00184			3.13839	2	2.88298
Lysine-specific demethylase hairless OS=Homo sapiens GN=HR PE=1 SV=5 - [HAIR_HUMAN]	Q5QJ38	0.04169		-2.72372		2	3.02873
Protein flightless-1 homolog OS=Homo sapiens GN=FLII PE=1 SV=2 - [FLII_HUMAN]	Q5TB30	0.01282			-2.00488	4	6.05445
N-lysine methyltransferase SETD8 OS=Homo sapiens GN=SETD8 PE=1 SV=3 - [SETD8_HUMAN]	Q5TCQ9	0.01065			2.28258	3	4.31950
Zinc finger and BTB domain-containing protein 21 OS=Homo sapiens GN=ZBTB21 PE=1 SV=2 - [ZBT21_HUMAN]	Q6WKZ4	0.00439			-2.38185	2	2.84799
Adenosylhomocysteinase OS=Homo sapiens GN=AHCY PE=1 SV=4 - [SAHH_HUMAN]	Q8WVS4	0.00005			2.84172	2	6.33454
Fez family zinc finger protein 2 OS=Homo sapiens GN=FEZF2 PE=2 SV=2 - [FEZF2_HUMAN]	Q96I25	0.00236			-2.80353	2	3.62646
Thyrotrophic embryonic factor (Fragment) OS=Homo sapiens GN=TEF PE=2 SV=1 - [E0Z557_HUMAN]	Q96N67	0.00445		-3.30112		2	3.05093
Zinc finger protein 831 OS=Homo sapiens GN=ZNF831 PE=2 SV=4 - [ZN831_HUMAN]	Q99457	0.01016		-2.41605		2	3.88755
Zinc finger protein 197 OS=Homo sapiens GN=ZNF197 PE=2 SV=1 - [ZN197_HUMAN]	Q9HC77	0.00689			-2.04134	2	2.64568
Bromodomain adjacent to zinc finger domain protein 2A OS=Homo sapiens GN=BAZ2A PE=1 SV=4 - [BAZ2A_HUMAN]	Q9UBC2	0.00341			3.84174	4	6.91875
Zinc finger Ran-binding domain-containing protein 2 OS=Homo sapiens GN=ZRANB2 PE=1 SV=2 - [ZRAB2_HUMAN]	Q9Y6N6	0.00666		-4.01604		2	2.70472
Other							
LINE-1 type transposase domain-containing protein 1 OS=Homo sapiens GN=L1TD1 PE=1 SV=1 - [LITD1_HUMAN]	Q15418	0.00085			-2.83500	2	3.23202

(*continued on next page*)

Table 2 (*continued*)

(b) continue

Description	Accession	Anova (p)	Ag1 vs C	Ag10 vs C	Ag1 vs Ag10	Peptide number	Confidence score
Protein Synthesis							
Ribosomal proteins							
Ribosomal protein S6 kinase alpha-1 OS=Homo sapiens GN=RPS6KA1 PE=1 SV=2 - [KS6A1_HUMAN]	O94913	0.00721			2.31355	2	4.42423
Probable ATP-dependent RNA helicase DDX31 OS=Homo sapiens GN=DDX31 PE=1 SV=2 - [DDX31_HUMAN]	Q8NEC7	0.00517			2.69316	3	5.10123
Other							
Elongation factor Tu, mitochondrial OS=Homo sapiens GN=TUFM PE=1 SV=2 - [EFTU_HUMAN]	Q6F5E8	0.00648		-2.26028		3	6.92413
La-related protein 1B OS=Homo sapiens GN=LARP1B PE=1 SV=2 - [LAR1B_HUMAN]	Q8WXA3	0.02839			2.38478	2	1.90011
Glutamine--tRNA ligase OS=Homo sapiens GN=QARS PE=1 SV=1 - [SYQ_HUMAN]	Q9BWV1	0.00451			3.48317	2	4.21209
Protein destination and storage							
Folding and stability							
Heat shock 70 kDa protein 1A OS=Homo sapiens GN=HSPA1A PE=1 SV=1 - [HS71A_HUMAN]	P41002	0.02705			2.67714	2	6.64383
DnaJ homolog subfamily C member 10 OS=Homo sapiens GN=DNAJC10 PE=1 SV=2 - [DJC10_HUMAN]	Q8WWN8	0.04471			2.14334	3	4.72374
Sacsin OS=Homo sapiens GN=SACS PE=1 SV=2 - [SACS_HUMAN]	Q9NSV4	0.03704			4.16629	3	4.38615
Targeting							
Modification							
Ubiquitin carboxyl-terminal hydrolase 35 OS=Homo sapiens GN=USP35 PE=1 SV=3 - [UBP35_HUMAN]	O95218	0.04842		-2.28345		2	3.37342
Protein zyg-11 homolog A OS=Homo sapiens GN=ZYG11A PE=2 SV=3 - [ZY11A_HUMAN]	Q8NHQ1;Q6	0.00000		-7.47438		2	3.51096
NEDD4-like E3 ubiquitin-protein ligase WWP2 OS=Homo sapiens GN=WWP2 PE=1 SV=2 - [WWP2_HUMAN]	Q8TDB8	0.00000			6.61215	2	3.28088
Polypeptide N-acetylgalactosaminyltransferase 9 OS=Homo sapiens GN=GALNT9 PE=2 SV=3 - [GALT9_HUMAN]	Q96N23	0.02514			-3.49380	2	2.94166
Proteolysis							
Sentrin-specific protease 1 OS=Homo sapiens GN=SENP1 PE=1 SV=2 - [SENP1_HUMAN]	Q12872	0.00714		-2.79629		2	2.64249
Ubiquitin carboxyl-terminal hydrolase 34 OS=Homo sapiens GN=USP34 PE=1 SV=2 - [UBP34_HUMAN]	Q5VT97	0.00055			3.35609	3	3.42914
Transporters							
Ions							
Sodium/calcium exchanger 1 OS=Homo sapiens GN=SLC8A1 PE=1 SV=3 - [NAC1_HUMAN]	P60709	0.00960			3.98218	2	2.20588
Sodium-dependent phosphate transport protein 2C OS=Homo sapiens GN=SLC34A3 PE=1 SV=2 - [NPT2C_HUMAN]	Q659C4	0.01414		-6.19983		3	3.16762
Short transient receptor potential channel 6 OS=Homo sapiens GN=TRPC6 PE=1 SV=1 - [TRPC6_HUMAN]	Q8NCX0	0.04305				2	2.16705
Acetylcholine receptor subunit epsilon OS=Homo sapiens GN=CHRNE PE=1 SV=2 - [ACHE_HUMAN]	Q9HCM1	0.03262			2.18623	2	2.24959
Voltage-dependent P/Q-type calcium channel subunit alpha-1A OS=Homo sapiens GN=CACNA1A PE=1 SV=2 - [CAC1A_HUMAN]	Q9NVC6	0.02023		2.27163		2	2.12242
H(+)/Cl(-) exchange transporter 5 OS=Homo sapiens GN=CLCN5 PE=1 SV=1 - [CLCN5_HUMAN]	Q9Y210	0.01110			7.01479	2	3.32427
Sugars							
Solute carrier family 2, facilitated glucose transporter member 14 OS=Homo sapiens GN=SLC2A14 PE=2 SV=1 - [GTR14_HUMAN]	A8MWP4	0.00224			2.79665	2	4.41859
Lipids							
Oxysterol-binding protein-related protein 7 OS=Homo sapiens GN=OSBPL7 PE=2 SV=1 - [OSBL7_HUMAN]	Q8WXG6	0.00072			-2.40060	2	1.73329
Transport ATPases							
Other							
Epidermal growth factor receptor substrate 15-like 1 OS=Homo sapiens GN=EPS15L1 PE=1 SV=1 - [EP15R_HUMAN]	Q14642	0.00874			2.92299	2	2.38211
Multidrug resistance-associated protein 5 OS=Homo sapiens GN=ABCC5 PE=1 SV=2 - [MRP5_HUMAN]	Q14684	0.01044			2.21202	2	3.79990
Rab11 family-interacting protein 1 OS=Homo sapiens GN=RAB11FIP1 PE=1 SV=3 - [RFIP1_HUMAN]	Q5JPB2	0.02292		-2.13091		3	4.21899
GRIP and coiled-coil domain-containing protein 2 OS=Homo sapiens GN=GCC2 PE=1 SV=4 - [GCC2_HUMAN]	Q86YR5;P81	0.04093		-5.47707		2	3.58415
Golgin subfamily A member 3 OS=Homo sapiens GN=GOLGA3 PE=1 SV=2 - [GOGA3_HUMAN]	Q96RW7	0.01692			6.08202	3	4.88172
Golgi-specific brefeldin A-resistance guanine nucleotide exchange factor 1 OS=Homo sapiens GN=GBF1 PE=1 SV=2 - [GBF1_HUMAN]	Q9P0U3	0.00317			2.95741	3	3.87289
Aftiphilin OS=Homo sapiens GN=AFTPH PE=1 SV=2 - [AFTIN_HUMAN]	Q9UNX4	0.00098			3.16596	2	3.40527
Cell structure							
Cytoskeleton							
SH3 and multiple ankyrin repeat domains protein 3 OS=Homo sapiens GN=SHANK3 PE=1 SV=3 - [SHAN3_HUMAN]	F8W8Y7	0.00001		-4.43196		2	4.05002
Dynein heavy chain 3, axonemal OS=Homo sapiens GN=DNAH3 PE=2 SV=1 - [DYH3_HUMAN]	P43304	0.00392			4.18829	6	9.04761
Ankyrin-1 OS=Homo sapiens GN=ANK1 PE=1 SV=3 - [ANK1_HUMAN]	P62258	0.00028			2.34921	3	4.81041
Dystonin OS=Homo sapiens GN=DST PE=1 SV=4 - [DYST_HUMAN]	Q12789	0.00083			4.00603	4	4.71133
Filamin-B OS=Homo sapiens GN=FLNB PE=1 SV=2 - [FLNB_HUMAN]	Q13045	0.00503		-2.62261		2	3.59954
ERC protein 2 OS=Homo sapiens GN=ERC2 PE=1 SV=3 - [ERC2_HUMAN]	Q16831	0.00261			-2.45522	2	2.42826
Actin, aortic smooth muscle OS=Homo sapiens GN=ACTA2 PE=1 SV=1 - [ACTA_HUMAN]	Q6DT37	0.00032			2.94955	5	18.25935
Leucine-rich repeat-containing protein 16C OS=Homo sapiens GN=RLTPR PE=1 SV=2 - [LR16C_HUMAN]	Q6NUP7	0.00107			2.21972	2	3.36603
Actin, cytoplasmic 1 OS=Homo sapiens GN=ACTB PE=1 SV=1 - [ACTB_HUMAN]	Q8IZC6	0.00801			2.47853	4	14.28794
Keratin, type I cuticular Ha6 OS=Homo sapiens GN=KRT36 PE=2 SV=1 - [KRT36_HUMAN]	Q8TCH5	0.00001		-3.96904		2	3.90489
Dynein heavy chain 10, axonemal OS=Homo sapiens GN=DNAH10 PE=1 SV=4 - [DYH10_HUMAN]	Q99590	0.00066		-5.71738		5	7.55736
Spatacsin OS=Homo sapiens GN=SPG11 PE=1 SV=3 - [SPTCS_HUMAN]	Q9BYB0	0.00001		-4.87535		2	2.83306
Putative beta-actin-like protein 3 OS=Homo sapiens GN=POTEKP PE=5 SV=1 - [ACTBM_HUMAN]	Q9H8H2	0.01128		-3.51727		2	8.55057
Protein diaphanous homolog 3 OS=Homo sapiens GN=DIAPH3 PE=1 SV=4 - [DIAP3_HUMAN]	Q9NQR1	0.00515		-5.58537		2	3.16517
Rotatin OS=Homo sapiens GN=RTTN PE=1 SV=3 - [RTTN_HUMAN]	Q9P267	0.01957			3.30145	5	5.80963
Chromosome							
Structural maintenance of chromosomes protein 6 OS=Homo sapiens GN=SMC6 PE=1 SV=2 - [SMC6_HUMAN]	Q7Z494	0.00098	-4.31645			2	1.79870
Centromere protein J OS=Homo sapiens GN=CENPJ PE=1 SV=2 - [CENPJ_HUMAN]	Q6ULP2	0.04541			2.05372	3	5.96051
Endocytosis							
Lymphocyte antigen 75 OS=Homo sapiens GN=LY75 PE=1 SV=3 - [LY75_HUMAN]	Q5T5U3	0.00018			6.70841	4	5.91814
Endosome							
Cell cycle							
Transforming acidic coiled-coil-containing protein 3 OS=Homo sapiens GN=TACC3 PE=1 SV=1 - [TACC3_HUMAN]	O75054	0.00012		-3.12906		3	5.15713
MAP kinase-activating death domain protein OS=Homo sapiens GN=MADD PE=1 SV=2 - [MADD_HUMAN]	O75437	0.00331		-3.39786		3	5.37250
Protein SFI1 homolog OS=Homo sapiens GN=SFI1 PE=1 SV=2 - [SFI1_HUMAN]	P42336	0.00031			8.25024	2	3.33097
Organelle transport							
Cell Adhesion							
Brother of CDO OS=Homo sapiens GN=BOC PE=1 SV=1 - [BOC_HUMAN]	Q5T5P2	0.03985		-2.37580		2	3.43105
Laminin subunit gamma-3 OS=Homo sapiens GN=LAMC3 PE=1 SV=3 - [LAMC3_HUMAN]	Q6TFL3	0.02197			2.23904	2	2.76056
Cell proliferation							
Other							
WD repeat-containing protein 60 OS=Homo sapiens GN=WDR60 PE=1 SV=3 - [WDR60_HUMAN]	O14827	0.00034		-2.70226		2	2.55201
Glutathione S-transferase C-terminal domain-containing protein OS=Homo sapiens GN=GSTCD PE=1 SV=2 - [GSTCD_HUMAN]	Q5TZA2	0.01914			-2.06842	2	3.56643
Collagen alpha-1(XXVII) chain OS=Homo sapiens GN=COL27A1 PE=1 SV=1 - [CORA1_HUMAN]	Q86VV8	0.03965		-2.49982		4	5.54561
Collagen alpha-1(XIX) chain OS=Homo sapiens GN=COL19A1 PE=1 SV=3 - [COJA1_HUMAN]	P20020	0.00003		-6.25696		2	3.73179

(*continued on next page*)

Table 2 (*continued*)

(b) continue

Description	Accession	Anova (p)	Ag1 vs C	Ag10 vs C	Ag1 vs Ag10	Peptide number	Confidence score
Signal transduction							
Receptors							
Kinases							
Inactive serine/threonine-protein kinase TEX14 OS=Homo sapiens GN=TEX14 PE=1 SV=2 - [TEX14_HUMAN]	E0ZS57	0.01839			2.90678	3	4.97882
Testis-specific serine kinase substrate OS=Homo sapiens GN=TSKS PE=1 SV=3 - [TSKS_HUMAN]	O14867	0.00000		-3.18889		4	6.89274
Phosphatidylinositol 4,5-bisphosphate 3-kinase catalytic subunit alpha isoform OS=Homo sapiens GN=PIK3CA PE=1 SV=2 - [PK3CA_HUMAN]	O43593	0.00443		-3.57290		3	4.90199
Serine/threonine-protein kinase MRCK gamma OS=Homo sapiens GN=CDC42BPG PE=1 SV=2 - [MRCKG_HUMAN]	O43663	0.01547			4.48832	4	8.81443
Mitogen-activated protein kinase-binding protein 1 OS=Homo sapiens GN=MAPKBP1 PE=1 SV=4 - [MABP1_HUMAN]	P49795	0.00347		-3.69116		3	5.56513
Microtubule-associated serine/threonine-protein kinase 4 OS=Homo sapiens GN=MAST4 PE=1 SV=3 - [MAST4_HUMAN]	Q5T7N2	0.00362			3.82310	4	5.22494
Serine/threonine-protein kinase NIM1 OS=Homo sapiens GN=NIM1K PE=1 SV=1 - [NIM1_HUMAN]	Q5TAX3	0.03678	2.00413			3	4.58566
Leucine-rich repeat serine/threonine-protein kinase 2 OS=Homo sapiens GN=LRRK2 PE=1 SV=2 - [LRRK2_HUMAN]	Q9BZF2	0.01450			-3.03391	4	6.06743
Phosphatases							
Serine/threonine-protein phosphatase 4 regulatory subunit 4 OS=Homo sapiens GN=PPP4R4 PE=1 SV=1 - [PP4R4_HUMAN]	P0CG00	0.00000		-8.25251		3	4.14620
G proteins							
Cadherin EGF LAG seven-pass G-type receptor 2 OS=Homo sapiens GN=CELSR2 PE=1 SV=1 - [CELR2_HUMAN]	O00308	0.01305			-2.55825	2	3.67914
Adhesion G-protein coupled receptor G2 OS=Homo sapiens GN=ADGRG2 PE=1 SV=2 - [AGRG2_HUMAN]	P10635	0.02958			4.06976	2	1.66623
Regulator of G-protein signaling 19 OS=Homo sapiens GN=RGS19 PE=1 SV=1 - [RGS19_HUMAN]	Q14993	0.00154			5.17953	2	2.48693
G-protein-signaling modulator 1 OS=Homo sapiens GN=GPSM1 PE=1 SV=2 - [GPSM1_HUMAN]	Q9UIF9	0.04013			4.00845	2	3.48646
Other							
Rho GTPase-activating protein 21 OS=Homo sapiens GN=ARHGAP21 PE=1 SV=1 - [RHG21_HUMAN]	O15440	0.00342			3.83642	2	2.50618
14-3-3 protein epsilon OS=Homo sapiens GN=YWHAE PE=1 SV=1 - [1433E_HUMAN]	O43149	0.00109		-5.48692		2	4.54105
Ras-specific guanine nucleotide-releasing factor 2 OS=Homo sapiens GN=RASGRF2 PE=1 SV=2 - [RGRF2_HUMAN]	O60318	0.00303			3.75864	2	2.61426
Rho GTPase-activating protein SYDE2 OS=Homo sapiens GN=SYDE2 PE=1 SV=2 - [SYDE2_HUMAN]	O75081	0.00290			5.16395	4	4.65012
Nephrocystin-3 OS=Homo sapiens GN=NPHP3 PE=1 SV=1 - [NPHP3_HUMAN]	P00734	0.01210			2.09231	2	3.83707
Rap guanine nucleotide exchange factor 1 OS=Homo sapiens GN=RAPGEF1 PE=1 SV=3 - [RPGF1_HUMAN]	P32418	0.00227			2.47944	4	5.23876
Nuclear receptor coactivator 5 OS=Homo sapiens GN=NCOA5 PE=1 SV=2 - [NCOA5_HUMAN]	Q59H19	0.00025			7.05167	2	2.86805
Paralemmin-3 OS=Homo sapiens GN=PALM3 PE=1 SV=2 - [PALM3_HUMAN]	Q8IVF4	0.02296			2.04222	2	3.69599
Calretinin OS=Homo sapiens GN=CALB2 PE=2 SV=2 - [CALB2_HUMAN]	Q8IWJ2	0.00801			2.11600	2	4.60129
DEP domain-containing protein 1A OS=Homo sapiens GN=DEPDC1 PE=1 SV=2 - [DEP1A_HUMAN]	Q8TD57	0.00198	-2.06581			2	3.90782
Ankyrin repeat and SOCS box protein 16 OS=Homo sapiens GN=ASB16 PE=1 SV=2 - [ASB16_HUMAN]	Q9HCQ5	0.01709			2.85468	2	2.90105
Disease / defence							
Cell death							
Membrane-associated guanylate kinase, WW and PDZ domain-containing protein 3 OS=Homo sapiens GN=MAGI3 PE=1 SV=2 - [MAGI3_HUM	Q8N3A8	0.02744			2.07453	2	3.16933
Rho guanine nucleotide exchange factor 6 OS=Homo sapiens GN=ARHGEF6 PE=1 SV=2 - [ARHG6_HUMAN]	Q92538	0.03960	2.31904			3	3.80856
Defence-related							
Stress response							
Plasma membrane calcium-transporting ATPase 1 OS=Homo sapiens GN=ATP2B1 PE=1 SV=3 - [AT2B1_HUMAN]	O14709	0.03023	2.37903			2	2.95243
Other							
Mitochondria-eating protein OS=Homo sapiens GN=SPATA18 PE=1 SV=1 - [MIEAP_HUMAN]	O75197	0.01188			2.69605	2	2.50270
Unclear classification							
Immunoglobulin superfamily member 3 OS=Homo sapiens GN=IGSF3 PE=2 SV=3 - [IGSF3_HUMAN]	O15021	0.00464			2.11344	4	7.36897
Low-density lipoprotein receptor-related protein 1B OS=Homo sapiens GN=LRP1B PE=1 SV=2 - [LRP1B_HUMAN]	O75665	0.00041			2.35993	4	6.48868
Protein-lysine methyltransferase METTL21D OS=Homo sapiens GN=VCPKMT PE=1 SV=2 - [MT21D_HUMAN]	Q0VFX3	0.00302			3.87951	2	1.87147
Type I inositol 1,4,5-trisphosphate 5-phosphatase OS=Homo sapiens GN=INPP5A PE=1 SV=1 - [I5P1_HUMAN]	Q8IXB1	0.01410	-2.79381			2	2.55432
Low-density lipoprotein receptor-related protein 5 OS=Homo sapiens GN=LRP5 PE=1 SV=2 - [LRP5_HUMAN]	Q8TBJ5	0.01552			4.06628	2	3.27132
Prothrombin OS=Homo sapiens GN=F2 PE=1 SV=2 - [THRB_HUMAN]	Q8TC71	0.00059			3.39024	2	3.46502
Low-density lipoprotein receptor-related protein 2 OS=Homo sapiens GN=LRP2 PE=1 SV=3 - [LRP2_HUMAN]	Q96N46	0.00837			3.43731	3	4.24653
Methyl-CpG-binding domain protein 5 OS=Homo sapiens GN=MBD5 PE=1 SV=3 - [MBD5_HUMAN]	Q96NU0	0.03195	2.16779			2	2.53358
Cilia- and flagella-associated protein 54 OS=Homo sapiens GN=CFAP54 PE=2 SV=3 - [CFA54_HUMAN]	Q9BXT5	0.03944	2.29659			2	2.47300
NLR family CARD domain-containing protein 4 OS=Homo sapiens GN=NLRC4 PE=1 SV=2 - [NLRC4_HUMAN]	Q9NPP4	0.03684			2.77833	4	5.45859
Testis-expressed sequence 15 protein OS=Homo sapiens GN=TEX15 PE=2 SV=2 - [TEX15_HUMAN]	Q9NZR2	0.00075			-2.52843	2	2.49528
Glutamine--fructose-6-phosphate aminotransferase [isomerizing] 1 OS=Homo sapiens GN=GFPT1 PE=1 SV=3 - [GFPT1_HUMAN]	Q9UJT2	0.00012			3.34586	2	3.13420
Semaphorin-4D OS=Homo sapiens GN=SEMA4D PE=1 SV=1 - [SEM4D_HUMAN]	Q9ULJ3	0.00694		-9.20221		2	3.18152
Arf-GAP with Rho-GAP domain, ANK repeat and PH domain-containing protein 3 OS=Homo sapiens GN=ARAP3 PE=1 SV=1 - [ARAP3_HUMAN	Q9UNS1	0.00436			2.88346	4	6.38147
Unclasified							
Proline-rich transmembrane protein 3 OS=Homo sapiens GN=PRRT3 PE=1 SV=3 - [PRRT3_HUMAN]	B7Z4Z6	0.00360			3.81189	2	3.20684
CDNA FLJ23893 fis, clone LNG14589 OS=Homo sapiens PE=2 SV=1 - [Q8TCH5_HUMAN]	O00411	0.00396			8.35905	2	3.53347
Armadillo repeat-containing X-linked protein 4 OS=Homo sapiens GN=ARMCX4 PE=1 SV=3 - [F8W8Y7_HUMAN]	O00555	0.03798			2.08180	2	3.61534
Putative uncharacterized protein (Fragment) OS=Homo sapiens PE=4 SV=1 - [Q59H19_HUMAN]	O15481	0.00154			5.43727	2	2.65952
Melanoma-associated antigen B4 OS=Homo sapiens GN=MAGEB4 PE=1 SV=1 - [MAGB4_HUMAN]	P22676	0.00873		-3.22099		2	2.60074
Ectonucleotide pyrophosphatase/phosphodiesterase family member 5 OS=Homo sapiens GN=ENPP5 PE=2 SV=1 - [ENPP5_HUMAN]	P23526	0.01350			3.99462	2	2.83146
Protein ANKUB1 OS=Homo sapiens GN=ANKUB1 PE=2 SV=2 - [ANKUB_HUMAN]	P47897	0.02489		-2.54458		2	3.29550
Putative uncharacterized protein ENSP00000401716 OS=Homo sapiens PE=5 SV=1 - [YU008_HUMAN]	P49411	0.00606			3.30317	2	3.20645
Coiled-coil domain-containing protein 15 OS=Homo sapiens GN=CCDC15 PE=2 SV=2 - [CCD15_HUMAN]	P98164	0.01787	2.33321			2	2.57983
FOXL2 neighbor protein OS=Homo sapiens GN=FOXL2NB PE=2 SV=1 - [FOXNB_HUMAN]	Q03167	0.00224			-2.84252	2	3.67873
FLJ44955 protein OS=Homo sapiens GN=FLJ44955 PE=2 SV=1 - [Q0VFX3_HUMAN]	Q08379	0.02168	-2.27411			2	2.88650
CDNA FLJ26166 fis, clone ADG02852 OS=Homo sapiens PE=2 SV=1 - [Q6ZPA5_HUMAN]	Q15052	0.01476		-4.49648		2	4.23955
cDNA FLJ53550 OS=Homo sapiens PE=2 SV=1 - [B7Z4Z6_HUMAN]	Q15170	0.04865			8.81191	2	3.43420
Epididymis luminal protein 109 OS=Homo sapiens GN=HEL-109 PE=2 SV=1 - [V9HVX8_HUMAN]	Q63HK5	0.00015	2.65774		2.57004	3	4.37475
Tetratricopeptide repeat protein 14 OS=Homo sapiens GN=TTC14 PE=1 SV=1 - [TTC14_HUMAN]	Q8IWB6	0.00000		-2.88793		2	4.12918
Coiled-coil domain-containing protein 171 OS=Homo sapiens GN=CCDC171 PE=2 SV=1 - [CC171_HUMAN]	Q96T58	0.00292			3.53981	3	3.82551
CAP-Gly domain-containing linker protein 4 OS=Homo sapiens GN=CLIP4 PE=1 SV=1 - [CLIP4_HUMAN]	Q9BYX7	0.02968			5.54663	2	4.16107
Poly [ADP-ribose] polymerase 8 OS=Homo sapiens GN=PARP8 PE=2 SV=1 - [PARP8_HUMAN]	Q9BZE4	0.00280			3.99443	2	2.74150
RUN and FYVE domain-containing protein 2 OS=Homo sapiens GN=RUFY2 PE=1 SV=2 - [RUFY2_HUMAN]	Q9C091	0.03833			4.05831	2	2.93673
Contactin-associated protein-like 3B OS=Homo sapiens GN=CNTNAP3B PE=2 SV=2 - [CNT3B_HUMAN]	Q9HCD5	0.00405			4.16334	3	4.27581
Uncharacterized protein KIAA1551 OS=Homo sapiens GN=KIAA1551 PE=1 SV=3 - [K1551_HUMAN]	Q9HCK1	0.00034			5.57074	5	8.57042
GREB1-like protein OS=Homo sapiens GN=GREB1L PE=2 SV=2 - [GRB1L_HUMAN]	Q9NZJ4	0.03791			2.21830	2	2.66118
Sickle tail protein homolog OS=Homo sapiens GN=KIAA1217 PE=1 SV=2 - [SKT_HUMAN]	Q9P2H5	0.00095			-2.57846	2	3.87869
Trichohyalin-like protein 1 OS=Homo sapiens GN=TCHHL1 PE=2 SV=1 - [TCHL1_HUMAN]	Q9UJA9	0.00165			4.87708	2	2.16440
Coiled-coil domain-containing protein 150 OS=Homo sapiens GN=CCDC150 PE=1 SV=2 - [CC150_HUMAN]	Q9UKV0	0.00145			4.03485	2	3.74387
Ankyrin repeat domain-containing protein 33B OS=Homo sapiens GN=ANKRD33B PE=3 SV=1 - [AN33B_HUMAN]	Q9Y6A5	0.00054			2.25318	3	5.69247
Catabolism							
Uridine phosphorylase 1 OS=Homo sapiens GN=UPP1 PE=1 SV=1 - [UPP1_HUMAN]	Q03001	0.00310			4.40521	4	8.77583

Table 3
Overlap of protein identifications between the two proteomics approaches at two experimental times. a) 24 h and b) 72 h experiment.

UniProt accession number	Name	Protein description
a)		
P0DMV8	HSPA1A	Heat shock 70 kDa protein 1A OS = *Homo sapiens* GN = HSPA1A PE = 1 SV = 1 - [HS71A_HUMAN]
P25705	ATP5A1	ATP synthase subunit alpha, mitochondrial OS = Homo sapiens GN = ATP5A1 PE = 1 SV = 1 - [ATPA_HUMAN]
P07355	ANXA2	Annexin A2 OS = Homo sapiens GN = ANXA2 PE = 1 SV = 2 - [ANXA2_HUMAN]
P04406	GAPDH	Glyceraldehyde-3-phosphate dehydrogenase OS = Homo sapiens GN = GAPDH PE = 1 SV = 3 - [G3P_HUMAN]
b)		
P49411	TUFM	Elongation factor Tu, mitochondrial OS = Homo sapiens GN = TUFM PE = 1 SV = 2 - [EFTU_HUMAN]
P0DMV8	HSPA1A	Heat shock 70 kDa protein 1A OS = Homo sapiens GN = HSPA1A PE = 1 SV = 1 - [HS71A_HUMAN]

control in our study.

The analysis of imaged gels returned a total of 960 (range 672–1112), 954 (range 674–1238) and 1015 (range 734–1258) protein spots for the control, 1 and 10 μg/mL AgNPs treated samples at 24 h. A total of 1103 (range 721–1303), 1013 (range 776–1264) and 1092 (range 818–1332) protein spots were detected for the control, 1 and 10 μg/mL AgNPs treated samples at 72 h, respectively. The average percentage of matched spots across gels was 91% for 24 h and 87% for 72 h.

The Mann-Whitney test was used to compare the overall protein expression profile. Among the protein spots detected, 4 were found to be down-regulated by at least 2-folds, and 13 were up-regulated by at least 2-folds in cells treated with 1 μg/mL AgNPs and 13 down-regulated and 15 up-regulated by 10 μg/mL AgNPs exposure for 24 h (Fig. 2Sa). In the case of 72 h exposure, 27 spots were down-regulated, and 10 spots were up-regulated with at least a two-fold change by the lower concentration tested, whereas 13 proteins were found down-regulated and 13 up-regulated by the highest dose used of 10 μg/μL (Fig. 2Sb). Differences were also found between the two doses of AgNPs-treated cells. Some spots were differentially expressed in cells treated with 1 μg/mL AgNPs with respect to 10 μg/mL AgNPs (10 up-regulated and 13 down-regulated at 24 h and 24 up-regulated and 17 down-regulated at 72 h of exposure) (Fig. 2Sa, 2Sb).

Proteins of interest (up- or down-regulated) were defined from the images of the control and treated samples, and their corresponding spots in the image of the preparative gel were matched. The 132 spots were selected from the preparative gel for spot picking (Fig. 3S). The aforementioned deregulated protein targets were identified using LC-MS/MS. Proteome Discoverer (Thermo Scientific®) with the Sequest workflow and UniProtKB/Swiss-Prot database was used for protein identification of the selected deregulated protein spots.

In total, 123 unique differentially regulated spots were identified. Table 2S reports the UniProt Accession Number, the protein symbol, the protein coverage, the number of identified peptides and amino acids, the molecular mass, a probability score, a description and a biological function, symbols and the level of de-regulation of the identified proteins (p value and fold change). UniProtKB/Swiss-Prot and Gene Ontology (GO) were used to gain insight into the cellular processes, molecular functions of the proteins differentially regulated by the AgNPs. In Table 1, deregulated proteins by 1 or 10 μg/mL AgNPs exposure at 24 or 72 h are visualised grouped for the main function.

3.5. Relative quantification of identified proteins using the label-free MS-based method

A label-free MS-based proteomics approach was also used to investigate the effects of 1 or 10 μg/mL AgNPs on Caco-2 cells. The analysis of imaged peptide maps returned a total of 9177 and 11,333 co-detected peaks after matching the control, 1 and 10 μg/mL AgNPs treated sample groups at 24 h and 72 h exposure, respectively. The relative quantification was based on all peptides. Data were filtered (MS/MS spectra: rank < 5; peptide charge: < 5) before exporting the MS/MS output files for protein identification. 105,729 and 94,213 MS/MS spectra were exported into Proteome Discoverer for the 24 h and 72 h experiment, respectively. 75,162 and 57,457 search hits were re-imported into Progenesis QI for Proteomics and assigned to peptide ions. After signal normalisation, the quantification was made for all peptides using the relative quantification method (use of all peptide identified as part of the protein). The total number of quantifiable proteins was 7232 and 7295 for the 24 h and 72 h experiment, respectively. One-way ANOVA was used to identify statistically significant differentially abundant proteins between non-treated Caco-2 cells (control) and cells treated with 1 or 10 μg/mL AgNPs for the two-time points considered in this study. Only deregulated proteins, by at least 2-folds in cells, were validated. This results in 39 and 71 deregulated proteins for 1 and 10 μg/mL regarding, with respect to the control at 24 h exposure. For the 72 h experiment, 12 and 44 proteins were deregulated for 1 and 10 μg/mL, with respect to the control. Differences were also found between the two doses of AgNPs treated cells. 181 and 123 proteins were differentially expressed in cells treated with 1 μg/mL AgNPs with respect to 10 μg/mL AgNPs at 24 h and 72 h exposure, respectively. Table 3S reports the UniProt Accession Number, the protein symbol, the protein coverage, the number of identified peptides and amino acids, the molecular mass, a probability score, a description and a biological function, symbols and the level of deregulation of the identified proteins (p value and fold change).

In Table 2, deregulated proteins after 1 or 10 μg/mL AgNPs exposure at 24 or 72 h are visualised and grouped for the main function.

3.6. Comparison of the two experimental approaches

Sample requirement is an important parameter when dealing with in vitro experiments. There is a difference in the total amount of proteins required to obtain an adequate dataset with each of the techniques. 200 μg of loaded proteins are needed in the 2D-gel based method to generate enough peptides from protein spots for their MS characterisation. Only 3 μg loaded in the UHPLC are sufficient in the MS-based for a qualitative and quantitative analysis of the peptide mixture. Furthermore, the 2D-gel based experiment requires a total instrumental time of 130 h (based on the number of selected spots for MS characterisation) whereas the label-free MS-based experiment is performed for 54 h (see Table 4S). The average data analysis time is similar to both approaches. The average number of peptides identified per confident protein assignment for the 2D gel-based method is 10, compared to an average of 7 for the label-free MS-based method, which is slightly lower. Fig. 4S shows the number of deregulated proteins identified by the two experimental approaches, label-free MS-based and 2D-gel based at 24 (a) and 72 h (b). It shows that 291 proteins were identified independently by the label-free MS-based and 56 proteins by the 2D-gel based methods at 24 h exposure. At 72 h exposure, 179 and 88 proteins were identified independently by the label-free MS-based and 2D-gel based methods, respectively. Four and two proteins were found in

common irrespective of the applied approach in the case of the 24 h and 72 h experiments, respectively (Table 3). For the 24 h experiment, the four proteins found in common were P0DMV8, P25705, P07355 and P04406; whereas for the 72 h experiment, the two proteins in common were P49411 and P0DMV8. The low overlap observed cannot only be interpreted as a poor performance, but also demonstrates the advantage of the multimodal approach to the characterisation of the proteome (Yeung et al., 2008).

It is important to note that the analysis by differential 2D gel can provide additional information on the analysis only by MS. This is quite a novelty as this work can provide a perfect integration between two proteomic techniques that are normally used independently. The results obtained show that the integration of both techniques is advantageous for two main reasons. On the one hand, the label-free MS-based proteomics analysis, which is less costly in terms of time, allows acquiring more information on the differentially expressed proteins. This technique does not have the limitations of the analysis 2D by which it is possible to investigate only a defined range of pI and molecular weights. In our work, we covered from about pI 4.5 to 8.5 and from about 20 to 200 kDa. Also, label-free MS-based proteomics analysis does not have any limitations, either in the case of proteins with a poor solubility (mainly hydrophobic proteins of the membrane) or proteins which tend to form protein aggregates due to bridges disulfide formation (the case of cytoskeleton proteins). Here, the latter problem was minimised by the sample preparation method applied. On the other hand, the 2D gel analysis provides the advantage of identifying the different isoforms of a protein e.g. due to post-translational modification (PTMs) and/or by alternative splicing, as well as altered by the action of proteases. This is a relevant factor considering that isoforms of the same protein might have different biological effects, ranging from a complete loss of function to its acquisition.

Specifically, referring to Fig. 3S, isoforms or proteolytic products of a particular protein found to be differently regulated by AgNPs exposure are highlighted. The data are presented in Table 5S.

3.7. De-regulated networks

The IPA software was used for the combination and interpretation of complex data for both proteomic platforms. The data were obtained by analysing the differentially expressed proteins. Several biological activities were found to be altered in Caco-2 cells exposed to AgNPs. Figs. 3 (a, b) and 4 (a, b) report the most significant molecular networks affected in response to 1 or 10 μg/mL AgNPs treatment for 24 h (a) and 72 h (b), for the 2D-gel based and label-free MS-based approach respectively. The focus molecules and de-regulation in response to 1 or 10 μg/mL AgNPs treatment for 24 h and 72 h are highlighted in Tables 4 (a, b) and 5 (a, b) for the 2D-gel based and label-free MS-based approach respectively.

Interestingly, the major proteins altered in response to AgNPs were associated with cell cycle, cell morphology, cellular function and maintenance.

3.8. Additional studies

To support our findings, we cross-linked omics data with a broad set of complementary techniques.

We investigated the effects of 72 h AgNPs exposure on the nuclei and cytoskeleton organisation of Caco-2 cells by immunocytochemistry. In the Supplementary information, Fig. 5S shows Hoechst and Alexa Fluor® 488 phalloidin staining, used to visualise nuclei and F-actin filaments respectively (63× magnification). Upon AgNPs incubation, some nuclei are fragmented; this phenomenon is not observed in untreated cells or cells exposed to the solvent control. The cytoskeleton organisation appears disrupted and damaged. The F-actin distribution shows to be altered in cells exposed to AgNPs, with a higher effect seen at 10 μg/mL concentration.

Also, to overcome the limited sensitivity of proteomics to investigate inflammatory cell response induced by AgNPs, we used antibody arrays, which can detect cytokines in the ranges of pg/mL. We performed a simultaneous screening of 42 human markers using a human cytokine specific antibody array.

For the completeness of the study, apoptosis-specific antibody array was performed. Arrays data are reported in Fig. 6S and 7S and highlight significant changes in the expression of several proteins involved in cytokines production, as well as in the apoptosis process, respectively.

4. Discussion

4.1. Biological significance of proteomic results obtained

The increased use of AgNPs in consumer production as dietary supplements or food packaging materials creates concerns for humans, which could directly or indirectly be exposed to the NPs. Oral exposure to AgNPs and its subsequent systemic absorption have been observed in rats (Kim et al., 2008), indicating that the gastrointestinal tract is a potential target organ. For this reason, the Caco-2 cells, extensively used over the last twenty years as an in vitro model of the intestinal barrier for toxicity testing of classical toxicants (Brandon et al., 2006) and more recently for nanomaterials (Sahu et al., 2016) (Gerloff et al., 2009) was selected for this study.

Effective assessment of the growing number of new nanomaterials benefits from a more comprehensive understanding of their toxicological mechanisms, which is difficult to achieve by traditional, single end-point approaches (Costa and Fadeel, 2016) (Matysiak et al., 2016). In this regard, system biology approaches have started to be applied to the nanotoxicological sciences to overcome the limitations of end-point assays.

Several key questions remain to be answered on the toxicity mechanism of AgNPs, in particular, the identification of the key signalling pathways involved (McShan et al., 2014). With this work, we aim to provide a valid contribution by applying a multimodal approach, which allows analysing Caco-2 cellular interactions with 30 nm citrate coated AgNPs.

Firstly, we deeply characterized the NPs used as particle size, surface area, aggregation/agglomeration state, parameters that are all likely to influence the biological availability and effects of the NPs. We demonstrated that the AgNPs selected were homogeneous, well dispersed and stable at the experimental conditions considered, including in complete cell culture medium. As next step, we performed in vitro cytotoxicity testing showing a concentration-dependent toxic effect of AgNPs. Based on these data, we selected two doses for the subsequent proteomic analysis: a low no toxic concentration of 1 μg/mL and a high concentration of 10 μg/mL. Acute exposure as the common exposure model in nanotoxicology was applied, which provide useful indication in terms of quantitative ranking of NPs hazards. Two exposure durations were considered: 24 and 72 h. Doses and time points selected were in line with available studies (Zhang et al., 2016) (Verano-Braga et al., 2014). At his regards, no specific exposure limits have been calculated for nanosilver in the EU, whereas for the general population the World Health Organisation (WHO) set a “No Observable Adverse Effect Level”-(NOAEL) related to the sum of all exposure routes of 5 μg/kg bw(body weight) AgNPs/day. Recently, for AgNP a NOAEL (for rats) was observed, based on a 90 day oral exposure of 30 mg/kg bw/day; this assessment was based on signs of liver toxicity (Hartemann et al., 2015, Kim et al., 2010).

Since silver ions might be slowly released from NPs due to surface oxidation, surface reactions, and dissolution of nanosilver in a biological medium, the toxicity contribution from the ionic form versus the nano-form of silver has been taken into account. We quantified the ions released from AgNPs, and investigated the cellular interaction and uptake of AgNPs using ICP-MS. Our results showed that approximately only 1% of the initial amount of AgNPs exposed to the cells is

internalised or strictly bound to the membrane of cells at the highest concentration (10 μg/mL) and exposure time (72 h) analysed. Based on literature data, AgNPs stability, in terms of ions release is of considerable variability. (Beer et al., 2012), detected between 39% and 71% of Ag^+ ion fraction from commercial available AgNPs powder, reporting that the high concentration of Ag ionic fraction is linked to the dispersion protocol. AgPure (listed as NM-300 reference material of the Joint Research Centre (JRC, Italy) used by (Oberemm et al., 2016) resulted in 15.1% as ionic silver after 24 h incubation in cell culture medium, whereas (Verano-Braga et al., 2014) reported a 6 to 17% of the silver content of the AgNPs suspensions to be in the ionic form (Ag^+) in LoVo cells treated with 20 and 100 nm AgNPs. In our experimental conditions, the amount of free ionic silver was found to be < 0.1% after incubation in cell culture media at the highest dose and time point considered. As we observed a very limited release of Ag^+, we account that the toxicity of AgNPs is mainly related to AgNPs per se.

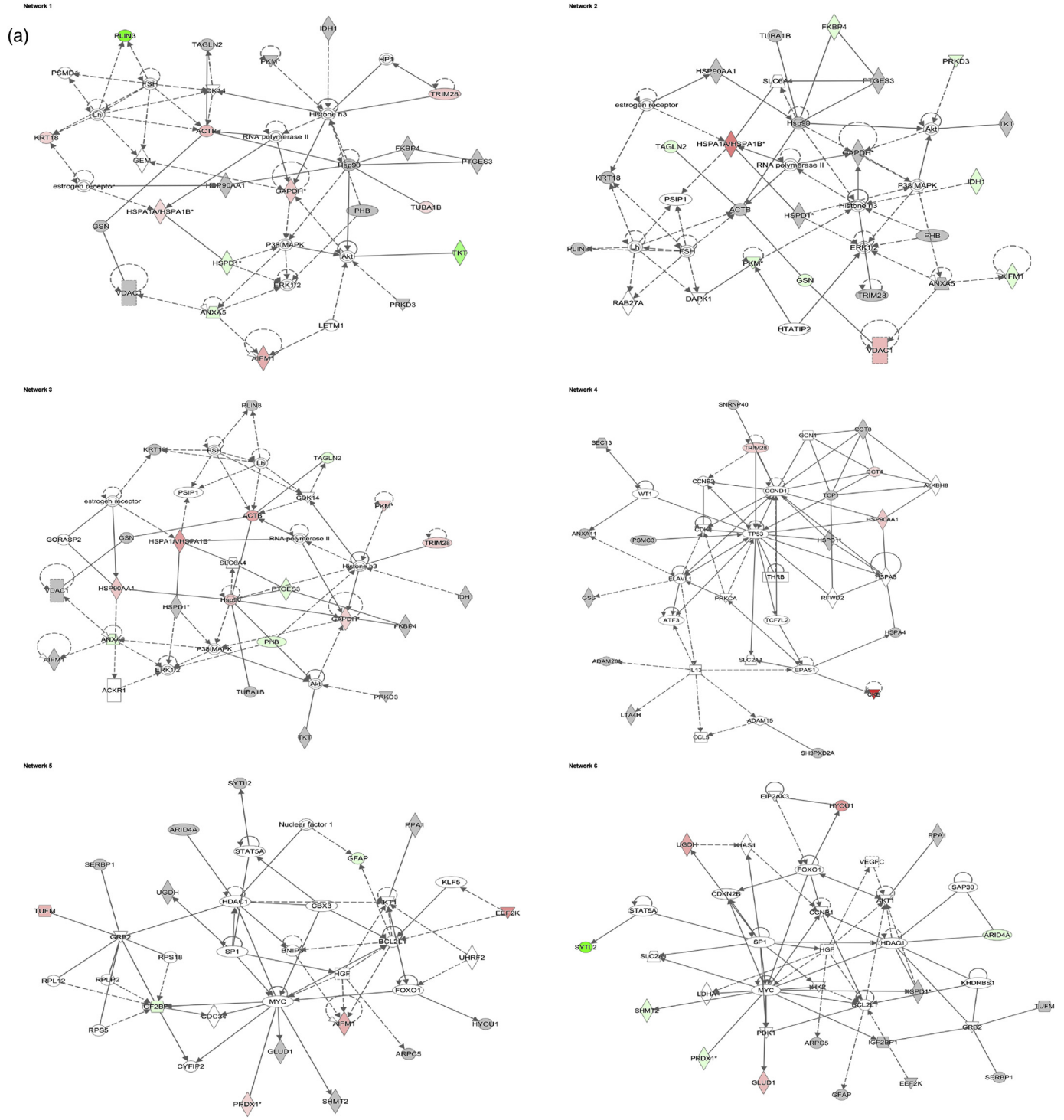

Fig. 3. Data analysis from the 2D gel-based approach - De-regulated molecular networks in response to 1 or 10 μg/mL AgNPs exposure in Caco-2 cells. a) 24 h and b) 72 h experiment. The networks are obtained by analysing the differentially expressed proteins using Ingenuity IPA. Identified deregulated proteins and metabolites involved in the network are highlighted in bold. The colour indicates the deregulation (red: up-regulated, green: down regulated). (For interpretation of the references to colour in this figure legend, the reader is referred to the web version of this article.)

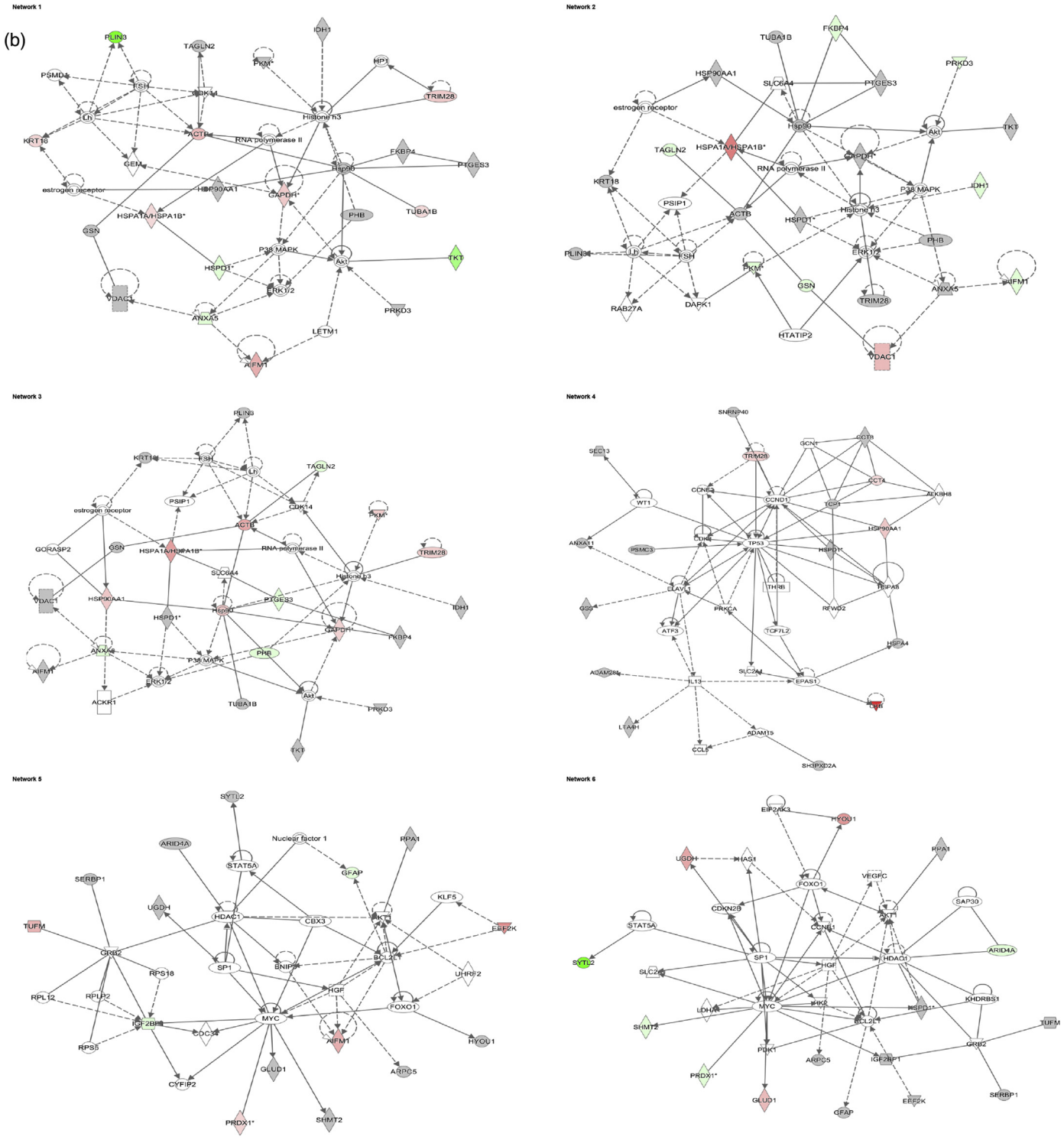

Fig. 3. (*continued*)

This is in agreement with several other previous studies that had reported that AgNPs-induced toxicity is primarily the result of oxidative damage and is independent of the toxicity of Ag^+ ions (Kim et al., 2009). Also, (Verano-Braga et al., 2014) and (Xu et al., 2015) have shown that more proteins were deregulated by AgNPs than by the free silver ions released into the solution by the NPs. More recently, (Oberemm et al., 2016) concluded that the high number of deregulated proteins in the AgNP-treated cells points towards particle-specific effects not exerted by silver ions. (Sahu et al., 2016) reported that 20 nm AgNPs nanoparticle are genotoxic in Caco-2 cell line, however, it is not dependent on the contribution of ionic silver. (Beer et al., 2012) concluded that for an AgNPs suspension containing 5.5% of Ag^+, they could not detect any difference in the toxicity between AgNPs suspension and its supernatant.

As a preliminary step, we assessed if there were any differences in the proteome profile of the untreated cells compared to cells exposed to the solvent of the NPs at the same doses intended to use in the study (1 or 10 μg/mL). The results showed that very few significant differences were found: two proteins in the case of control vs. solvent of 1 μg/mL AgNPs and three proteins in the case of control vs. solvent of 10 μg/mL

Table 4

Data analysis from the 2D gel-based approach - Identified molecular networks using Ingenuity IPA. a) 24 h and b) 72 h experment. The table reports the most significant molecular networks in response to 1 and 10 μg/mL AgNP treatments, by analysing the differentially expressed proteins from the cells. The network number, the list of all proteins and metabolites involved in the network, the number of molecules overlapping between our data set and the network and the top functions related to the network are shown. Focus molecules are indicated in bold and deregulation is indicated with a coloured arrow (red: up-regulated, green: down-regulated).

Network ID	Analysis	Molecules in Network	Score	Focus Molecules	Top Functions
1	Ag1 vs Ag10	AIFM1, Akt, ANXA2, ↓ANXA5, BCL2L2, ↓CALM1 (includes others), ↓CFL1, ↑DLAT, ENO1, ERK1/2, ↓GAPDH, HNRNPK, Hsp90, HSP90AB1, ↓HSPA5,↑ HSPA1A/HSPA1B, HSPD1, Jnk, KDELR1, ↑KHSPR, KRT8, NCK1, NFATC2, NFkB (complex), P38 MAPK, p85 (pik3r), PI3K (complex), ↑PLCG1, Ras, RBP3, RNA polymerase II, SDF4, SHC1, TCR, VCL	36	18	**Cell morphology, Cellular Assembly and Organization**
2	Ag1 vs C	AIFM1, Akt, ↓ANXA2, ↑ANXA5, CACNA1C, CALM1 (includes others), CD3G, CFL1, CSNK1A1, DLAT, ↑EN01, ERK1/2, Fc receptor, ↓GAPDH, ↑HNRNPK, Hsp90, HSP90AB1, HSPA5, ↓HSPA1A/HSPA1B, HSPD1, Jnk, KHSRP, KRT8, ↑NFATC2, NFkB (complex), P38 MAPK, p85 (pik3r), PI3K (complex), PLCG1, RNA polymerase II, SLC6A4, TCR, TP53I3, VCL, ZMAT3	36	18	**Post-Translational Modification, Protein Folding**
3	Ag10 vs C	A2M, ↑AIFM1, Akt, ANXA2, ANXA5, BCL2L2, CALM1 (includes others),CFL1, ↑DLAT, ↓ENO1, ERK1/2, ↓GAPDH, HNRNPK, Hsp90, ↑HSP90AB1, ↓HSPA5, ↑HSPA1A/HSPA1B, ↑HSPD1, Jnk, KDELR1, KHSPR, ↓KRT8, MAT2B, NCK1, NFATC2, NFkB (complex), P38 MAPK, p85 (pik3r), ↑PLCG1, RBP3, RNA polymerase II, SDF4, TCR, ↓VCL	36	18	**Cellular Movement, Cellular Compromise**
4	Ag1 vs C	ACO2, ↑ACTG1, ↑ALDH2, AR, Calmodulin, CALU, CCT5, CSNK1A1, CTNNB1, Cyclin E, ↓GAPDH, ↓HSPA1A/HSPA1B, HSPD1, IFITM1, IFNG, IL7, ↑KRT5, LDHB, Lh, LONP1P4HA1, ↓P4HB, PLIN3, PKL1, PPP1R12A, PSMA5, PTHLH, RACK1, RCN1, SMARCA4, SVIL, TAGLN, TP53, TUBB3, YWHAG	24	13	**DNA Replication, Recombination and Repair**
5	Ag1 vs Ag10	ACO2, ACTG1, ↑ALDH2, AR, ↓CALU, CASP4, CTNNB1, DDIT3, DYNLL1, ↓GAPDH, HLA-C, HSP90B1, IFITM1, IFNG, IL7, KAT2B, KRT5, LDHB, Lh, P4HB, ↓PLIN3, PKL1, PPP1R12A, ↓PSMA5, PSMC2, ↑RACK1, RAF1, Ras, RCN1, SMARCA4, SUZ12, TP53, TUBB3, YWHAG, YY1	21	12	**Cell Death and Survival**
6	Ag10 vs C	↑ACO2, ACTG1, ↑ALDH2, AR, ↓CALU, CASP4, CCT5, CTNNB1, DAPK3, DDIT3, ↓GAPDH, HSP90B1, IFITM1, IFNG, IL7, KAT2B, KRT5, ↓LDHB, Lh, MAP2K1, MPRIP, P4HB, PIK3R1,↓PLIN3, PKL1, ↓PPP1R12A, PRKG1, ↓PSMA5, RACK1, ↓RCN1, SMARCA4, SUZ12, TP53, YWHAG, YY1	20	12	**Cell cycle**

Network ID	Analysis	Molecules in Network	Score	Focus Molecules	Top Functions
1	Ag1 vs Ag10	↑ACTB, ↑AIFM1, Akt, ↓ANXA5, CDK14, ERK1/2, estrogen receptor, FKBP4, FSH, ↑GAPDH, GEM, GSN, Histone h3, HP1, Hsp90, HSP90AA1, ↑HSPA1A/HSPA1B, ↓HSPD1, IDH1, ↑KRT18, LETM1, Lh, P38 MAPK, PHB, PKM, ↓PLIN3, PRKD3, PSMD1, PTGES3, RNA polymerase II, TAGLN2, ↓TKT, ↑TRIM28, ↑TUBA1B, VDAC1	40	21	**Post-Translational Modification, Protein Folding**
2	Ag1 vs C	ACTB, ↓AIFM1, Akt, ANXA5, DAPK1, ERK1/2, estrogen receptor, ↓FKBP4, FSH, GAPDH, ↓GSN, Histone h3, Hsp90, HSP90AA1, ↑HSPA1A/HSPA1B, HSPD1, HTATIP2, ↓IDH1, KRT18, Lh, P38 MAPK, PHB, ↓PKM, PLIN3, ↓PRKD3, PSIP1, PTGES3, RAB27A, RNA polymerase II, SLC6A4, ↓TAGLN2, TKT, TRIM28, TUBA1B, ↑VDAC1	40	21	**Cell Death and Survival**
3	Ag10 vs C	ACKR1, ↑ACTB, AIFM1, Akt, ↓ANXA5, CDK14, ERK1/2, estrogen receptor, FKBP4, FSH, ↑GAPDH, GORASP2, GSN, Histone h3, Hsp90, ↑HSP90AA1, ↑HSPA1A/HSPA1B, HSPD1, IDH1, KRT18, Lh, P38 MAPK, ↓PHB, ↑PKM, PLIN3, PRKD3, PSIP1, ↓PTGES3, RNA polymerase II, SLC6A4, ↓TAGLN2, ↑TRIM28, TUBA1B, VDAC1	40	21	**Post-Translational modification**
4	Ag1 vs C	ADAM15, ADAM28, ALKBH8, ANXA11, ATF3, CCL5, CCDN1, CCEN2, ↑CCT4, CCT8, CDK2, ↑CKB, ELAVL1, EPAS1, GCN1, GSS, ↑HSP90AA1, HSPA4, HSPA8, HSPD1, IL13, LTA4H, PRKCA, PSMC3, RFWD2, SEC13, SH3PXD2A, SLC2A1, SNRNP40, TCF7L2, TCP1, THRB, TP53, ↑TRIM28, WT1	28	16	**Injury and Abnormalities**
5	Ag10 vs C	↑AIFM1, AKT1, ARID4A, ARPC5, BCL2L1, BNIP3, CBX3, CDC34, CYFIP2, ↑EEF2K, FOXO1, ↓GFAP, GLUD1, GRB2, HDAC1, HYOU1, ↓IGF2BP1, KLF5, MYC, Nuclear factor 1, PPA1, ↑PRDX1, RPL12, RPLP2, RPS5, RPS18, SERBP1, SHMT2, SP1, STAT5A, SYTL2, ↑TUFM, UGDH, UHRF2	25	15	**Cell Morphology, Cellular Function and Maintenance**
6	Ag1 vs Ag10	AKT1, ↓ARID4A, ARPC5, BCL2L1, CCNB1, CDKN2B, EEF2K, EIF2AK3, FOXO1, GFAP, ↑GLUD1, GRB2, HAS1, HDAC1, HGF, HK2, HSPD1, ↑HYOU1, IGF2BP1, KHDRBS1, LDHA, MYC, PDK1, PPA1, ↓PRDX1, SAP30, SERBP1, ↓SHMT2, SLC2A1, SP1, STAT5A, ↓SYTL2, TUFM, ↑UGDH, VEGFC	25	15	**Cell Cycle**

AgNPs-treated cells (Data not shown). This indicates no specific effects of the coating matrix on cells. Solvent control did not also show any decrease in cell viability on the control. Based on these observations, we focused on the analysis of the differentially regulate proteins by only the NPs and we compared the profiling among controls and AgNPs-treated Caco-2 cells at the two different doses and at two different exposure time (24 and 72 h).

In analysing the molecular effects of AgNPs in the most comprehensive manner, the combination of two proteomic approaches, complemented with other techniques were applied. In contrast with classical end-points methods, the strength of omics methods is to provide the opportunity for an unbiased assessment and may result in identifying novel and/or unanticipated end-points, which could also yield to novel biomarkers (Costa and Fadeel, 2016). Also, when coupled with

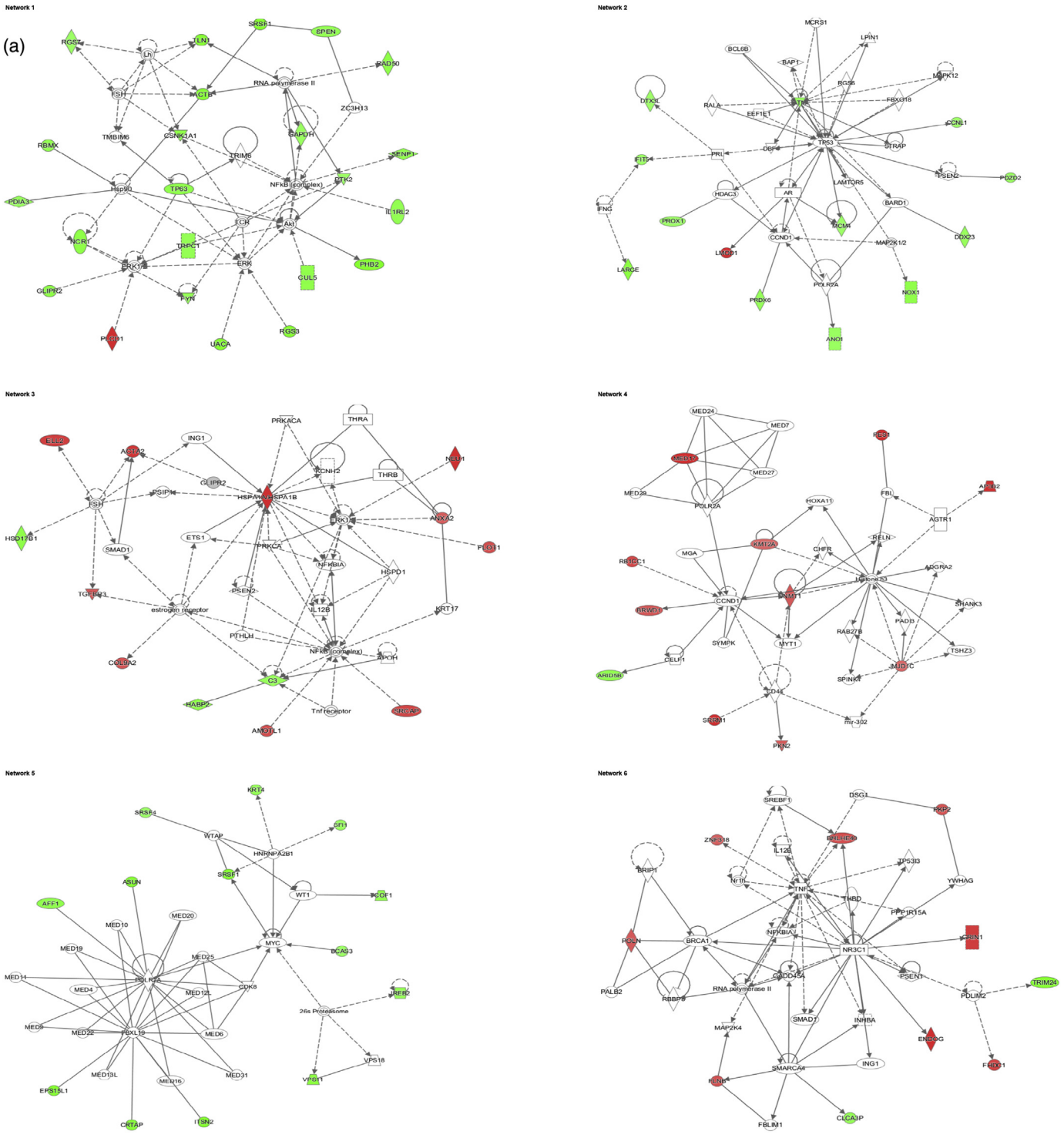

Fig. 4. Data analysis from the label-free MS-based approach - Deregulated molecular networks in response to 1 or 10 μg/mL AgNPs exposure in Caco-2 cells. a) 24 h and b) 72 h experiment. The networks are obtained by analysing the differentially expressed proteins using Ingenuity IPA. Identified deregulated proteins and metabolites involved in the network are highlighted in bold. The colour indicates the deregulation (red: up-regulated, green: down regulated). (For interpretation of the references to colour in this figure legend, the reader is referred to the web version of this article.)

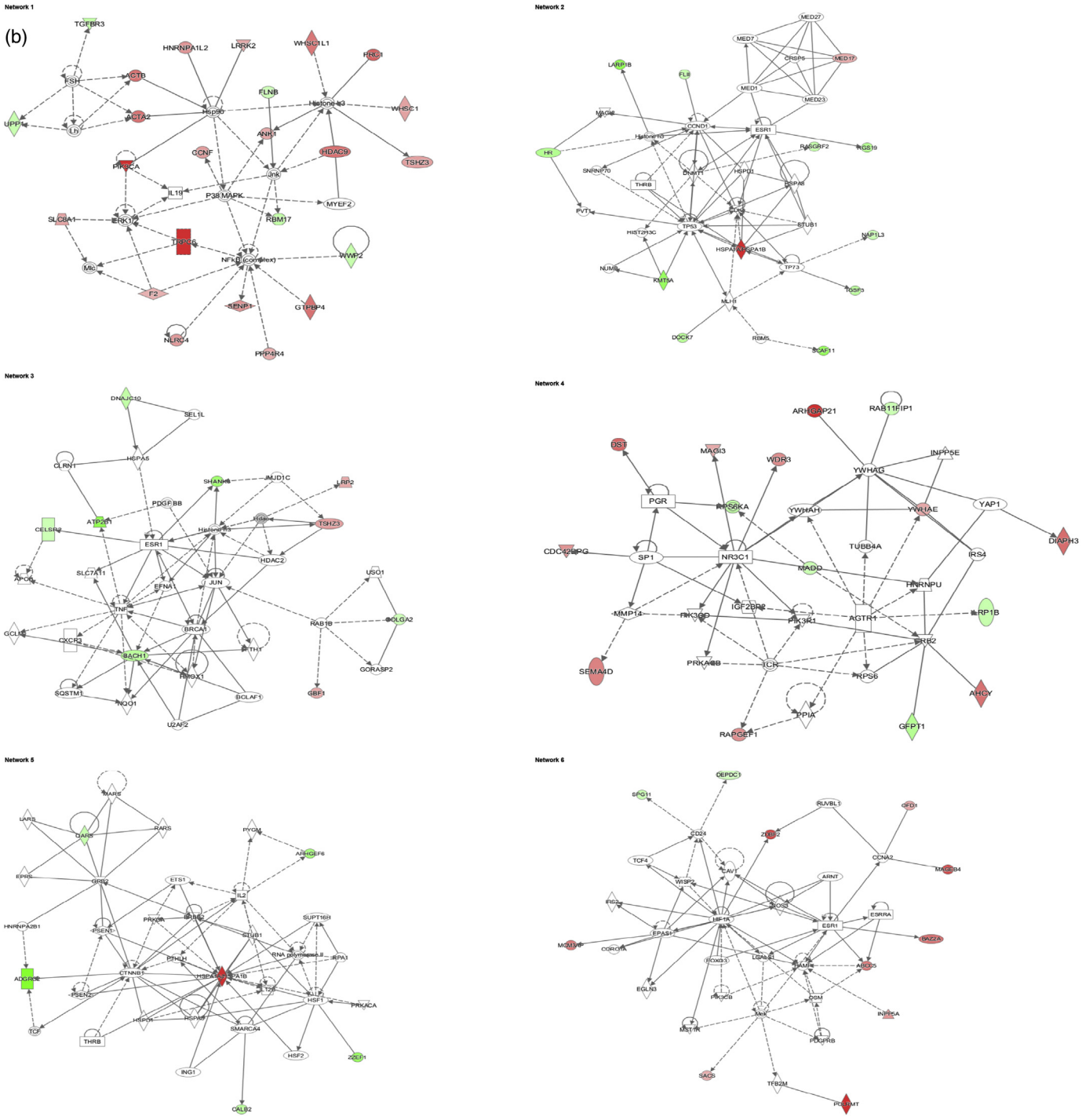

Fig. 4. (*continued*)

bioinformatics, it may lead to indicate novel and/or low dose effects, not detected by conventional cellular assays. Although only a small amount of AgNPs was taken up by the cells and as ICP-MS data have shown and in accordance with literature (Bouwmeester et al., 2011), image analysis and biostatistics of the 2-DE gel image spot data revealed noticeable differences in protein spot expression in a concentration and timely manner. De-regulated proteins were classified through biological functions. In particular, a considerable fraction of the proteins identified as altered by AgNPs was related to energy and metabolism, protein synthesis or stability/transcription, cell morphology and transport, as well as stress response.

For example, citrate coated-AgNPs 30 nm triggered a deregulation of several cytoskeleton proteins. Among the most affected proteins are: Tubulin beta-4B (TUBB4), one of the major constituents of microtubules; Actin-related protein 2/3 complex subunit 5 (ARPC5), which functions as a component of the Arp2/3 complex and it is involved in the regulation of actin polymerization and, together with an activating nucleation-promoting factor (NPF), mediates the formation of branched actin networks.

Cofilin expression (CFL1) was sharply decreased at 24 h in 10 μg/mL treated cells; this protein belongs to the actin-binding proteins which disassemble actin filaments. T-complex protein (TCP1 and CCT8) involved in complex folds, including actin and tubulin, were also found deregulated by AgNPs. Isoform 4 of Perilipin-3 (PLIN3), a cadherin

Table 5
Data analysis from the label-free MS-based approach - Identified molecular networks using Ingenuity IPA. a) 24 h and b) 72 h experment. The table reports the most significant molecular networks in response to 1 and 10 μg/mL AgNP treatments, by analysing the differentially expressed proteins from the cells.

Network ID	Analysis	Molecules in Network	Score	Focus Molecules	Top Functions
1	Ag1 vs Ag	↓ACTB,Akt,↓CSNK1A1,CUL5,ERK,ERK1/2,FSH,↓FYN,↓GAPDH,↓GLIPR2,Hsp90,↓IL1RL2,Lh,↓NCR1,NFkB (complex),↓PDIA3,↓PHB2,↑PLCD1,↓PTK2,↓RAD50↓,RBMX,↓RGS3,↓RGS7,RNA polymerase II,↓SENP1,↓SPEN,↓SRSF1,TCR,↓TLN1,TMBIM6,↓TP63,TRIM6,↓TRPC1,↓UACA,ZC3H13	39	23	**Cellular Movement**
2	Ag1 vs C	↓ANO1,AR,↓ATM,BAP1,BARD1,BCL6B,CCND1,↓CCNL1,DBF4,↓DDX23,↓↓DTX3L,EEF1E1,FBXO18,HDAC3,↓IFIT5,IFNG,LAMTOR5,↓LARGE,↑LMOD1,LPIN1,MAP2K1/2,MAPK12,↓MCM4,MCRS1,↓NOX1,↓PDZD2,POLR2A,↓PRDX6,PRL,↓PROX1,PSEN2,RALA,RGS6,STRAP,TP53	28	13	**Cell Cycle**
3	Ag10 vs C	↑ACTA2,↑AMOTL1,↑ANXA2,APOH,↓C3,↑COL9A2,↑ELL2,ERK1/2,estrogen receptor,ETS1,↑FLOT1,FSH,GLIPR2,↓HABP2,↓HSD17B1,↑HSPA1A/HSPA1B,HSPD1,IL12B,ING1,KCNH2,KRT17,↑NEU1,NFkB (complex),NFKBIA,PRKACA,PRKCA,PSEN2,PSIP1,PTHLH,SMAD1,↑SRCAP,↑TGFBR3,THRA,THRB,Tnf receptor	24	13	**Cellular Movement**
4	Ag10 vs C	ADGRA2,AGTR1,↑AP3B2,↓ARID5B,↑BRWD1,CCND1,CD44,CELF1,CHFR,↑DNMT1,FBL,Histone h3,HOXA11,JMJD1C,↑KMT2A,MED7,↑MED17,MED24,MED27,MED29,MGA,mir-302,MYT1,PADI3,↑PES1,↑PKN2,POLR2A,RAB27B,↑RB1CC1,RELN,SHANK3,SPINK4,↑SRRM1,SYMPK,TSHZ3	19	11	**Cellular Function and Maintenance**
5	Ag1 vs Ag	26s Proteasome,↓AFF1,↓ASUN,↓BCAS3,CDK8,↓CRTAP,↓EPS15L1,FBXL19,HNRNPA2B1,↓IREB2,↓ITSN2,↓KRT4,MED4,MED6,MED9,MED10,MED11,MED16,MED19,MED20,MED22,MED25,MED31,MED12L,MED13L,MYC,POLR2A,↓SFI1,↓SRSF1,↓SRSF4,↓TCOF1,↓VPS11,VPS18,WT1,WTAP	18	13	**RNA Post-Transcriptional Modification, Cell Cycle**
6	Ag10 vs C	↑BHLHE40,BRCA1,BRIP1,↓CLCA3P,DSG1,↑ENDOG,FBLIM1,↑FHDC1,↑FLNB,GADD45A,↑GRIN1,IL12B,ING1,INHBA,MAP2K4,NFKBIA,Nr1h,NR3C1,PALB2,PDLIM2,↑PKP2,↑POLN,PPP1R15A,PSEN1,RBBP8,RNA polymerase II,SMAD1,SMARCA4,SREBF1,THBD,TNF,TP53I3,↓TRIM24,YWHAG,↑ZNF318	17	10	**Cell Death and Survival**

Network ID	Analysis	Molecules in Network	Score	Focus Molecules	Top Functions
1	Ag1 vs Ag1	↑ACTA2,↑ACTB,↑ANK1,↑CCNF,ERK1/2,↑F2,↓FLNB,FSH,↑GTPBP4,↑HDAC9,Histone h3,↑HNRNPA1L2,Hsp90,IL19,Jnk,Lh,↑LRRK2,Mlc,MYEF2,NFkB (complex),↑NLRC4,P38 MAPK,↑PIK3CA,↑PPP4R4,↑PRC1,↓RBM17,↑SENP1,↑SLC8A1,↓TGFBR3,↑TRPC6,↑TSHZ3,↓UPP1,↑WHSC1,↑WHSC1L1,↓WWP2	45	24	**Cell Development, Cell Morphology**
2	Ag10 vs C	CCND1,CDK1,CRSP5,DNMT1,↓DOCK7,ESR1,↓FLII,HIST2H3C,Histone h3,↓HR,HSPA8,↑HSPA1A/HSPA1B,HSPD1,↓IGSF3,↓KMT5A,↓LARP1B,MAGI2,MED1,MED7,↑MED17,MED23,MED27,MLH1,↓NAP1L3,NUMB,PVT1,↓RASGRF2,RBM5,↓RGS19,↓SCAF11,SNRNP70,STUB1,THRB,TP53,TP73	26	12	**Post-Translational Modification, Protein Folding**
3	Ag1 vs C	APOB,↓ATP2B1,↓BACH1,BCLAF1,BRCA1,↓CELSR2,CLRN1,CXCR3,↓DNAJC10,EFNA1,ESR1,FTH1,↑GBF1,GCLM,↓GOLGA2,GORASP2,Hdac,HDAC2,Histone h3,HMOX1,HSPA5,JMJD1C,JUN,↑LRP2,NQO1,PDGFBB,RAB1B,SEL1L,↓SHANK3,SLC7A11,SQSTM1,TNF,↑TSHZ3,U2AF2,USO1	20	9	**Cell Death and Survival**
4	Ag1 vs Ag1	AGTR1,↑AHCY,↑ARHGAP21,↑CDC42BPG,↑DIAPH3,↑DST,↓GFPT1,GRB2,HNRNPU,IGF2BP2,INPP5E,IRS4,↓LRP1B,↓MADD,↑MAGI3,MMP14,NR3C1,PGR,PIK3CD,PIK3R1,PPIA,PRKACB,↓RAB11FIP1,↑RAPGEF1,RPS6,RPS6KA,↑SEMA4D,SP1,TCR,TUBB4A,↑WDR3,YAP1,↑YWHAE,YWHAG,YWHAH	21	14	**Organismal Injury and Abnormalities**
5	Ag10 vs C	↓ADGRG2,↓ARHGEF6,↓CALB2,CTNNB1,EPRS,ERBB2,ETS1,GRB2,HNRNPA2B1,HSF1,HSF2,HSPA8,↑HSPA1A/HSPA1B,HSPD1,IL2,IL12B,ING1,LARS,MARS,PRKACA,PRKCA,PSEN1,PSEN2,PTHLH,PYGM,↓QARS,RARS,RNA polymerase II,RPA1,SMARCA4,STUB1,SUPT16H,TCF,THRB,↓ZZEF1	11	6	**Cell Cycle, Gene Expression**
6	Ag1 vs Ag1	↑ABCC5,ARNT,↑BAZ2A,CAV1,CCNA2,CD24,CORO1A,↓DEPDC1,EGLN3,EPAS1,ESR1,ESRRA,FOXO3,HAMP,HIF1A,↑INPP5A,IRS2,LGALS1,↑MAGEB4,↑MCM3AP,Mek,MST1R,NOS3,↑OFD1,OSM,PDGFRB,PIK3CB,↑POLRMT,RUVBL1,↑SACS,↓SPG11,TCF4,TFB2M,WISP2,↑ZDBF2	15	11	**Cellular Movement, Cell-To-Cell Signaling and Interaction**

binding protein involved in cell-cell adhesion was found to be strongly down-regulated at 24 h at both tested concentrations. Of interest is the deregulation of KRT8 and KRT18, which are essential proteins for the integrity of the epithelial cells, and playing an important role under stress. As (Wang et al., 2007) and (Georgantzopoulou et al., 2016) have reported, KRT8 and KRT18 are involved in IL-6 mediated cell protection. Accordingly, our cytokines array data shows a significant increase in IL-6 expression in cells exposed to 10 μg/mL of AgNPs for 72 h.

Also, 10 μg/mL AgNPs treatment for 72 h led to a significant deregulation of glutathione synthetase (GSS), a protein involved in inflammatory response and oxidative stress neutralisation. As a defence mechanism against oxidative injury, cells expressed altered levels of glutaredoxin-3 (GLRX3) and peroxiredoxin-1 (PRDX1) when exposed to 10 μg/mL of AgNPs for 72 h. Moreover, several heat shock proteins among which mitochondrial heat shock 60KDa (HSPD1), Serpin H1 (SERPINH1), Heath shock 70 KDa (HSPA1A) were found deregulated to counteract the oxidative damage. Altered expression of several heat shock proteins was in line with published observations (Oberemm et al., 2016). Protein disulphide-isomerase (P4HB), which catalyses the formation, breakage and rearrangement of disulfide bonds and 3-mercaptopyruvate sulfurtransferase (MPST) that acts as an antioxidant by transfering sulfur ion to cyanide or to other thiol compounds, were found deregulated at both time points tested (24 and 72 h) only at the lower concentration examined (1 μg/mL).

(Miethling-Graff et al., 2014) reported that AgNPs increased ROS level in LoVo cells at 24 h of exposure and correlated this finding with changes in the proteomic response of proteins involved in oxidative stress.

Both concentrations tested led to altered levels of Annexin A5 (ANXA5), a key apoptosis regulator, suggested to be an early marker of apoptosis (Herzog et al., 2004). (van der Zande et al., 2016) also reported that at gene levels, among the most dominant functional pathways affected by AgNPs exposure in CaCo-2 cells were the ones connected to oxidative stress and apoptosis.

In addition, by 2D technique, different isoforms of proteins have been identified. Glyceraldehyde-3- Phosphate dehydrogenase (GADPH), which is involved in several biological processes such as apoptosis, glycolysis, translational, presents three different isoforms whose expression levels were altered by AgNPs cell exposure. These results are in a good agreement with literature data on the influence of post-translational modification and oxidation of GADPH (Zhang et al., 2015, Kosova et al., 2017).

Oxidative stress can promote the formation of high molecular weight disulfide-linked GAPDH aggregates through a process called nucleocytoplasmic coagulation. Oxidation at Met-46 may play a pivotal role in the formation of these insoluble structures. This modification has been proposed to destabilise nearby residues, increasing the likelihood of secondary oxidative damages (Samson et al., 2014).

Also of interest was elongation factor 2 (EEF2), whose proteolytic product was found to be over expressed in cells treated with 10 μg/mL AgNPs for 72 h, also reported as among the top deregulated proteins by (Oberemm et al., 2016). Phosphorylation by EEF-2 kinase completely inactivates EEF-2, resulting in a drastic inhibition of polyphenylalanine synthesis in poly(U)-directed translation, therefore, completely inactive in translation (Ryazanov et al., 1988).

When results of the nanoparticle-cell interaction mechanisms induced by nanogold (AuNPs) obtained from previous studies (Gioria et al., 2014, Gioria et al., 2016) were compared with the data obtained by AgNPs in the present study, both the similarities and differences underlying biological processes and proteins regulation were found. To highlight is the expression of ENO1, IDH1 and P4HB, proteins involved in glycolysis, isocitrate metabolic process and cell redox homeostasis respectively, resulted altered in Caco-2 when exposed to AgNPs, as well as in Caco-2 or Balb-3 T3 cells exposed to AuNPs. Their modified expression could be suggested as a general response of cells exposed to NMs, whereas ETFA, HSPD1, PP1r7/PPP1R12A, Anx2, NUDC deregulation could potentially be considered as a specific Caco-2 response to NPs. It should be noted that no similar pathways were found to be activated in the two studies (Caco-2 cells exposed to AgNPs or AuNPs). This revealed that even if common deregulated proteins are found, they may link and coordinate different molecular pathways in the same Caco-2 cells model when exposed to different metal NPs.

Due to the extensively documented difficulties to quantitate in 2D gels proteins with high net charges, high pI and low M_r values, (Rabilloud et al., 2009), for a complete study, we employed in parallel label-free MS-based proteomics. Gel-free approaches were initially pitched as replacements for 2DE-MS; however, due as well to their limitations, they turned out to be complementary. It is evident that both approaches, with their respective advantages and disadvantages, should be used in parallel to get a complete comprehension of protein expression and interactions in a certain physiological condition (Abdallah et al., 2012).

De-regulated proteins identified using the label-free technique was also classified by biological functions. After 24 and 72 h of treatment with the selected AgNPs particles, a large number of proteins were found to be deregulated, particularly related to energy and metabolism, protein synthesis or stability/transcription, cell structure and transport, signal transduction.

As expected, the higher AgNPs concentration caused more protein deregulation. Interestingly, by label-free approach, more deregulated spots were observed for cells treated for 24 h, as compared to 72 h. Furthermore, 24 h exposure resulted in a predominant up-regulation of proteins, in particular, for the high dose tested, whereas, at 72 h exposure, altered proteins were mainly down regulated. Several zinc finger proteins involved in transcription regulation were found to be altered by AgNPs at the dose of 10 μg/mL at both time points analysed, in line with what was observed by (Oberemm et al., 2016) and co-workers who identified six different zinc finger proteins specifically deregulated by AgNPs treatment.

The low overlap observed between the two techniques that we found demonstrates the advantage of the multimodal approach in the characterisation of the proteome (Yeung et al., 2008).

Omics techniques provide more holistic approaches than offered by conventional techniques, in particular, here we addressed the advantage of a multimodal proteomics approach in the characterisation of the proteome (Yeung et al., 2008), definitely of great value for mechanistic (Adverse Outcome Pathway) studies and further integration of knowledge obtained from in vitro data for the safety assessment of NMs.

It is accepted that due to the complexity of NPs- cell interactions, comprehensive computational modelling approaches are needed to understand the cellular mechanisms, evolution, and dynamics of cellular proteins. Since omics approaches, as proteomics allows for computational modelling, we applied Ingenuity pathway analysis for interpreting the data of both proteomic platforms and gained insights into the main networks affected by the deregulated proteins.

The most significant molecular networks affected in response to 1 or 10 μg/mL AgNPs treatment for 24 h and 72 h were presented. Interestingly, the major proteins altered in response to AgNPs were associated with cell morphology, cellular assembly and organisation, cell cycle, cell death and survival. The findings are in line with what was reported by (Ma et al., 2011) at the level of global gene expression profiles, analysed by the integration of clustering, gene ontology (GO) and biological pathway analysis. By investigating the molecular mechanisms of interaction between AgNPs and human dermal fibroblasts-fetal (HDF-f), the results of Ma and co-workers suggest that AgNPs may cause the disruption of the cytoskeleton and cellular membrane, disturbance of energy metabolism and gene expression associated pathways, DNA damage, accompanied by cell cycle arrest.

At first glance, this work might not see as of any progress beyond the current status of knowledge. However, by conducting the experiments flawlessly and by interpreting the proteomics findings as much as possible, this work contributes to the goal of cooperation and openness

in the pursuit of scientific progress. Indeed, data sharing in mass-spectrometry (MS)-based proteomics opens a plethora of opportunities for data scientists (Martens and Vizcaíno, 2017). Standardization efforts have ensured that a large proportion of the public data can be read and processed by any interested researcher with the great opportunity for (orthogonal) reuse of public data or integration with other public omics data sets. Unfortunately, the lack of experimental and technical metadata has been highlighted many times as the main issue for the reuse of biological data, and particularly in proteomics (Griss et al., 2015).

4.2. Additional studies

At proteomics level, we reported alterations of molecular networks involved in cell morphology, cellular assembly and organisation, cell death and survival. We supported our findings, by cross-linking omics data with a broad set of complementary techniques. Cell morphology investigation revealed apparent dose-dependent changes in cell shape and a less define cytoskeleton structure in AgNPs treated cells compared to the controls.

The inflammatory response was also examined. Treatment with AgNPs resulted in an increase of IL-8, both at 24 and 72 h only at the highest dose tested of 10 μg/mL, whereas IL-6 was found overexpressed at the highest dose tested only at 72 h. AgNPs are reported to have both stimulatory and suppressive effects on the production of cytokines. Furthermore, the differential effects are dependent on dose and cell type (Nguyen et al., 2016). Treatment with low doses of AgNPs resulted in inhibitor effects, and higher doses led to increased pro-inflammatory cytokine levels. The dose and time-dependent effects in cytokine production however, need to be further investigated.

At proteome level, we identified several proteins involved in oxidative stress and apoptosis, in line with previous studies that reported apoptosis induced by various AgNPs (Gopinath et al., 2010). Based on the data achieved by using a human apoptosis antibody array membrane, we suggest that following the exposure of Caco-2 cells to AgNPs, TRAIL proteins, which are members of the tumor necrosis factor (TNF) family of ligands, are capable of initiating apoptosis through engagement of its death receptors (Wiley et al., 1995).

Some members of the Bcl-2 family inhibit apoptosis, while others facilitate this physiological process of cell death (O'Connor et al., 1998). In particular, AgNPs exposed to Caco-2 cells for 72 h increase BIM expression, a protein that binds to Bcl-2 provoking apoptosis.

Normally, DNA damage and cellular stress signalling activate p53, which, through DNA-specific transcription activation, transcriptional repression, and protein-protein interactions, triggers cell cycle arrest and apoptosis. One of the genes induced by p53 was identified as that encoding the insulin-like growth factor binding protein IGFBP-3, which is reported as the primary regulator of the amount of free IGF-I available to interact with the IGF-1 receptor. By sequestering IGFs from stimulating the IGF-1R, IGFBP-3 inhibits the IGF-survival signalling, thus functioning as a pro-apoptotic agent (Grimberg, 2000). There are accumulating evidences that IGFBP-3 can also cause apoptosis in an IGF-independent manner. Thus, IGFBP-3 induction by p53 constitutes a means of cross talk between the p53 and IGF axes. Also, by down regulating IGF-II, as we reported, P53 reduces the IGF/IGF-1R survival and mitogenic stimulation.

5. Conclusions

In this work, we have focused specifically on how systematic proteomic and structural studies could be used to define the critical protein interaction networks affecting Caco-2 human cells when exposed to AgNPs. We applied two different proteomic platforms for the assessment of the potential human health risks of AgNPs present e.g. in consumer products or medical applications. We have shown how this integration of techniques is crucial to obtaining biological insight for a correct hazard assessment. With these two proteomic platforms, we were able to detect significant changes in the protein profiles of Caco-2 cells that were treated with 30 nm AgNPs at the concentrations of 1 and 10 μg/mL at 24 or 72 h exposure.

We believe that these techniques could support an informed decision-making platform to assess the potential health effects of existing nanomaterials. This work is intended to contribute to an in-depth understanding of the mechanisms of action of AgNPs and should help in the development of safe NMs for nanotechnology-based consumer products without harmful side effects. As additional value, it contributes to the accumulation of data in the public domain, with the potential to generate new knowledge.

Funding

The research described in this work was supported by the European Commission's Joint Research Centre (JRC) within the Consumer Products Safety of the Directorate of Health, Consumers and Reference Materials through the JRC Multiannual Work Programme.

Supplementary data to this article can be found online at https://doi.org/10.1016/j.tiv.2018.03.015.

Acknowledgements

We are very thankful to Angela Kaempfer, François Rossi and Agnieszka Kinser-Ovaskainen for their helpful discussions. We acknowledge Emmanuel Duh for proofreading.

Conflict of interest

The authors declare that there are no conflicts of interest.

References

Abdallah, C., Dumas-Gaudot, E., Renaut, J., Sergeant, K., 2012. Gel-based and gel-free quantitative proteomics approaches at a glance. International Journal of Plant Genomics 2012.

Bar-Ilan, O., Albrecht, R.M., Fako, V.E., Furgeson, D.Y., 2009. Toxicity assessments of multisized gold and silver nanoparticles in zebrafish embryos. Small 5, 1897–1910.

Beer, C., Foldbjerg, R., Hayashi, Y., Sutherland, D.S., Autrup, H., 2012. Toxicity of silver nanoparticles—nanoparticle or silver ion? Toxicol. Lett. 208, 286–292.

Bouwmeester, H., Poortman, J., Peters, R.J., Wijma, E., Kramer, E., Makama, S., Puspitaninganindita, K., Marvin, H.J., Peijnenburg, A.A., Hendriksen, P.J., 2011. Characterization of translocation of silver nanoparticles and effects on whole-genome gene expression using an in vitro intestinal epithelium coculture model. ACS Nano 5, 4091–4103.

Brandon, E.F., Bosch, T.M., Deenen, M.J., Levink, R., van DER Wal, E., van Meerveld, J.B., Bijl, M., Beijnen, J.H., Schellens, J.H., Meijerman, I., 2006. Validation of in vitro cell models used in drug metabolism and transport studies; genotyping of cytochrome P450, phase II enzymes and drug transporter polymorphisms in the human hepatoma (HepG2), ovarian carcinoma (IGROV-1) and colon carcinoma (CaCo-2, LS180) cell lines. Toxicol. Appl. Pharmacol. 211, 1–10.

Calderón-Jiménez, B., Johnson, M.E., Bustos, A.R.M., Murphy, K.E., Winchester, M.R., Baudrit, J.R.V., 2017. Silver nanoparticles: technological advances, societal impacts, and metrological challenges. Front. Chem. 5.

Costa, P.M., Fadeel, B., 2016. Emerging systems biology approaches in nanotoxicology: towards a mechanism-based understanding of nanomaterial hazard and risk. Toxicol. Appl. Pharmacol. 299, 101–111.

Dadosh, T., 2009. Synthesis of uniform silver nanoparticles with a controllable size. Mater. Lett. 63, 2236–2238.

Georgantzopoulou, A., Serchi, T., Cambier, S., Leclercq, C.C., Renaut, J., Shao, J., Kruszewski, M., Lentzen, E., Grysan, P., Eswara, S., 2016. Effects of silver nanoparticles and ions on a co-culture model for the gastrointestinal epithelium. Particle fibre Toxicol. 13, 9.

Gerloff, K., Albrecht, C., Boots, A.W., Förster, I., Schins, R.P., 2009. Cytotoxicity and oxidative DNA damage by nanoparticles in human intestinal Caco-2 cells. Nanotoxicology 3, 355–364.

Gioria, S., Chassaigne, H., Carpi, D., Parracino, A., Meschini, S., Barboro, P., Rossi, F., 2014. A proteomic approach to investigate AuNPs effects in Balb/3T3 cells. Toxicol. Lett. 228, 111–126.

Gioria, S., Lobo Vicente, J., Barboro, P., La Spina, R., Tomasi, G., Urbán, P., Kinsner-Ovaskainen, A., François, R., Chassaigne, H., 2016. A combined proteomics and metabolomics approach to assess the effects of gold nanoparticles in vitro. Nanotoxicology 10, 736–748.

Gopinath, P., Gogoi, S.K., Sanpui, P., Paul, A., Chattopadhyay, A., Ghosh, S.S., 2010. Signaling gene cascade in silver nanoparticle induced apoptosis. Colloids Surf. B:

Biointerfaces 77, 240–245.
Grimberg, A., 2000. P53 and IGFBP-3: apoptosis and cancer protection. Mol. Genet. Metab. 70, 85–98.
Griss, J., Perez-Riverol, Y., Hermjakob, H., Vizcaíno, J.A., 2015. Identifying novel biomarkers through data mining—A realistic scenario? PROTEOMICS-Clin. Appl. 9, 437–443.
Hartemann, P., Hoet, P., Proykova, A., Fernandes, T., Baun, A., DE Jong, W., Filser, J., Hensten, A., Kneuer, C., Maillard, J.-Y., 2015. Nanosilver: safety, health and environmental effects and role in antimicrobial resistance. Mater. Today 18, 122–123.
Herzog, A., Kuntz, S., Daniel, H., Wenzel, U., 2004. Identification of biomarkers for the initiation of apoptosis in human preneoplastic colonocytes by proteome analysis. Int. J. Cancer 109, 220–229.
Kim, Y.S., Kim, J.S., Cho, H.S., Rha, D.S., Kim, J.M., Park, J.D., Choi, B.S., Lim, R., Chang, H.K., Chung, Y.H., 2008. Twenty-eight-day oral toxicity, genotoxicity, and gender-related tissue distribution of silver nanoparticles in Sprague-Dawley rats. Inhal. Toxicol. 20, 575–583.
Kim, S., Choi, J.E., Choi, J., Chung, K.-H., Park, K., Yi, J., Ryu, D.-Y., 2009. Oxidative stress-dependent toxicity of silver nanoparticles in human hepatoma cells. Toxicol. in Vitro 23, 1076–1084.
Kim, Y.S., Song, M.Y., Park, J.D., Song, K.S., Ryu, H.R., Chung, Y.H., Chang, H.K., Lee, J.H., Oh, K.H., Kelman, B.J., 2010. Subchronic oral toxicity of silver nanoparticles. Particle Fibre Toxicol. 7, 20.
Kosova, A., Khodyreva, S., Lavrik, O., 2017. Role of glyceraldehyde-3-phosphate dehydrogenase (GAPDH) in DNA repair. Biochem. Mosc. 82, 643–654.
Lefebvre, D.E., Venema, K., Gombau, L., Valerio Jr, L.G., Raju, J., Bondy, G.S., Bouwmeester, H., Singh, R.P., Clippinger, A.J., Collnot, E.-M., 2015. Utility of models of the gastrointestinal tract for assessment of the digestion and absorption of engineered nanomaterials released from food matrices. Nanotoxicology 9, 523–542.
Li, Y., Zhang, W., Niu, J., Chen, Y., 2013. Surface-coating-dependent dissolution, aggregation, and reactive oxygen species (ROS) generation of silver nanoparticles under different irradiation conditions. Environ. Sci. & Technol. 47, 10293–10301.
Lomer, M.C., Thompson, R.P., Powell, J.J., 2002. Fine and ultrafine particles of the diet: influence on the mucosal immune response and association with Crohn's disease. In: Proceedings of the Nutrition Society. 61. pp. 123–130.
Ma, J., Lü, X., Huang, Y., 2011. Genomic analysis of cytotoxicity response to nanosilver in human dermal fibroblasts. J. Biomed. Nanotechnol. 7, 263–275.
Martens, L., Vizcaíno, J.A., 2017. A golden age for working with public proteomics data. Trends Biochem. Sci. 42 (5), 333–341. http://dx.doi.org/10.1016/j.tibs.2017.01.001. (Epub 2017 Jan 22).
Matysiak, M., Kapka-Skrzypczak, L., Brzóska, K., Gutleb, A.C., Kruszewski, M., 2016. Proteomic approach to nanotoxicity. J. Proteome 137, 35–44.
Mcshan, D., Ray, P.C., Yu, H., 2014. Molecular toxicity mechanism of nanosilver. J. Food Drug Anal. 22, 116–127.
Miethling-Graff, R., Rumpker, R., Richter, M., Verano-Braga, T., Kjeldsen, F., Brewer, J., Hoyland, J., Rubahn, H.-G., Erdmann, H., 2014. Exposure to silver nanoparticles induces size-and dose-dependent oxidative stress and cytotoxicity in human colon carcinoma cells. Toxicol. in Vitro 28, 1280–1289.
Nguyen, K.C., Richards, L., Massarsky, A., Moon, T.W., Tayabali, A.F., 2016. Toxicological evaluation of representative silver nanoparticles in macrophages and epithelial cells. Toxicol. in Vitro 33, 163–173.
Oberemm, A., Hansen, U., Böhmert, L., Meckert, C., Braeuning, A., Thünemann, A.F., Lampen, A., 2016. Proteomic responses of human intestinal Caco-2 cells exposed to silver nanoparticles and ionic silver. J. Appl. Toxicol. 36, 404–413.
O'connor, L., Strasser, A., O'reilly, L.A., Hausmann, G., Adams, J.M., Cory, S., Huang, D.C., 1998. Bim: a novel member of the Bcl-2 family that promotes apoptosis. EMBO J. 17, 384–395.
Panáček, A., Kvítek, L., Prucek, R., Kolář, M., Večeřová, R., Pizúrová, N., Sharma, V.K., Nevěčná, T.J., Zbořil, R., 2006. Silver colloid nanoparticles: synthesis, characterization, and their antibacterial activity. J. Phys. Chem. B 110, 16248–16253.
Rabilloud, T., Vaezzadeh, A.R., Potier, N., Lelong, C., Leize-Wagner, E., Chevallet, M., 2009. Power and limitations of electrophoretic separations in proteomics strategies. Mass Spectrom. Rev. 28, 816–843.
Ryazanov, A.G., Shestakova, E.A., Natapov, P.G., 1988. Phosphorylation of Elongation Factor 2 by EF-2 Kinase Affects Rate of Translation.
Sahu, S.C., Njoroge, J., Bryce, S.M., Zheng, J., Ihrie, J., 2016. Flow cytometric evaluation of the contribution of ionic silver to genotoxic potential of nanosilver in human liver HepG2 and colon Caco2 cells. J. Appl. Toxicol. 36 (4), 521–531. http://dx.doi.org/10.1002/jat.3276. (Epub 2016 Jan 6).
Samson, A.L., Knaupp, A.S., Kass, I., Kleifeld, O., Marijanovic, E.M., Hughes, V.A., Lupton, C.J., Buckle, A.M., Bottomley, S.P., Medcalf, R.L., 2014. Oxidation of an exposed methionine instigates the aggregation of glyceraldehyde-3-phosphate dehydrogenase. J. Biol. Chem. 289, 26922–26936.
Teow, Y., Asharani, P., Hande, M.P., Valiyaveettil, S., 2011. Health impact and safety of engineered nanomaterials. Chem. Commun. 47, 7025–7038.
Van Der Zande, M., Undas, A.K., Kramer, E., Monopoli, M.P., Peters, R.J., Garry, D., Antunes Fernandes, E.C., Hendriksen, P.J., Marvin, H.J., Peijnenburg, A.A., 2016. Different responses of Caco-2 and MCF-7 cells to silver nanoparticles are based on highly similar mechanisms of action. Nanotoxicology 10, 1431–1441.
Verano-Braga, T., Miethling-Graff, R., Wojdyla, K., Rogowska-Wrzesinska, A., Brewer, J.R., Erdmann, H., Kjeldsen, F., 2014. Insights into the cellular response triggered by silver nanoparticles using quantitative proteomics. ACS Nano 8, 2161–2175.
Wang, L., Srinivasan, S., Theiss, A.L., Merlin, D., Sitaraman, S.V., 2007. Interleukin-6 induces Keratin expression in intestinal epithelial cells potential role of keratin-8 in interleukin-6-induced barrier function alterations. J. Biol. Chem. 282, 8219–8227.
Wiley, S.R., Schooley, K., Smolak, P.J., Din, W.S., Huang, C.-P., Nicholl, J.K., Sutherland, G.R., Smith, T.D., Rauch, C., Smith, C.A., 1995. Identification and characterization of a new member of the TNF family that induces apoptosis. Immunity 3, 673–682.
Win, K.Y., Feng, S.-S., 2005. Effects of particle size and surface coating on cellular uptake of polymeric nanoparticles for oral delivery of anticancer drugs. Biomaterials 26, 2713–2722.
Xu, L., Shi, C., Shao, A., Li, X., Cheng, X., Ding, R., Wu, G., Chou, L.L., 2015. Toxic responses in rat embryonic cells to silver nanoparticles and released silver ions as analyzed via gene expression profiles and transmission electron microscopy. Nanotoxicology 9, 513–522.
Yeung, A.T., Patel, B.B., Li, X.-M., Seeholzer, S.H., Coudry, R.A., Cooper, H.S., Bellacosa, A., Boman, B.M., Zhang, T., Litwin, S., 2008. One-hit effects in cancer: altered proteome of morphologically normal colon crypts in familial adenomatous polyposis. Cancer Res. 68, 7579–7586.
Zhang, J.-Y., Zhang, F., Hong, C.-Q., Giuliano, A.E., Cui, X.-J., Zhou, G.-J., Zhang, G.-J., Cui, Y.-K., 2015. Critical protein GAPDH and its regulatory mechanisms in cancer cells. Cancer Biol. & Med. 12, 10.
Zhang, X.-F., Shen, W., Gurunathan, S., 2016. Silver nanoparticle-mediated cellular responses in various cell lines: an in vitro model. Int. J. Mol. Sci. 17, 1603.